

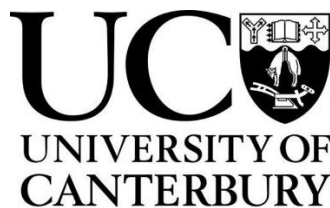
**HYDROGEOLOGICAL INVESTIGATION OF  
EARTHQUAKE RELATED SPRINGS  
IN THE HILLSBOROUGH VALLEY  
CHRISTCHURCH, NEW ZEALAND**

---

A thesis  
submitted in partial fulfilment  
of the requirements for the Degree of  
Master of Science in Geology  
in the  
University of Canterbury  
by  
Mitchell James Green

---

University of Canterbury  
2015



## **Abstract**

This thesis is concerned with springs that appeared in the Hillsborough, Christchurch during the 2010-2011 Canterbury Earthquake Sequence, and which have continued to discharge groundwater to the surface to the present time. Investigations have evolved, measurements of discharge at selected sites, limited chemical data on anions and isotope analysis. The springs are associated with earthquake generated fissures (extensional) and compression zones, mostly in loess-colluvium soils of the valley floor and lower slopes. Extensive peat swamps are present in the Hillsborough valley, with a groundwater table at ~1m below ground.

The first appearance of the ‘new’ springs took place following the Mw 7.1 Darfield Earthquake on 4 September 2010, and discharges increased both in volume and extent of the Christchurch Mw 6.3 Earthquake of 22 February 2011. Five monitored sites show flow rates in the range of 4.2-14.4L/min, which have remained effectively constant for the duration of the study (2014-2015). Water chemistry analysis shows that the groundwater discharges are sourced primarily from volcanic bedrocks which underlies the valley at depths  $\leq 50\text{m}$  below ground level.

Isotope values confirm similarities with bedrock-sourced groundwater, and the short term (hours-days) influence of extreme rainfall events. Cyclone Lusi (2013-2014) affects were monitored and showed recovery of the bedrock derived water signature within 72 hours. Close to the mouth of the valley sediments interfinger with Waimakiriri River derived alluvium bearing a distinct and different isotope signature. Some mixing is evident at certain locations, but it is not clear if there is any influence from the Hunsbury reservoir which failed in the Port Hills Earthquake (22 February 2011) and stored groundwater from the Christchurch artesian aquifer system (Riccarton Gravel).

## **Acknowledgements**

- First and foremost I must thank my supervisory team David Bell and Travis Horton.
- Technical staff for helping in the field and the lab.
- My family for their support
- The office for the good times
- The shilling club for a drink when required
- My teddy bear for the cuddles and companionship during the hard times

# Contents

Abstract .....	i
Acknowledgements .....	i
Chapter 1. Introduction .....	1
1.1 Project Background .....	1
1.2 Thesis Objectives .....	3
1.3 Geology of the Christchurch Area .....	3
1.4 Tectonic Setting and Seismicity of the Christchurch area .....	9
1.5 Geology of the Canterbury 2010-2011 Earthquake Sequence (CES) .....	10
1.6 Hydrogeology of Christchurch .....	14
1.7 Climate .....	15
1.8 Hydrogeological Terminology and Previous Work .....	18
1.8.1 Spring Terminology .....	18
1.8.2 Previous Work .....	18
1.9 Thesis Format .....	21
Chapter 2. Groundwater and Spring Hydrogeology .....	23
2.1 Introduction .....	23
2.2 Occurrence and Classification of springs .....	23
2.2.1 Types of springs .....	23
2.2.2 Classification of springs .....	24
2.2.3 Thermal and mineral springs .....	27
2.2.4 Source and recharge of springs .....	27
2.2.5 Groundwater-surface water interactions .....	28
2.3 Earthquakes and Hydrological Response .....	28
Chapter 3. STUDY AREA: THE HILLSBOROUGH VALLEY .....	30
3.1 Introduction .....	30
3.2 The Geology of Hillsborough Valley .....	32



3.2.1	Introduction.....	32
3.2.2	The Lyttelton Volcanic Group (11-9.7ma) .....	32
3.2.3	Regolith Material types and their Distribution .....	36
3.3	Geomorphology.....	43
3.3.1	Erosional Geomorphology .....	43
3.3.2	Earthquake Geomorphology .....	45
3.4	Sample Site Locations .....	47
3.5	Study area site plans .....	49
Chapter 4.	Methodology .....	54
4.1	Introduction .....	54
4.2	Site Investigation and Mapping.....	54
4.2.1	Field Investigations .....	54
4.2.2	Mapping and LiDAR .....	55
4.2.3	Geotechnical Data.....	57
4.3	Sampling and Monitoring Schedule .....	59
4.4	Piezometer installation and Monitoring .....	60
4.5	Spring Discharge Monitoring and Weir Installation .....	61
4.6	Water Sampling Analysis.....	63
4.7	Isotope Testing .....	64
4.8	Anion Testing.....	64
Chapter 5.	Hillsborough Valley Physical Hydrogeology .....	65
5.1	Introduction .....	65
5.2	Groundwater in the Hillsborough Valley .....	65
5.2.1	Earthquake response .....	67
5.3	Spring Distribution and Classification .....	67
5.3.1	Spring Features .....	68
5.4	Spring Discharge and Piezometric Investigation results.....	70

5.4.1	Spring Discharge.....	70
5.4.2	Groundwater Levels.....	71
Chapter 6.	Hillsborough Valley Chemical Hydrogeology .....	76
6.1	Introduction .....	76
6.2	Hydrogeological Geochemistry.....	76
6.3	Groundwater in the Christchurch area .....	77
6.3.1	Composition of Banks Peninsula Water. ....	78
6.3.2	The Christchurch Artesian Aquifers. ....	81
6.4	Aquifers of the Hillsborough Area.....	81
6.5	Hydrochemistry of the Hillsborough Valley .....	82
6.6	Stable Isotope Analysis .....	85
6.6.1	Oxygen-18.....	85
6.6.2	Deuterium .....	87
6.6.3	Stable Isotope samples compared with the Global Meteoric Water Line.....	89
6.7	Ionic Analysis.....	90
6.8	Ex-Tropical Cyclone Lusi .....	100
6.8.1	Significance.....	101
6.8.2	High frequency sampling .....	101
6.8.3	Spring and Groundwater response .....	101
6.9	Hydrochemical comparison with Canterbury natural water .....	104
Chapter 7.	Summary and Conclusions .....	107
7.1	Thesis Objectives and Methodology .....	107
7.2	Physical Hydrogeology .....	108
7.2.1	Spring discharge.....	108
7.2.2	Piezometric levels .....	109
7.3	Chemical Hydrogeology .....	109
7.4	Isotope Hydrogeology .....	110

7.5	Principal Conclusions.....	110
7.6	Future Research.....	111
	References.....	112

## List of Figures

Figure 6.1: Map showing the location of Canterbury and Christchurch within New Zealand (inset). The locations of the Southern Alps and Banks Peninsula are also shown. (Google Earth 2015) .....	1
Figure 6.2: Oblique view of the Hillsborough Valley looking south showing the extent of residential development, roads and the Huntsbury Reservoir on the western slope of the valley. (Google Earth 2015) .....	2
Figure 6.3: A Digital Elevation Model (DEM) of the proposed Lyttelton Volcanic Complex as described in Hampton (2010). Volcanic deposits younger than the Lyttelton Volcanic Group are shown overlying the proposed cone structures of Lyttelton Volcano. The inset provides a geological map and stratigraphic sequence for Banks Peninsula. ....	4
Figure 6.4: Schematic diagram detailing the formation of cone-controlled and radial valleys associated with volcanic cones. The Hillsborough Valley study area is most likely a radial valley associated with an eruptive centre of the Lyttelton Volcanic complex. (Hampton 2010) .....	5
Figure 6.5: Shallow subsurface geology of the Christchurch area. Major road and rail networks are shown as reference. (modified from Brown et al. 1995) .....	1-7
Figure 1.6: The plate tectonic setting for the South Island of New Zealand. Shown are key crustal fault structures, the Hikurangi Plateau and the Chatham Rise (from Ring & Hampton 2012). ....	<b>Error! Bookmark not defined.</b>
Figure 1.7: The $M_w$ 7.1 Darfield main shock (green star) and aftershock sequence up to 11th April 2014. The epicentre of the 22 <sup>nd</sup> February 2011 Christchurch earthquake (red star), 13 <sup>th</sup> June 2011 (blue star) and 23 <sup>rd</sup> December 2011 (pink star) are also displayed. Note the general eastward trend of seismic activity during the earthquake sequence. (GNS Science 2015) ....	11
Figure 1.8(a): Proposed blind fault locations in Christchurch, with various seismic station names and locations displayed (left) (modified from Beavan et al. 2012). Figure 1.8(b): Map of the	

Hillsborough Valley area showing the location of the upper edge of the Port Hills Fault plane at a depth of 1000m, and projected to sea level. Fissure traces and areas of spring activity are also shown (Right). (after Stephen-Brownie 2012, plotted with data from Kaiser et al. 2012)	13
Figure 1.9: Schematic cross-section through the Canterbury Plains highlighting the confined and unconfined/semi-confined aquifers beneath Christchurch. (modified from Cox et al. 2012)	14
Figure 6.10: Average monthly rainfall for the Christchurch area during the period 1980-2010 from the Botanical Gardens monitoring station. Total annual rainfall during this period averaged 618mm. (NIWA 2015)	16
Figure 6.11: Mean annual rainfall amount (mm) isoline map for the Christchurch area. (Christchurch City Council 2010)	17
Figure 6.12: Summary of spring discharge against rainfall results for the 'Abattoir' springs in Akaroa County, Banks Peninsula by Sanders (1986).	19
Figure 6.1: Types of gravity springs (modified from Fetter 2001)	25
Figure 6.2: Thermal ground waters from throughout the South Island of New Zealand, with location and maximum temperatures (°C) recorded. (Hunt & Bibby 1992)	27
Figure 6.3: Figure showing the type of earthquake related response seen in piezometers proximal to Christchurch during the Darfield earthquake. Also shown are areas of liquefaction and new spring development (modified from Cox et al. 2012)	29
Figure 3.1: Map of greater Christchurch, with the Hillsborough Valley area highlighted by box section (see figure 2.2).	30
Figure 3.2 Map of the Hillsborough Valley study area with notable roads and waterways shown. Elevation contours are also displayed.	31
Figure 3.3: Lava flows outcropping along the Rapaki Spur, image is oriented to the east.	33
Figure 3.4: Typical aa lava flow morphology of Banks Peninsula. Note the rubbly layers, breccia and cooling shrinkage fractures (after Namjou 1988)	34
Figure 3.5: Hawaiite flow exposed at the entrance to the Mt. Vernon gorge, Note the irregular and platy cooling joints and fractures.	34
Figure 3.6: Generalised cross-section of a Port Hills ridge, showing the relationships between landforms, slope, regolith and erosion. (Bell & Trangmar 1987)	36
Figure 3.7: Waterways, wetlands and vegetation cover as detailed in the 1856 Black Maps of the Christchurch area. The Hillsborough Valley study area is highlighted in the red box, note the presence of marshy land at the mouth of the valley (Christchurch City Council 2010).	44

Figure 3.8: Geological map of the Hillsborough Valley. Note the contact with the Springston Formation at the Valley entrance and the extensive peat deposits in the Valley floor. ....	42
Figure 3.9: LiDAR derived Hillslope map of the Hillsborough Valley. Alluvial fan features in the valley floor are highlighted by the dashed red line. ....	<b>Error! Bookmark not defined.</b>
Figure 3.10: Hillshade map of the Hillsborough Valley. Earthquake related springs, fissure traces and compressional feature locations are displayed, as is the extent and thickness of peat deposits in the valley floor. (Data is sourced from CERA 2015) .....	46
Figure 3.11: LiDAR derived hill shade and contour map of the Hillsborough Valley study area with spring, waterway and site locations displayed. The extent of peat deposits in the valley floor are also displayed. ....	48
Figure 3.12: Hydrogeological sketch plan for the Site A study area. ....	49
Figure 3.13: Hydrogeological sketch plan for the Site B study area .....	50
Figure 3.14: Hydrogeological sketch plan for the Site C study area. Note the presence of compressional zone fractures along hard surfaces such as the asphalt driveway and the paved area at the house entranceway.....	51
Figure 3.15: Site plan for the Site D study area. The pre-existing house has been demolished allowing full access to the site. Note the location of the groundwater sampling pipe and seepage interception trenches. ....	52
Figure 3.16: DEM and Hillshade map of the Hillsborough Valley. The hydrological catchment (watershed) area is highlighted as this was used as a conservative measure to calculate the groundwater catchment area for the valley. This was also used to collect Storativity values .....	<b>Error! Bookmark not defined.</b>
Figure 4.1: Bare-Earth DEM map of the Hillsborough Valley/ Mt. Vernon Area with 20 metre contours shown. ....	56
Figure 4.2: Map of the Hillsborough valley with spring, borehole and mass movement features displayed over DEM derived Hillshade map .....	58
Figure 4.3: The V-Notch weir installation under the house at Site B. Where: .....	62
Figure 5.1: Cross-Section #1 through the Hillsborough Valley. Data was obtained via deep boreholes drilled by Tonkin & Taylor Ltd (CERA 2015), and deeper valley fill units have been inferred based on Port Hills Valley morphology presented in previous research (Namjou 1988; Parker 1989; Sanders 1986; Brown & Weeber 1994). Borehole log data is located in appendix 1.....	69
Figure 5.2: Site A Spring Discharge and Daily Rainfall .....	<b>Error! Bookmark not defined.</b>
Figure 5.3: Site B Spring #1 Discharge and Hourly Rainfall ..	<b>Error! Bookmark not defined.</b>

Figure 5.4: Site A Piezometer monitoring levels and. Daily rainfall **Error! Bookmark not defined.**

Figure 5.5: Groundwater levels and. Daily rainfall for Site B Piezometer #1.....**Error! Bookmark not defined.**

Figure 5.6: Groundwater levels and. Hourly rainfall for Site B Piezometer #2. ....**Error! Bookmark not defined.**

Figure 5.7: Graph showing the comparison between spring discharge and groundwater levels at the LV study site .....**Error! Bookmark not defined.**

Figure 5.8: Groundwater levels for Site C Piezometer #2 plotted against rainfall .....**Error! Bookmark not defined.**

Figure 5.9: Hydrogeological model of the Vernon Terrace area (Z-axis is not to scale) .**Error! Bookmark not defined.**

Figure 6.1: Plot of  $\delta^{18}\text{O}$  (V-SMOW) values and Daily Rainfall .....86

Figure 6.2: Plot of  $\delta^2\text{H}$  (V-SMOW) and Daily Rainfall for Hillsborough Valley water samples. ....88

Figure 6.3:  $\delta\text{D}$  vs.  $\delta^{18}\text{O}$  plotted against the Global Meteoric Water Line (GMWL). Tap water collected at the Hillsborough Valley sites plots towards lower along the GMWL with more depleted stable isotope values compared to the springs and groundwater of the area. Both the Ex-Tropical Cyclone Lusi rainwater and 6th March 2014 1/100 rainfall deluge waters are also highlighted, These were collected in the rain gauge at the Site A. Rainwater collected the 29th April 2014 at Matipo Street plots closer toward the more negative  $\delta$  values of the Christchurch tap water.....89

Figure 6.4: Fluoride anions (mg/L) for Hillsborough Valley water samples vs. rainfall .....93

Figure 6.5: Nitrate anions (mg/L) for Hillsborough Valley water vs. rainfall.....94

Figure 6.6: Sulphate anions (mg/L) for Hillsborough Valley water samples vs. rainfall.....96

Figure 6.7: Phosphate anions (mg/L) for Hillsborough Valley water vs. rainfall .....97

Figure 6.8: Chloride anions (mg/L) for Hillsborough Valley water vs. rainfall.....99

Figure 6.9: Piper plot of various spring and groundwater water samples from the greater Christchurch area .....104

Figure 6.10: Stiff plots for selected Christchurch spring and well waters. Spring water samples from the Hillsborough Valley study sites are shown in the inset. PW=Palatine Place and MP= Colombo Street “Main Pumps” Community water Supply well waters, HV= Heathcote Valley Well, FS= Ferrymead Spring, LRT= Lyttelton Railway Tunnel Spring, RB=Rapaki Bay Spring.....105



# Chapter 1. Introduction

## *1.1 Project Background*

The city of Christchurch is located on the southeast of the South Island of New Zealand, on the coastal Canterbury Plains and the northern fringe of the Port Hills (Figure 1.1). The Port Hills comprise the northern rim of Lyttleton Volcano, part of the Miocene volcanic centre which forms Banks Peninsula, which itself is built on Cretaceous volcanic and sedimentary basement rocks. The region was affected by a series of major earthquake events beginning with the 4th September 2010  $M_w$  7.1 Darfield earthquake and its subsequent aftershocks, the largest of which was the 22<sup>nd</sup> February 2011  $M_w$  6.3 Christchurch earthquake.

The earthquakes had a two-fold set of physical impacts for the region, particularly in the Christchurch area following the February 2011 (Christchurch) earthquake. One was that shaking caused significant structural damage and destruction to buildings, and damaged infrastructure which affected water supply, power, waste-water disposal and communications. Secondly, widespread ground deformation, lateral spreading, liquefaction and spring formation caused further damage to roads, infrastructure and property (Gulley et al. 2013).



**Figure 1.1:** Map showing the location of Canterbury and Christchurch within New Zealand (inset). The locations of the Southern Alps and Banks Peninsula are also shown. (Google Earth 2015)



This thesis study focuses on the formation of earthquake-related springs in the areas surrounding the base of the Port Hills, and specifically in the Hillsborough Valley (Figure 1.2). The 0.9km<sup>2</sup> Hillsborough Valley is located on the northeast of the Port Hills, and is flanked by the loess-covered Lyttleton basaltic lava flow packages that form the Huntsbury and Murray-Aynsley hills (Ogilvie 2009). It is a predominantly residential area of Christchurch, with development of both the valley floor and upwards on the valley slopes, although it was originally a mostly horticultural area of early Christchurch (Wilson 2005). The Hillsborough Valley is also referred to as the St. Martins Valley by others, as in Ogilvie (2009). Springs and seepages emerged within the valley in previously dry areas along and adjacent to footslope positions within 24 hours following the Darfield 2010 earthquake, with the number and magnitude of springs greatly increasing following the February 2011 Christchurch earthquake. The spring features have flowed persistently since their initial appearance, and continued to flow throughout this study.

According to Rutter (2011), earthquake-related springs may be the result of:

- 1) Reactivation of old, sealed artesian bores.
- 2) Reactivation of pre-existing (paleo) springs.
- 3) Discontinuities developed in confining layers.
- 4) Permeability developed in consolidated rocks.



**Figure 1.2: Oblique view of the Hillsborough Valley looking south showing the extent of residential development, roads and the Huntsbury Reservoir on the western slope of the valley. (Google Earth 2015)**

## ***1.2 Thesis Objectives***

The primary aims of this project are to determine the locations, morphology, source and causes of springs formed in the Hillsborough Valley at the base of the Port Hills as a result of the 2010-2012 Canterbury earthquake sequence (CES), and particularly following the 22<sup>nd</sup> February 2011 Christchurch earthquake. The key outcomes are to better understand the source of water and the mechanism(s) for formation of springs in the area. This has applications for future planning work, and the thesis documents the geotechnical and geomorphological implications and impacts of the springs. It also provides knowledge and understanding of the springs for the residents and local authorities in the area. Specific objectives are as follows:

- Produce relevant maps and site plans documenting the geospatial features of the study area, infrastructure, areas of particular spring activity and ground deformation, and the locations of springs that were studied.
- Measure and record physical and chemical data for the springs over a 10-12 month period to better understand both short-term and seasonal fluxes in spring discharge and chemistry.
- Produce hydrogeological models of the valley based on geotechnical and hydrochemical investigations which detail the spring morphologies, water source and flow mechanism(s) within the Hillsborough Valley.
- Display the results of the investigations in clear and understandable outputs that are of use to third parties, and are scientifically accurate and consistent.

## ***1.3 Geology of the Christchurch Area***

Key to understanding the hydrogeology of the Hillsborough Valley is to first determine the geological structures and evolution of the wider Christchurch area (Figure 1.3). The basement in the wider Canterbury region is the Torlesse Composite Terrane rocks, consisting of predominant greywackes and semi-schistose argillite in places, with minor volcanics, chert and limestone, that are late Palaeozoic to Mesozoic in age and represent deposition in a deeper marine setting in offshore basins. The Rakaia Terrane rocks of the Torlesse Supergroup are the immediate basement rocks in the Christchurch area, and these outcrop in the Gebbies Pass area of Banks Peninsula, 15km south of the study area, and underlie the Canterbury Plains (Brown & Weeber 1992). Overlying the Torlesse Supergroup greywackes are a sequence of terrestrial

to marine transgressive sedimentary rocks. These rocks date from the late Cretaceous through to the Pliocene, and consist of conglomerates, sandstones limestones through to mudstones. This sedimentary succession of rocks represents the New Zealand continent (Zealandia), proceeding initially through a period of erosion of the Rangitata mountain belt, large scale continental to then sea floor crustal extensional spreading; and finally to a period of crustal cooling and continental subsidence. The Tertiary sedimentary rock units underlie, but do not outcrop, in the immediate Christchurch area (Coates 2002).

The Hillsborough Valley is part of the extinct volcanic complex collectively known as Banks Peninsula. It is the largest accumulation of Cenozoic volcanic rocks in the South Island of New Zealand, which lay unconformably over the Rakaia Terrane rocks and earlier Cretaceous Volcanics of the Mt. Somers Formation (Forsyth et al. 2008). The northern section of Banks Peninsula is dominated by the structure of Lyttelton Volcano. Hampton (2010) provides a detailed account of the geology and formation of Lyttelton Volcano.

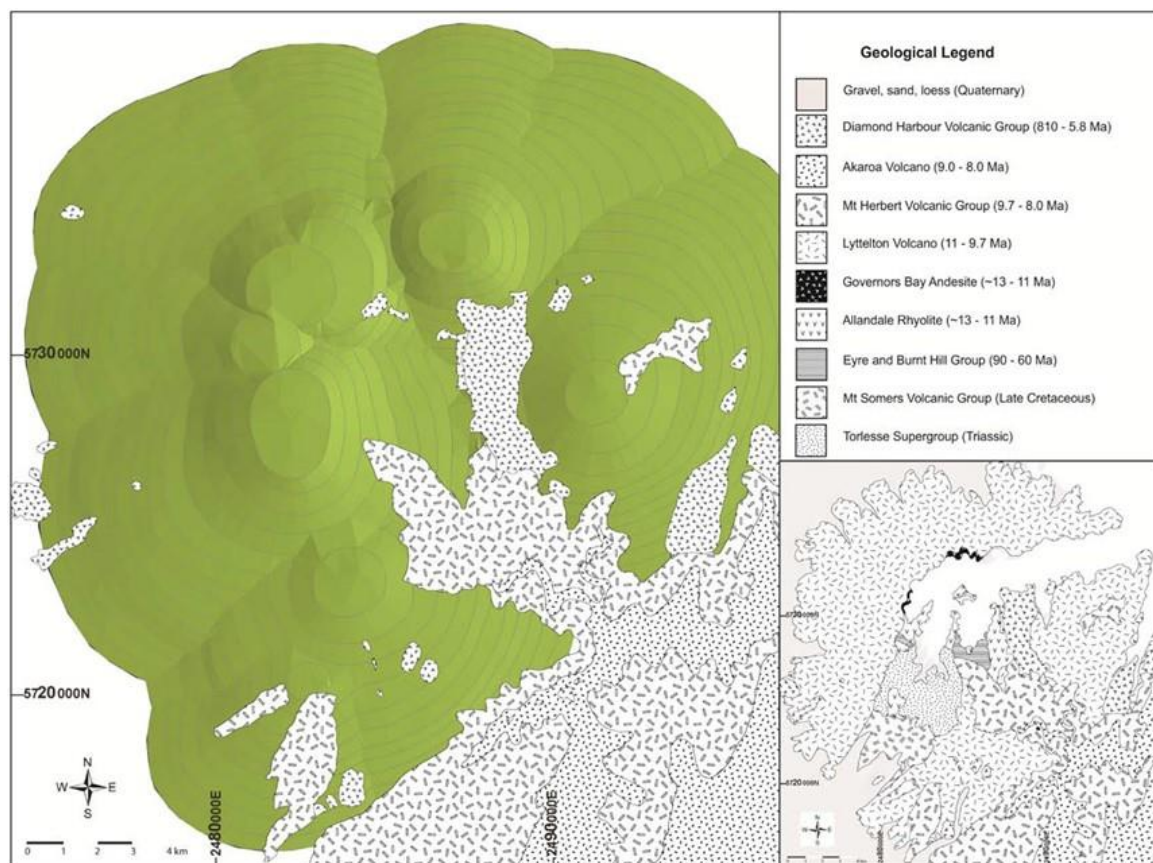


**Figure 1.3: A Digital Elevation Model (DEM) of the proposed Lyttelton Volcanic Complex as described in Hampton (2010). Volcanic deposits younger than the Lyttelton Volcanic Group are shown overlying the proposed cone structures of Lyttelton Volcano. The inset provides a geological map and stratigraphic sequence for Banks Peninsula.**

Hampton (2010) proposed two key erosional structures which form the present morphology of Lyttelton Volcano, these being radial valleys and cone-controlled valleys (Figure 1.4). Cone-controlled valleys form in regions where two sets of eruptive packages and cones meet, and form the somewhat larger valleys and low points in Lyttelton Volcano, such as Lyttelton Harbour, Gebbies Pass and the Herbert Depression. The smaller, radial valleys are the result of radial erosion centred on a cones summit. The Hillsborough Valley study site, based on its smaller size, series of overlapping lava flow packages and location, is therefore most likely a paleo-radial valley within the greater Lyttelton Volcanic complex cone structure. Evidence of the depth and extent of the Lyttelton volcanics beneath Christchurch is obtained from well-log data from deep boreholes, where the depth of bedrock has been mapped to 50 and 100 metre depth contours below the ground surface along the margins of the Port Hills (Brown & Weeber 1994). These investigations show that the volcanic bedrock extends to variable depths along the margin of the Port Hills, with the 100m depth to bedrock contour extending to a maximum distance of 2km from volcanic rock outcrops in areas such as Woolston, Christchurch. Beneath the Hillsborough Valley, volcanic bedrock varies between 50 and 100m in depth beneath the valley entrance.

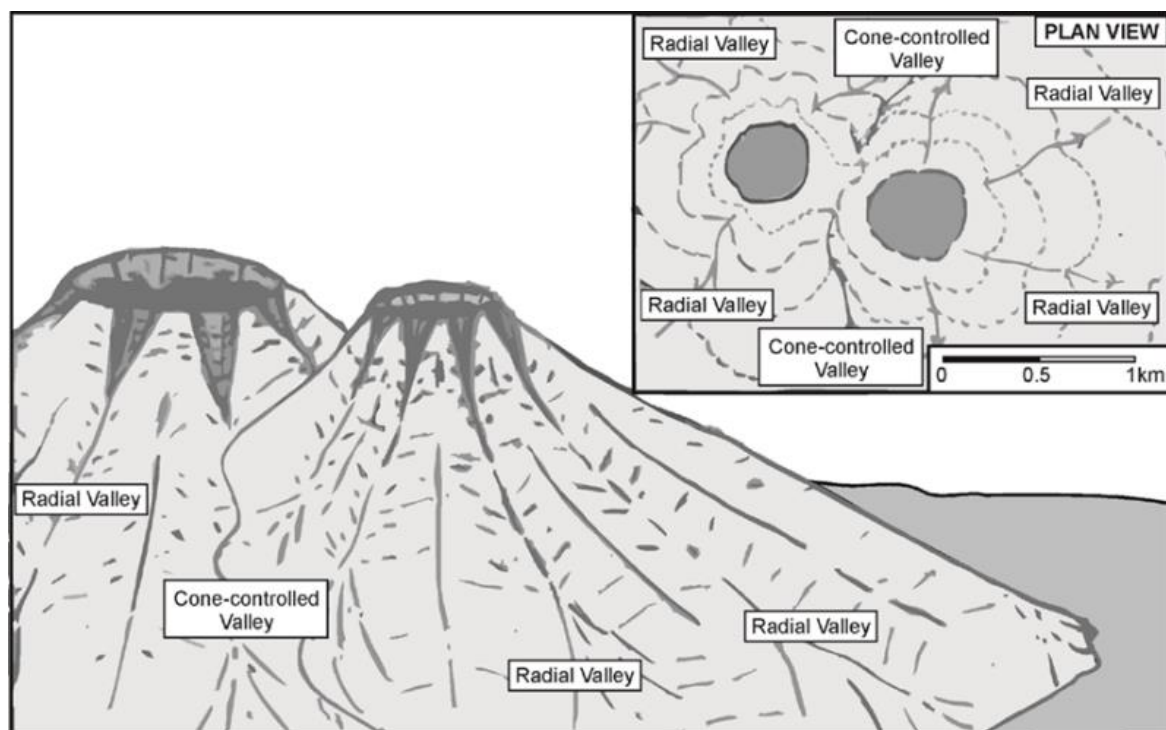


**Figure 1.4: Schematic diagram detailing the formation of cone-controlled and radial valleys associated with volcanic cones. The Hillsborough Valley study area is most likely a radial valley associated with an eruptive centre of the Lyttelton Volcanic complex. (Hampton 2010)**



The majority of the rock types described above are overlain by varying thicknesses of more recent sedimentary deposits associated with a number of glacial and interglacial periods which occurred during the Quaternary. The Canterbury Plains consist of a series of coalescing alluvial fans derived predominantly from Torlesse greywacke gravels which were deposited during the last 5 million years over the latest Tertiary and Quaternary strata during glacial periods (Brown & Weeber 1992). Alternatively, inland reworking and coastal redeposition of these gravels occurred during interglacial periods (Stewart 2012). Higher sea levels were another aspect of the interglacial periods, where as a consequence the sea encroached inland resulting in the deposition of fine grained marine sediments, beach and dune sands, and peats from coastal swamps and estuaries in the transgression-regression zone. Pockets of peat are also found in hillside valley outwash fans adjacent to the Port Hills, where swamps formed due to the low relief and lack of drainage (Christchurch City Council 2010). The uppermost coastal deposit is known as the Christchurch Formation, whereas the alternative inland equivalent is known as the Springston Formation, which overlies much of the Christchurch Formation in Eastern Christchurch (Figure 1.5; Table 1.1).

Aeolian (wind-blown) yellow-brown silty loess deposits with local fine sands and clay occur throughout Canterbury, and are draped over much of the eroded volcanics of Banks Peninsula (Forsyth et al. 2008). Loess found on Banks Peninsula has been blown from the river beds of the Canterbury Plains by northwest winds during glaciations, with some loess being derived from the seabed east of Banks Peninsula exposed due to the lower sea level at the time. Rates of deposition varied due to slope and location on Banks Peninsula, thicknesses range from 1-20 metres (+) with the thickest deposits now occurring towards the base of slopes and in valley floors due to reworking and redeposition from higher slopes (Brown & Weeber 1992).

The exact age of the loess has proven difficult to measure, with the last major accumulation of loess on Banks Peninsula beginning between 35,000 and 43,000 years ago based on OSL dating (Almond et al. 2007), and the uppermost paleosol ages signalling a cessation of deposition ~ 17,450  $\pm$  2070 years ago. Soils and alluvial deposits on the Port Hills are predominantly derived from loess material and to a lesser extent, eroded rocks from the Lyttelton Volcanic Group (Brown & Weeber 1992). Loess deposits are prone to erosion often due to their dispersive nature, especially when wetted. Erosional processes in the Port Hills loess consist of soil creep, mass-movements, sheet and rill erosion, tunnel-gullyng and wind erosion (Bell & Trangmar 1987).

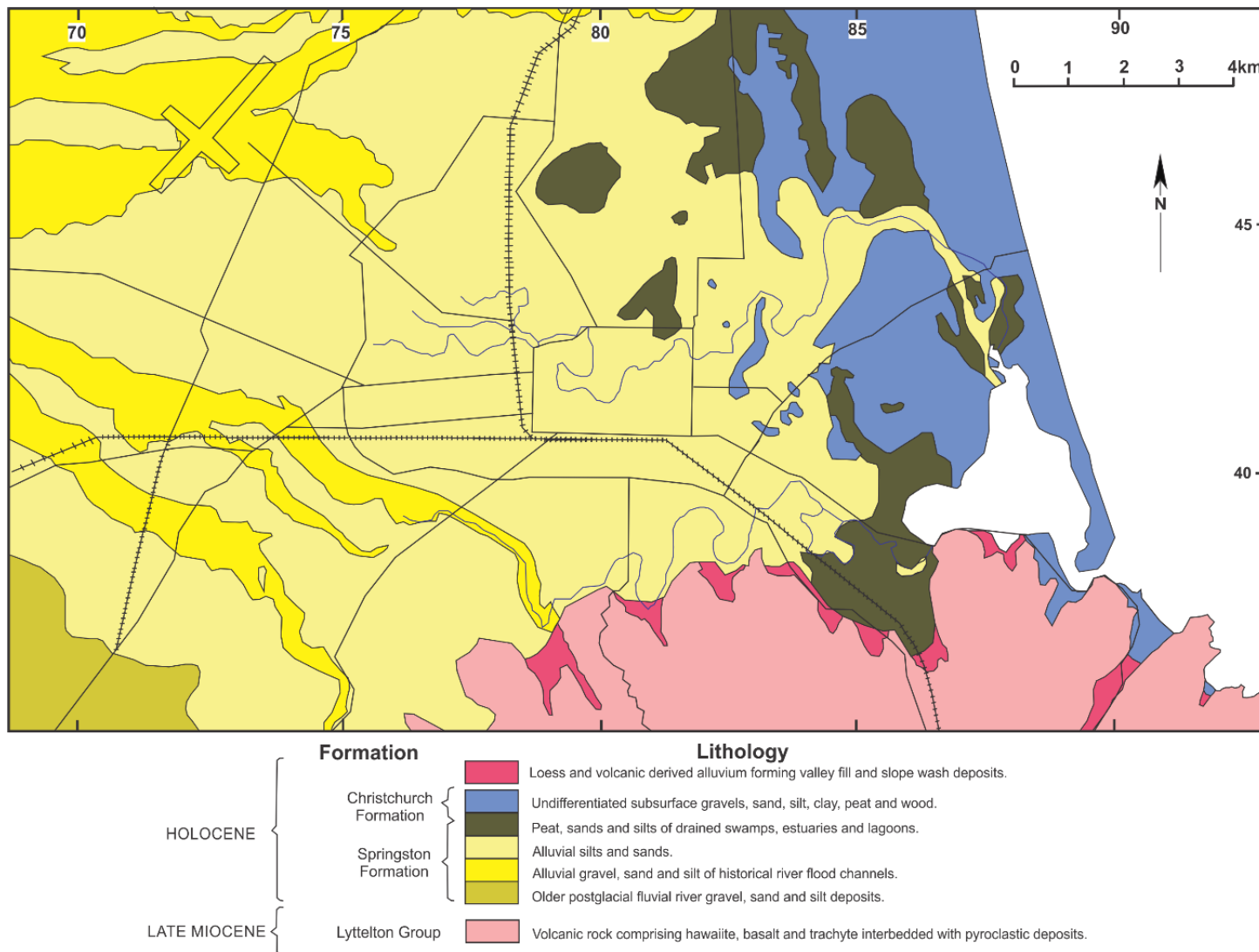


Figure 1.5: Shallow subsurface geology of the Christchurch area. Major road and rail networks are shown as reference. (modified from Brown et al. 1995)

Table 1.1: Stratigraphic column for the Christchurch area (From Brown & Weeber 1992).

International Series			New Zealand Series		Began (Years ago)	Strati- Graphic Column	Local Stratigraphic Units	Regional Geologic Events
Era	Period	Epoch	Epoch	Climatic Stage				
CENOZOIC	QUATERNARY	HOLOCENE	HAWERA	ARANUIAN	14000		Springston Formation	Marine progradation Marine transgression Sea level rise Glacial retreat
				OTIRAN	70000		Burnham Fm. Riccarton Gravel Wind whistle Fm.	Glacial advance Interstadial warming Glacial advance
		LATE PLEISTOCENE		KAIHINUAN	120000		Bromley Formation	Glacial retreat
				WAIMEAN	200000		Woodlands Fm. Linwood Gravel	Glacial advance
				KAROROAN	250000		Heathcote Fm.	Glacial retreat
				WAIMAUNGAN	310000		Hororata Fm. Burwood Gravel	Glacial advance
				SCANDINAVIAN	350000		Shirley Fm.	Glacial retreat
				NEMONAN	380000		Hororata Fm. Wainoni Gravel	Glacial advance
		EARLY PLEISTOCENE	CASTLECLIFFIAN				Unnamed	Glacial retreat /advance
							Unnamed	Glacial retreat /advance
							Unnamed	Glacial retreat /advance
					1200000		Undefined	Early glacial and interglacial sequence
			WANGANUI	NUKUMARUAN			Undefined	Marine and coastal swamp at present day coast
				PORIKAN ROSS	2400000		Sequence Uncertain	Glacial advance Glacial advance
	TERTIARY	PLIOCENE	MANGAPANIAN		7000000		Kowai Formation	Period of uplift, folding, and faulting followed by erosion, creating present landscape of Southern Alps KAIKOURA OROGENY
							Banks Peninsula Volcanics	Volcanic activity forming Banks Peninsula (island). Deposition of sand during period of slow alpine uplift causing eastwards shift of shoreline.
		MIOCENE	TARANAKI				Burnt Hill Group	
			SOUTHLAND					
			PAREORA		26000000			
		OLIGOCENE	LANDON		38000000		Motunau Group	Deposition of transgres- sive marine sequence from Late Cretaceous.
		EOCENE	ARNOLD		54000000		Eyre Group	Deposits formed in a sea which transgressed slowly westward over flat land- scape out on Torlesse Supergroup "greywacke"
			PALEOCENE	DANNIEVIRKE		65000000		Charteris Bay Sandstone Broken River Fm. Mount Somers Volcanics Mt. Misery Volcanics
		MESOZOIC		CRETACEOUS		MATA		
					136000000			Severe folding and faulting of Triassic-Jurassic sedi- ments. RANGITATA OROGENY
JURASSIC					190000000		Torlesse Supergroup	Deposition of sands and clays of enormous thickness throughout most of "New Zealand" region. Occasional episodes of volcanism.
TRIASSIC					225000000			

#### 1.4 Tectonic Setting and Seismicity of the Christchurch area

The present day tectonic structure of South Island New Zealand is dominated by oblique continental convergence, accommodating 39-48mm/yr of movement between the Pacific and Australian tectonic plates (DeMets et al. 2010). The plate boundary is defined throughout the South Island by the ~600km long Alpine Fault, 160km west of Christchurch, which links the oppositely dipping Hikurangi Subduction Trench to the northeast and the Puysegur Trench to the southwest (**Error! Reference source not found.**) (Browne et al. 2012). The transitional region between the two subduction zones sees continent-continent collision between the Chatham Rise and Australian continental plate, which is accommodated by a distributed area of active faults spanning the lower North Island and the South Island, all of which are capable of large earthquakes. The Marlborough Fault Zone (MFZ) represents the South Island continuation of these faults and consists of a series of northwest trending right-lateral ‘transpressional’ faults in the north-east of the South Island. These ultimately link westwards to the Alpine Fault, which accommodates 70-75% of the relative plate movement between the two tectonic plates. The ~30% of remaining plate motion is accommodated by numerous other faults throughout the Southern Alps and Canterbury.

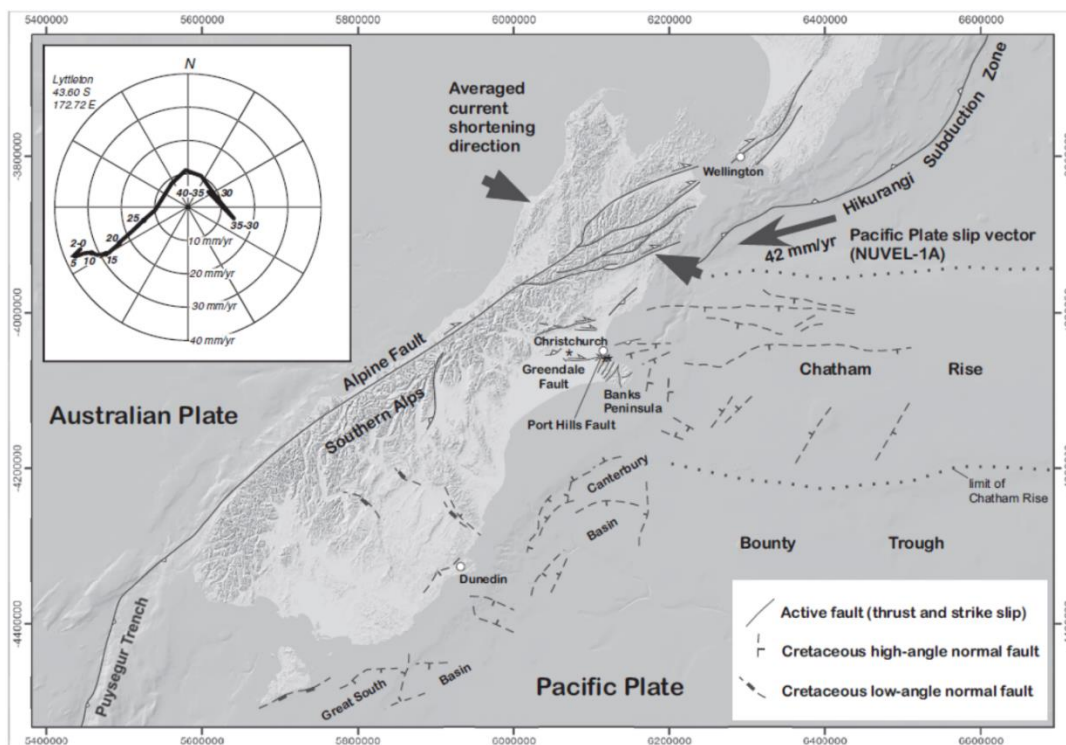


Figure 1.6: The plate tectonic setting for the South Island of New Zealand. Shown are key crustal fault structures, the Hikurangi Plateau and the Chatham Rise (from Ring & Hampton 2012).



There are several mapped structures in the Canterbury region which are either features with surface expression, or those that are ‘hidden’ in the subsurface which pose a known earthquake hazard to Christchurch and the surrounding area (including the Hororata Fault and Anticline, Springbank Fault and the Bobby’s Creek Fault). However, the faults responsible for the recent Darfield and Christchurch earthquakes were not previously recognised (GEER 2011).

### ***1.5 Geology of the Canterbury 2010-2011 Earthquake Sequence (CES)***

The 2010-2011 Canterbury Earthquake Sequence began with the 4th September 2010 Mw7.1 Darfield Earthquake, with an epicentre ~44km west of the Christchurch CBD near the township of Darfield (Gledhill et al. 2011). The earthquake sequence includes three subsequent earthquakes greater than Mw5.9, and over 12,000 aftershocks (Figure 1.7; Table 1.2). The aftershocks propagated eastwards following the initial rupture, and include the notable Mw6.2 22<sup>nd</sup> February 2011 Christchurch Earthquake, the 13<sup>th</sup> June and the 23<sup>rd</sup> December 2011 earthquake events, with seismic activity diminishing in both magnitude and frequency following the last of these (Kaiser et al. 2012). The major earthquakes from each significant event are summarised in Table 1.2.

**Table 1.2: Major earthquake events of the Canterbury Earthquake Sequence. The largest earthquakes of each event are shown.**

<b>Earthquake Event</b>	<b>Focal Depth (km)</b>	<b>PGA<sub>H</sub> (g)</b>	<b>PGA<sub>V</sub> (g)</b>	<b>Comments</b>
4 <sup>th</sup> September 2010 <u>M<sub>w</sub>7.1</u>	10	0.76	1.26	Recorded near Greendale (8km from epicentre)
22 <sup>nd</sup> February 2011 <u>Mw 6.2</u>	5	1.41	2.21	Measured at Heathcote Valley School (2km E of epicentre)
13 <sup>th</sup> June 2011 <u>M<sub>w</sub>6.0</u>	7	2.13	–	Measured in Sumner (epicentre)
23 <sup>rd</sup> December 2011 <u>M<sub>w</sub>6.0</u>	7	0.65	–	Measured at Heathcote Valley School (10km SW of epicentre)

The initial Darfield Earthquake produced a pronounced east-west striking  $29.5 \pm 0.5$  km long rupture surface along the previously unmapped Greendale Fault, ~4km south of the epicentre. The Greendale Fault gross rupture morphology is expressed as three definable segments. The central and eastern segments are at an east-west orientation and are separated by a ~950m northward step-over, while the western segment is oriented towards the NW, separated from the central segment by an ~550m step-over feature.

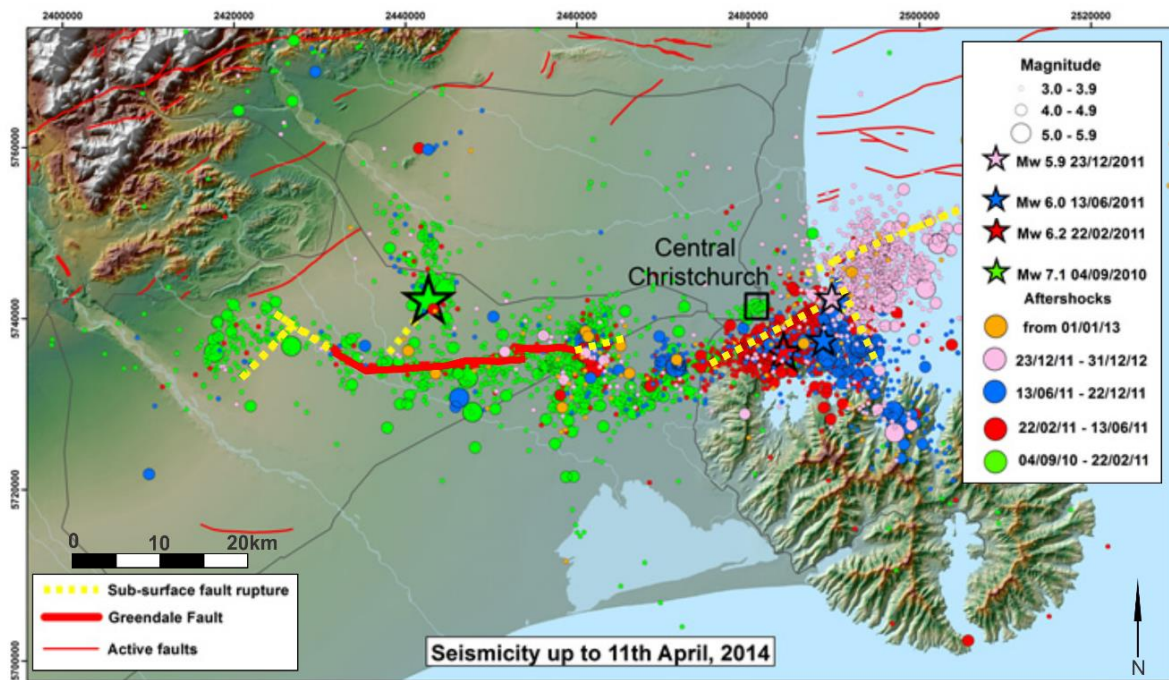


**Figure 1.7: The Mw 7.1 Darfield main shock (green star) and aftershock sequence up to 11th April 2014. The epicentre of the 22<sup>nd</sup> February 2011 Christchurch earthquake (red star), 13<sup>th</sup> June 2011 (blue star) and 23<sup>rd</sup> December 2011 (pink star) are also displayed. Note the general eastward trend of seismic activity during the earthquake sequence. (GNS Science 2015)**

Net right lateral fault displacements of  $\leq 1.5$ m were recorded within 6km of either end of the fault, and  $\geq 4$ m within the central 8km section, with maximum dextral displacement exceeding 5.2m horizontally and 1.5m vertically over typically 50-150m wide deformation surfaces. Offsets were clearly observable along previously linear structures such as roads, fences and hedgerows (Elliott et al. 2012; Quigley et al. 2012). Of the  $29 \pm 0.5$ km of the Canterbury Plains displaced by the Greendale Fault, ~80% ruptures through the Quaternary alluvial deposits known as the Burnham Formation of Last Glacial Maximum age (Table 1.1). According to Hornblow et al. (2014), the absence of a clear fault trace on the upper surface of the Burnham Formation suggest that penultimate surface rupturing from the Greendale Fault predates ~16-

18ka, with the last offset of paleo-channels suggesting movement on the Greendale Fault occurring between ~20-30ka.

The majority of faulting associated with the Canterbury Earthquake Sequence occurred on blind faults, where no surface rupture was observed, including ~5-8km of hidden faulting associated with the Greendale Fault, and the subsequent Port Hills Fault responsible for the subsequent 22<sup>nd</sup> February 2011 Christchurch Earthquake (Figure 1.8) (Li et al. 2014). The  $M_w$  6.2 Christchurch earthquake was the largest aftershock of the Darfield earthquake sequence. Occurring five and a half months after the initial earthquake, the Christchurch earthquake occurred 6km southeast of the Christchurch CBD rupturing the previously unrecognised Port Hills Fault and up to two other blind faults beneath southeast Christchurch, as shown in Figure 1.8(b) from Beavan et al. (2012). The inferred fault ruptures terminate 500-1000m below the surface, suggesting termination in the overlying Miocene Lyttleton volcanic rocks. The Port Hills fault segment propagates adjacent to the base of the Port Hills, with Stephen-Brownie (2012) modelling the fault plane as being located beneath the Hillsborough Valley.

Maximum inferred fault slip for the Port Hills fault during the Christchurch earthquake was 2.5-3m at a depth of ~5-6km, with a combination of reverse and strike-slip movement (Elliott et al. 2012). High vertical and horizontal Peak Ground Accelerations (PGA) were recorded during the Christchurch earthquake, most notable in the Heathcote Valley (4km SE of Hillsborough Valley), where a vertical PGA of 2.21g was recorded, with shaking causing extensive rock fall, land deformation, widespread liquefaction and extensive building damage in Christchurch (Cubrinovski et al. 2011), particularly the eastern suburbs, city centre and hillside areas (Kaiser et al. 2012).

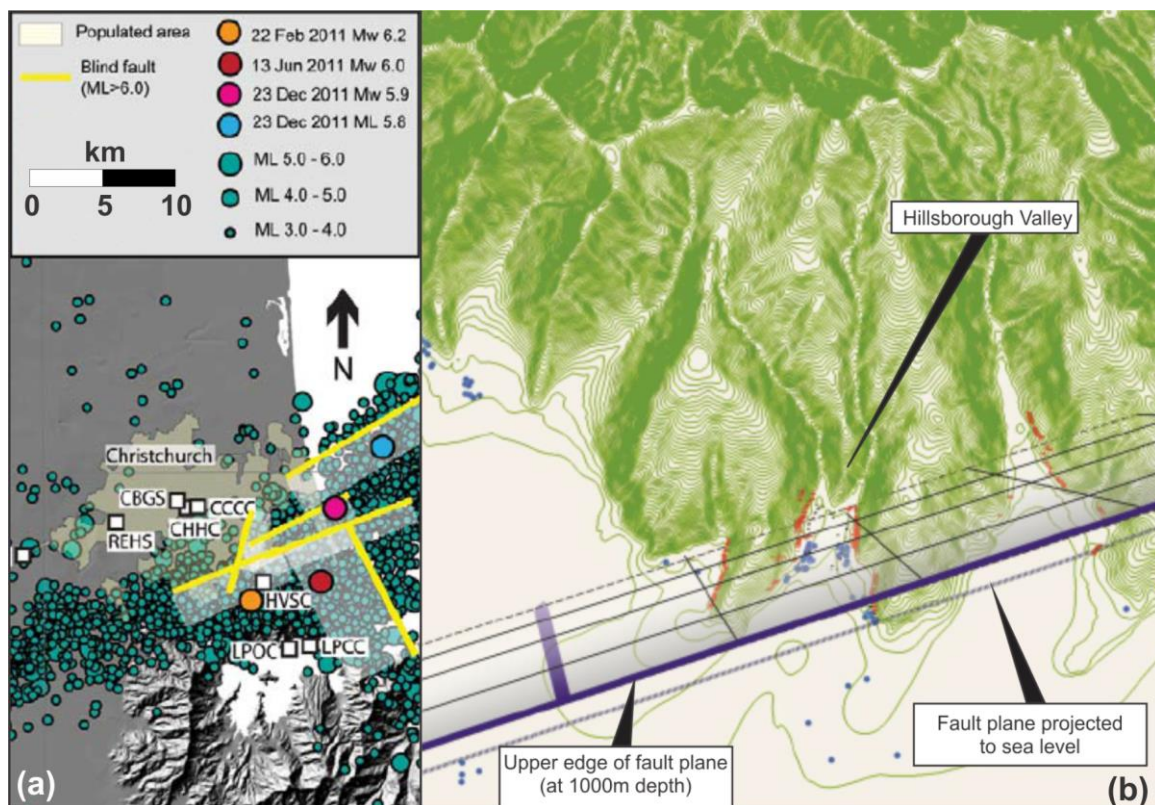


**Figure 1.8(a): Proposed blind fault locations in Christchurch, with various seismic station names and locations displayed (left) (modified from Beavan et al. 2012). Figure 1.8(b): Map of the Hillsborough Valley area showing the location of the upper edge of the Port Hills Fault plane at a depth of 1000m, and projected to sea level. Fissure traces and areas of spring activity are also shown (Right). (after Stephen-Brownie 2012, plotted with data from Kaiser et al. 2012)**

Aftershock activity increased following the Christchurch earthquake across the Canterbury region. On the 13<sup>th</sup> June 2011, a  $M_w$  5.3 earthquake occurred near the suburb of Sumner, followed an hour later by a  $M_w$  6.0 in a similar location. Henceforth referred to as the 13<sup>th</sup> June earthquake event, these earthquakes caused further damage and ground deformation (Bannister & Gledhill 2012). These two earthquakes likely involved an intersecting ENE-striking reverse right-lateral fault and a NW-striking left-lateral fault with maximum rupture slip of ~1m at a depth of 1km. A similar sequence of events occurred on the 23<sup>rd</sup> December 2011, where a  $M_w$  5.8 and  $M_w$  5.9 earthquakes ruptured 1-2 NE-striking, reverse-right-lateral blind faults occurring largely offshore of North and South New Brighton suburbs at a depth of ~2-5km with >1.4m slip.

## 1.6 Hydrogeology of Christchurch

The alluvial gravel outwash fans that comprise the Canterbury Plains extend from the foothills of the Southern Alps to the eastern continental shelf of the South Island, with predominantly alluvial gravels forming the subsurface lithologies through to the western margin of the central Christchurch area. The Christchurch urban area and eastern suburbs are underlain to a depth of 250-300m by complex interlayering of glacial outwash gravels which act as aquifers, and interglacial estuarine muddy sediments acting as aquitards (Figure 1.9). These alternating deposits resulted from sea level fluctuations of up to 150m between the glacial periods of the Quaternary, and continuing until about 14 000 B.P. (Coates 2002). Another consequence of interglacial sea level rise was the reworking of inland gravels. This has resulted in the inland subsurface being heterogeneous with variable well yields and transmissivity of the deposits over relatively short distances. Nevertheless, the alluvial deposits of the Canterbury Plains are highly permeable in comparison to most aquifer types (Stewart 2012).

The fluvial gravel outwash forms a large aquifer system which adjoins the coast of the Canterbury Plains adjacent to Banks Peninsula. The gravels form a series of confined alluvial aquifers underlying much of Christchurch because of a wedge of interglacial sediment, with recharge derived from influent seepage from the bed of the Waimakariri River to the northwest of Christchurch (Figure 1.9) (Brown & Weeber 1994).

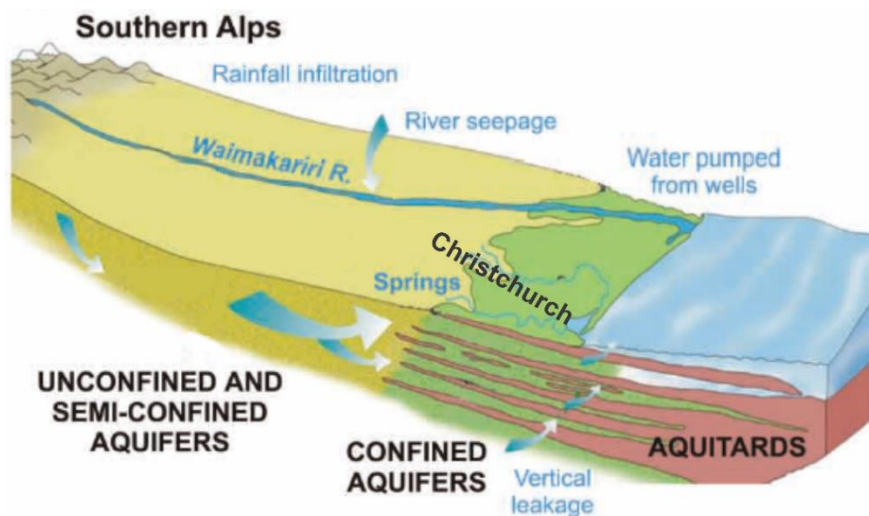


Figure 1.9: Schematic cross-section through the Canterbury Plains highlighting the confined and unconfined/semi-confined aquifers beneath Christchurch. (modified from Cox et al. 2012)

The volcanic rocks of Banks Peninsula form the second major aquifer system in the Christchurch area, consisting of layered lava flows interbedded with ash and debris flows with intersecting dikes and faults to form a large fractured rock mass. Groundwater is transmitted and stored in cooling fractures, cracks and fissures within the volcanic rock which formed due to cooling and faulting. As discussed in Chapter 2, these aquifers are predominantly recharged by deep slow-circulating locally derived Banks Peninsula rainfall (Brown & Weeber 1994).

## ***1.7 Climate***

The climate of Canterbury is influenced by two controlling factors, the region's location within the global atmospheric circulation, and local to regional effects associated with topography or sea surface temperatures (Sturman 2008). New Zealand lies in the geographical region of mid-latitude known as the roaring-forties. This mid-latitude location ensures the country is affected by very changeable weather due to the interactions between warm sub-tropical and cold polar air masses. The interacting air masses result in fluctuating low and high pressure systems. Low pressure systems are associated with more disturbed weather with increased wind speed, precipitation and either warmer or cooler weather, whereas high pressure systems are associated with more stable weather with generally warmer temperatures, less precipitation and less cloudiness. The influence of the Southern Alps 65km to the west of Christchurch on the prevailing winds dominate the climate of Christchurch.

Two key climate zones are present in the Christchurch area (Ryan 1987), these being:

- The Plains, with prevailing winds from the north-east and south-west, low rainfall and a large annual temperature fluctuation, with mean daily high-low variation values of ~10°C.
- Banks Peninsula, with mild winters, warm summers and higher rainfall; that peaks during late autumn-winter.

Historically, Christchurch on average receives less rainfall during the summer months than the wetter winter months, as shown in Figure 1.10. The increased precipitation during autumn-winter months is due to increased south-westerly flow accompanying colder weather, which coincides with increased moisture fluxes such as frosts contributing evaporation over the 30° to 50° S latitudes (Sodemann & Stohl 2009).



The mean annual rainfall in the Christchurch area varies from less than 600mm along the coast to more than 800mm towards the summits of the west Port Hills (as shown in Figure 1.11), and up to 2000mm at higher elevations throughout Banks Peninsula (Christchurch City Council 2010). The predominant rain-bearing winds are of south-west origin, which blow less than 20% of the time, and are in contrast to the prevailing warm north-west winds (McGann 1983).

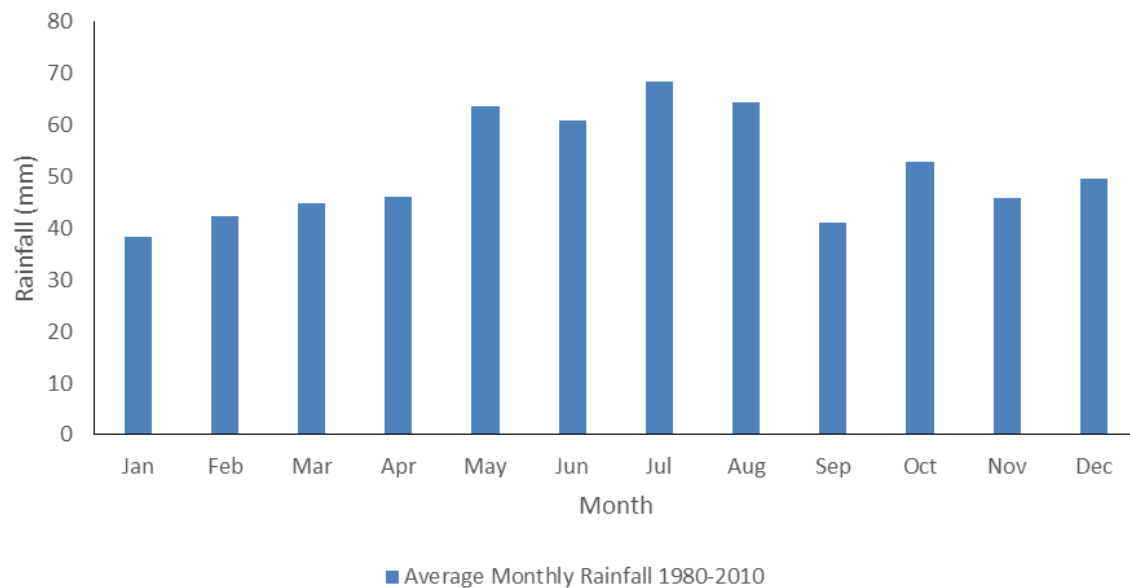


**Figure 1.10: Average monthly rainfall for the Christchurch area during the period 1980-2010 from the Botanical Gardens monitoring station. Total annual rainfall during this period averaged 618mm (NIWA 2015)**

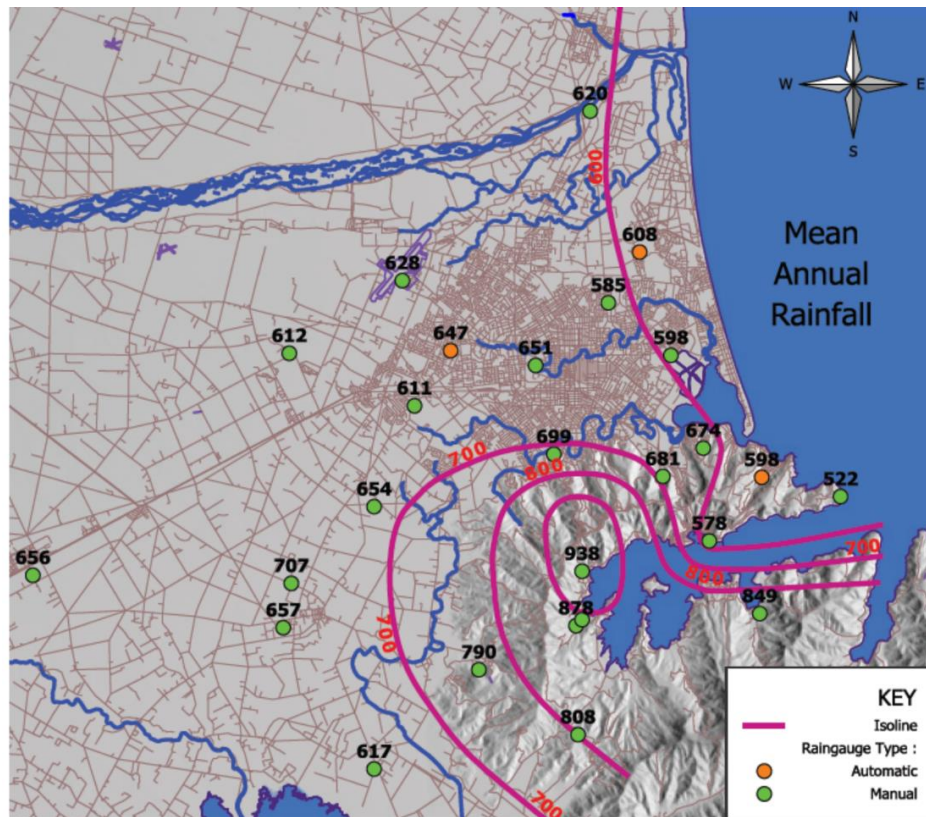


**Figure 1.11: Mean annual rainfall amount (mm) isoline map for the Christchurch area (Christchurch City Council 2010).**

Table 1.3 shows the mean monthly temperatures of Christchurch. Between the years 2004 and 2014, January has been the warmest month with average temperatures of 17.6°C. In contrast the coldest month is July with average daily air temperatures of 6.6°C. The mean annual temperatures on Banks Peninsula are up to 1.4°C warmer than the surrounding plains. The warmer temperatures observed on Banks Peninsula are due to the area being less exposed to the effects of katabatic drainage of cold air from the Plains and its closer proximity to the sea (Jayet 1986).



**Table 1.3: Summary of mean air temperatures measured in Christchurch for the ten year period from 2004-2014. (NIWA 2015)**

Year	Jan	Feb	Mar	Apr	May	Jun	Jul	Aug	Sep	Oct	Nov	Dec	Annual
2004	17.4	15	13.6	10	9.9	7.6	4.4	5.3	8.6	11.7	14.4	13.3	10.9
2005	17.6	18.7	15.4	12	10.1	6.5	7.8	9.4	10.7	11.7	13.9	17.4	12.6
2006	17.3	17.2	13.2	14.4	9.7	5.5	6.5	8.1	11.8	-	13.8	13.8	-
2007	16.3	16.9	16.5	12.3	12.5	6.4	6.8	7.9	10.3	12	14.2	17.2	12.4
2008	18.9	17.9	16.8	13.7	8.3	7.7	7.3	6.7	10.5	11.9	14.5	15.7	12.5
2009	18.6	15.9	14.6	12.7	7.7	6.5	6.2	10	10.8	10.7	14.3	16.1	12
2010	17.1	17.7	16.4	14.2	10.7	7	6.3	9	11.4	12.4	15.8	18.7	13.1
2011	18.1	18.1	16	12.1	11.8	8.5	5.8	6.9	9.4	11.9	13.8	15.7	12.3
2012	16.6	16.1	14	12.4	9.2	5.7	6.6	9.5	11	12.4	12.7	18	12
2013	18.4	17.3	16.6	12.9	9.5	7	8.1	9.8	10.3	13.5	15.2	17.2	13
2014	<u>16.9</u>	<u>17.5</u>	<u>14.7</u>	<u>13.1</u>	<u>10.4</u>	<u>8.4</u>	<u>6.7</u>	<u>7.7</u>	<u>10.1</u>	<u>12.8</u>	<u>14.8</u>	<u>16.2</u>	<u>12.4</u>
Average	17.6	17.1	15.3	12.7	10.0	7.0	6.6	8.2	10.4	12.1	14.3	16.3	12.3

## ***1.8 Hydrogeological Terminology and Previous Work***

### **1.8.1 Spring Terminology**

A ‘spring’ in the context of hydrology and hydrogeology is defined as a concentrated discharge of groundwater appearing at the ground surface as a current of flowing water from an aquifer (Todd & Mays 2005). This definition of a spring applies throughout this thesis. Spring occurrence and classification are discussed in detail in Chapter 2 of this thesis.

### **1.8.2 Previous Work**

Previous studies of the springs and groundwater have been carried out in the Christchurch area. Studies include Master of Science theses, reports by Crown Research Institutions (GNS Science and Environment Canterbury) and post-earthquake investigations carried out by industry organisations (Tonkin and Taylor Pty Ltd. and Aqualinc Research).

Three MSc theses project carried out in the 1980’s focussed on the pre-existing groundwater and spring hydrogeology of Banks Peninsula. These were Sanders (1986), Namjou (1988) and Parker (1989), and are further detailed in Chapter 2 of this thesis.

Sanders (1986) MSc thesis researched the viability of the springs of Akaroa County, Banks Peninsula, to cope with future increases in water demands as the tourist town develops (Figure 1.12). This required studies on both the physical discharge properties and the geochemical qualities of the springs.

Namjou (1988) MSc thesis studied the hydrogeological properties of Kaituna Valley to assess the groundwater resource potential in the area. Geophysical, hydrogeological and hydrogeochemical investigations were carried out in order to establish the quantitative and qualitative properties of the groundwater in the Kaituna Valley

Parker (1989) MSc thesis investigated the properties and resource potential of the Diamond Harbour groundwater system to assess the viability of it being able to sustainably produce the necessary quantity and quality of water to supplement the local water supply. Various geotechnical and hydrogeological investigations were carried out such as sieve analysis, resistivity analysis, geophysical logging, pump testing, isotope analysis, water balance calculations, and spring discharge analysis and piezometric analysis.

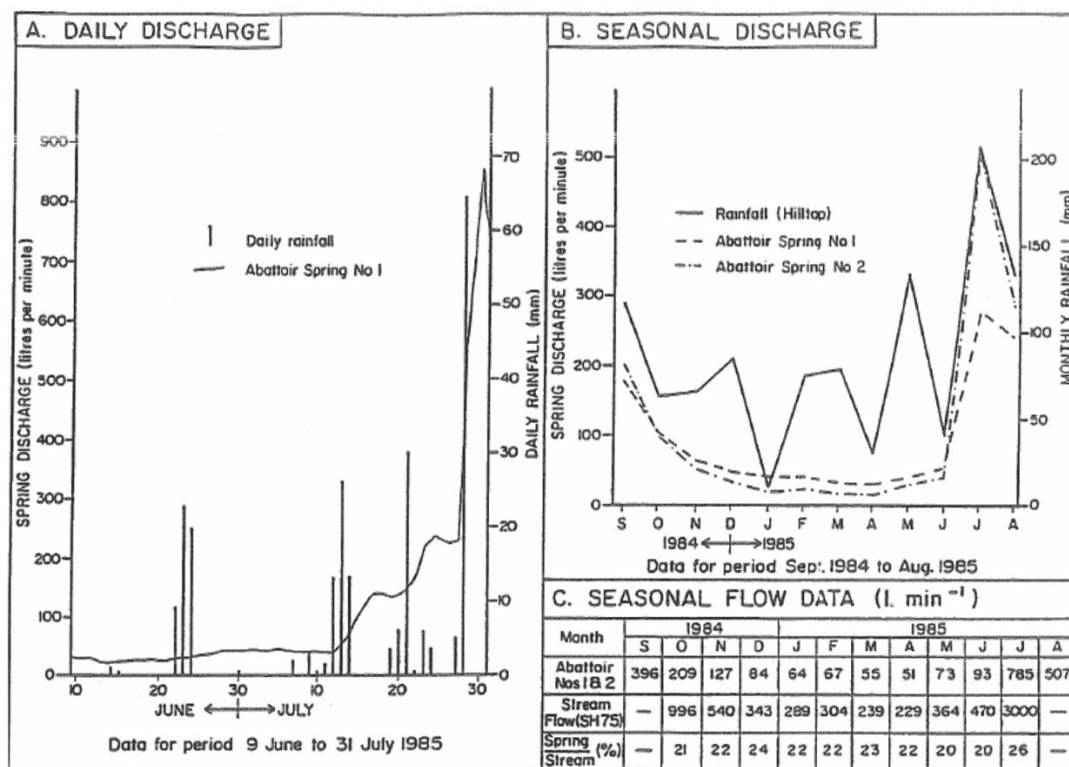


Figure 1.12: Summary of spring discharge against rainfall results for the 'Abattoir' springs in Akaroa County, Banks Peninsula by Sanders (1986).

Brown & Weeber (1994) is a study on the hydrogeological implications of geology at the boundary of Banks Peninsula volcanic rock aquifers and Canterbury Plains fluvial gravel aquifers. Data for the study is provided by well logs, water level and temperature measurements and chemical and Isotope (Tritium and O18) analysis. These findings were then compared to similar results measured over a ~100-year period.

Cox et. al. (2012) studied the hydrological effects of the Mw 7.1 Darfield (Canterbury) earthquake on local and regional hydrology, as follows:

a) Local Effects:

- Near instantaneous co-seismic liquefaction in susceptible areas.
- Changes in piezometric levels, +20m in near fault aquifers, with deeper aquifers rising +80m. But coastal aquifers recorded decreases in Piezometric levels. These changes persisted for up to 12 hours near the epicentre.

b) Regional Effects:

- Groundwater levels and spring discharges were affected from Southland >350km away to >1000km away in Northland.

Data provided by springs and boreholes that were actively monitored before, during and after the moment of the earthquake, showed the various responses of the groundwater levels in Christchurch during earthquake shaking events.

Stephen-Brownie (2012) is an MSc thesis project that was undertaken to provide explanations for the fissuring behaviour observed on the Port Hills of Christchurch following the series of significant earthquakes that occurred near the city in 2010 and 2011, in particular the Christchurch Earthquake of 22 February 2011. Her study is directly associated with the Hillsborough Valley area with extensive literature, laboratory and field studies on the properties and failure mechanisms of loess, a sequence of which underlies the Hillsborough area. A preliminary study was also conducted on the springs and groundwater features of the area by Stephen-Brownie (2012) and Aqualinc Research.

Testing methods included:

- Extensive literature study focusing on the properties and failure mechanism of loess, including international case studies of similar sites/ loess deposits
- Documentation and mapping of fissure features and prevalence
- Separation of Fissure features into three distinct categories.
- Laboratory tests including loess laser sizing analysis and shear box testing
- Documentation of spring occurrence, flow rates and water chemistry

## ***1.9 Thesis Format***

The present thesis comprises seven chapters in total. The layout and contents of each chapter is summarised as follows:

### Chapter Two: Springs and Groundwater Review.

The physical and chemical properties of springs and groundwater are covered in chapter two. Physical aspects such as types and classification of springs, the recharge of groundwater, and groundwater and surface water interactions are discussed. Chapter two also provides a review of the hydrological effects of the Canterbury Earthquake Sequence.

### Chapter Three: Study Area.

Chapter Three describes the physical setting, geology, geomorphology and earthquake effects of the Hillsborough Valley study area. Details and locations of the specific sampling sites are also covered.

### Chapter Four: Methodology.

The site investigation, sampling and testing methodology for this thesis study are described in Chapter four. Site investigation methodology covers the rationale behind choosing the specific monitoring sites, based on location, whether or not the spring features on the site can be sampled and are accessible, and whether or not permission was granted by the tenant or owner of a dwelling for site access. Methodologies include spring discharge, groundwater (piezometric) and rainwater sampling, as well as infield, isotopic and anionic testing methods.

### Chapter Five: Physical Hydrogeology.

The results of the spring discharge, piezometric groundwater level and rainfall collection are analysed and discussed in Chapter five. Seasonal variations in both the spring discharge and groundwater levels were observed following the ten month monitoring period that was carried out. Hydrogeological models are also displayed showing the proposed spring mechanisms and hydrogeological structure of the Hillsborough Valley.

#### Chapter Six: Chemical Hydrogeology.

The chemical composition of the Hillsborough Valley spring and ground water is analysed and discussed in Chapter six. These waters are compared and contrasted against other natural waters that have previously been tested in the greater Christchurch area in an effort to determine the source of the spring waters in the study area. Short-term and long-term anionic and isotopic composition of spring, ground and rain water samples are also plotted, with variations in spring discharge composition observed and discussed.

#### Chapter Seven: Summary and Conclusions.

Chapter seven is a summary of the findings from the previous chapters, with specific conclusions made on the formation and source of the earthquake related springs in the Hillsborough Valley based on hydrogeological characteristics.

## **Chapter 2. Groundwater and Spring Hydrogeology**

### ***2.1 Introduction***

This chapter discusses the physical and chemical aspects of groundwater-associated springs such as the morphology and types of springs, the various sources of spring water, and the recharge of groundwater. In addition, an overview of the occurrence of springs on Banks Peninsula and the greater Christchurch area, especially prior to the Canterbury Earthquake Sequence, is given in this chapter. The observed effects of the Canterbury Earthquake Sequence on the groundwater of Christchurch are also discussed.

### ***2.2 Occurrence and Classification of springs***

Groundwater represents the largest accumulation of fresh water within the reservoirs of the hydrological cycle, accounting for 98% of the liquid water in land masses (Heath 1983; Fetter 2001; Hiscock 2005). Springs represent a concentrated discharge of groundwater from an aquifer at the ground surface.

#### ***2.2.1 Types of springs***

Springs occur at the point where groundwater intersects the land surface, creating a visible flow of water. This discharge of ground water in a specific area is due to the elevation of the aquifer's hydraulic head being higher than that of the surrounding land. Springs flow through openings in the ground surface known as the spring orifice. Springs which issue from consolidated rocks usually have a well-defined orifice, whereas springs issuing from softer and unconsolidated sediments may not, although it is possible for the latter to have a clearly visible orifice (e.g. if issuing from cohesive, clayey substrate). At times, an orifice may not be readily visible, such as where a spring is discharging into the bottom of a deep spring pool, or where the orifice is covered by sediments and rock debris (Kresic 2010).

Where no visible spring orifice is observed, yet an area of land is wet when compared to its surroundings, groundwater discharge is referred to as a seep. These features are also known as *seepage springs*, where diffuse groundwater flow occurs beneath unconsolidated sediments such as sand, gravel and loose soil (Kresic 2010). According to Bryan (1919), where seepages occur on a large scale, the resulting land surface saturation often creates the appropriate conditions for the formation of marshes or swamps.

A *fracture or fissure spring* is a concentrated discharge of water which emerges from features in consolidated rock, such as bedding planes, joints, cleavage and faults. Water in fracture or fissure springs can come from great depth and such springs are often thermal (Todd & Mays 2005).

*Secondary springs* are springs which issue from locations sited away from the primary spring discharge, which is covered by material such as colluvium or other natural debris and is therefore not visible. Secondary spring discharge sites often tend to migrate over time (Kresic 2010).

Most springs ultimately discharge at the land surface due to the force of gravity, the exception being springs that are associated with young volcanism or hydrothermal activity, where discharge is controlled by geothermal gradients and gases. Springs are usually divided into two main groups based on the nature of the hydraulic head in the associated aquifer at the point of discharge:

- **Gravity Springs** form under unconfined conditions, where the groundwater table intersects the land surface. Alternatively, these are also known as *descending springs*.
- **Artesian Springs** are discharged under pressure due to confined conditions in the source aquifer. These are also known as *ascending springs*.

### 2.2.2 Classification of springs

Spring classification has been discussed since Bryan (1919), who observed various spring types such as fissure, depression, contact, barrier, artesian and springs which occur in impervious rock (Hiscock 2005). Todd & Mays (2005) and Kresic (2010) have described these six main classes of springs as follows:

- *Depression Springs* – Occur where the ground surface intersects the groundwater table, such as at topographical low spot (Figure 2.1-A).
- *Contact Springs* – Formed where a permeable water-bearing formation overlies a less permeable formation which intercepts the land surface (Figure 2.1-B).
- *Barrier Springs* – Which form where a lateral contact between an aquifer and a low permeability rock or sediment meet, channelling groundwater towards the ground

surface and allowing spring formation. Lateral barriers include faults (Figure 2.1-C), dykes, and folds. Faults are a major reason for the emergence of springs, especially in fractured rock type aquifers where they often form prominent fractures which become conduits for water flow. They are also common in unconsolidated and semi-consolidated sediments. In any setting, faults may play one or more of the following three roles (Kresic 2010):

- (a) Conduits for groundwater flow
  - (b) Areas of groundwater storage due to increased porosity in the fault zone
  - (c) A barrier to groundwater flow due to a decrease in porosity within the fault zone.
- *Artesian Springs* – Resulting from the release of groundwater under pressure from confined aquifers, and may occur at an outcrop of the aquifer or through an opening in the confining bed known as the artesian vent.
  - *Impervious Rock Springs* – Which occur in tubular channels such as solution weathered sink holes or joints/fractures in impervious rock, and are not hydrologically connected with local groundwater tables.
  - *Tubular or Fracture Springs* – that issue from rounded channels such as lava tubes, solution channels, joints or fractures in impermeable rock that connect with groundwater (Figure 2.1 D and E)

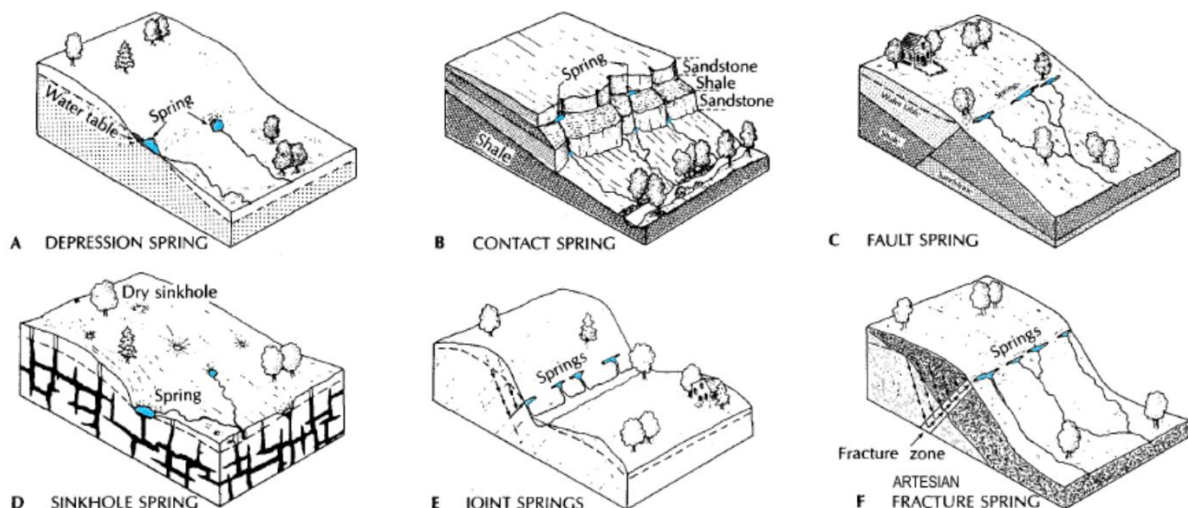


Figure 2.1: Types of gravity springs (modified from Fetter 2001)



Springs can also be classified according to magnitude. Meinzer (1923) categorised springs according to mean discharge as shown in **Table 2.1**. The amount of spring discharge is dependent on the size of the spring's source aquifers catchment area and the rate of recharge to the aquifer. Springs generally fluctuate in their rate of discharge. These fluctuations are due to variations in the rate of recharge, with periods ranging from minutes to years as dependant on geological and hydrological conditions, see Section 2.2.4 below (Todd & Mays 2005).

**Table 2.1: Classification of springs by discharge.**  
(after Meinzer 1923)

<b>Magnitude</b>	<b>Mean discharge</b>
First	>10 m <sup>3</sup> /s
Second	1-10 m <sup>3</sup> /s
Third	0.1-1 m <sup>3</sup> /s
Fourth	10-100 l/s
Fifth	1-10 l/s
Sixth	0.1-1 l/s
Seventh	10-100 ml/s
Eighth	<10 ml/s

Meinzer proposed the following equation to measure variability of discharge due to rate of recharge, expressed as a percentage:

$$V = \frac{Q_{max} - Q_{min}}{Q_{av}} \times 100 (\%) \quad (2.1)$$

Where  $Q_{max}$ ,  $Q_{min}$  and  $Q_{av}$  are the maximum, minimum and average discharge. Based on this equation, a constant spring would have a variability of less than 25 percent and variable springs would have a value of over 100 percent.

### 2.2.3 Thermal and mineral springs

Thermal springs are those which discharge water that has a temperature in excess of the normal local groundwater. Locations of thermal springs in the South Island of New Zealand are shown in Figure 2.2. A warm spring is also defined as having a water temperature higher than the average air temperature at the point of discharge. The spring-water temperature may also be variable over time due to the amount of surficial influence.

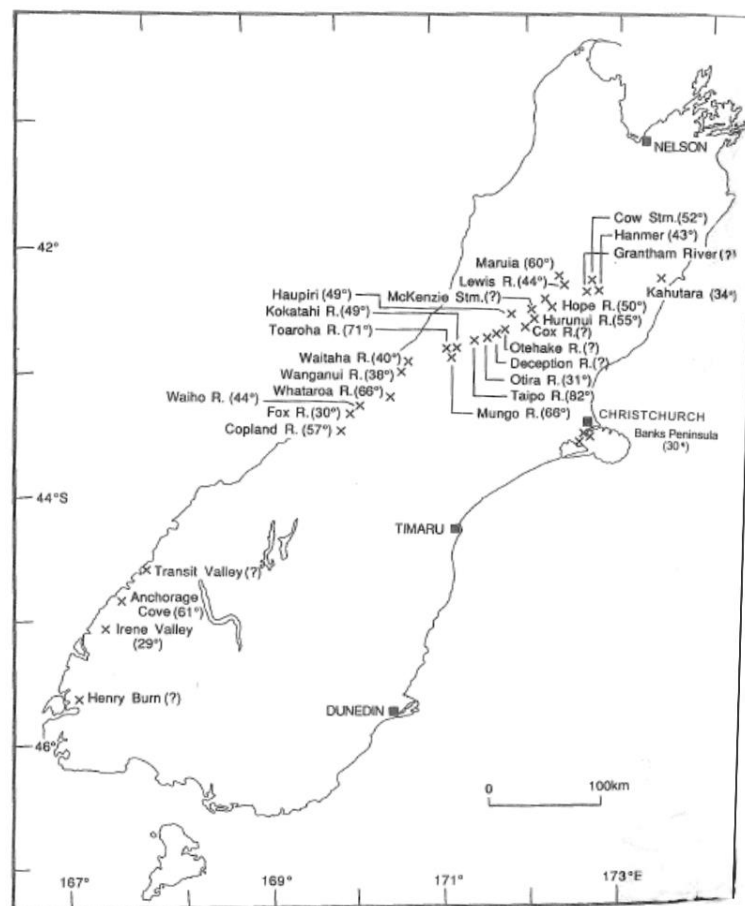


**Figure 2.2: Thermal ground waters from throughout the South Island of New Zealand, with location and maximum temperatures (°C) recorded.**  
(Hunt & Bibby 1992)

### 2.2.4 Source and recharge of springs

Groundwater recharge occurs predominately by rainfall (Trček & Zojer 2010). The primary factors affecting the natural recharge of groundwater according to Trček & Zojer (2010) include:

At the land surface and are influenced by topography and catchment drainage. They suggest that you can expect higher rainfall at higher altitude.

At the soil zone runoff and ponding of water provide additional inputs, while cropping of water and evapotranspiration are outputs.

Of these mechanisms, rainfall infiltration through the soil zone is the most relevant to this study.

### **2.2.5 Groundwater-surface water interactions**

Surface water and groundwater have historically been viewed as separate entities between disciplines, and have been investigated separately in most cases. While chemical, biological and physical properties of surface water differ, a variety of processes occur in the transition zone between the two, leading to transport, degradation, transformation precipitation or sorption of substances. (Kalbus et al. 2006). Essentially, groundwater and surface water are interconnected, and the knowledge of an underlying groundwater system is a basic prerequisite for the study and understanding of ground surface spring features (Trček & Zojer 2010).

However, it is important to note that these hydraulic interactions can be significant, although appear circular. When groundwater infiltration is down, less water is available, whereas when groundwater infiltration increases and there is an excess of water for the aquifer to hold, springs occur.

## **2.3 Earthquakes and Hydrological Response**

The hydrogeological response after a significant earthquake event, such as the Canterbury Earthquake Sequence (CES), according to Manga and Wang (2007); Cox et al (2012) and Rojstaczer and Carolina (1992) results in hydrologic changes, such as temporary excess streamflow, dropping water table, and changes in stream chemistry (Figure 2.3). The mechanism that most likely explains the postseismic hydrologic observations is a permeability increase caused by seismically induced fractures and microfractures. Rojstaczer and Wolf (1992) noted that the fracture networks that control ground-water flow in a region were enhanced by earthquake groundwater flow rates and would initially increase in proportion to permeability increase. They suggest the water table would drop because the groundwater

system would be effectively drained by the increased discharge. Areas of high elevation are most susceptible to water table drops because these areas tend to have the highest water table elevations prior to an earthquake. The increased fractures and microfracture in the ground-water system may also be expected to alter temporarily the chemistry of the groundwater.

The initial surge in discharge and the fracturing would effectively increase the permeability in parts of the aquifers. Rojstaczer and Wolf (1992) state that streamflow would decay rapidly because the hydraulic gradient that drives fluid flow would decay as the water table dropped. The declines in a water-table elevation would be expected to decay at a rate similar to the decay of streamflow.

In contrast, the relatively shallow depth of the water table suggests that permeability increases and watertable drops are only temporary. Rojstaczer and Wolf (1992) propose that permeability in this region is a time dependant parameter, increasing during times of seismicity and decreasing during interseismic periods.

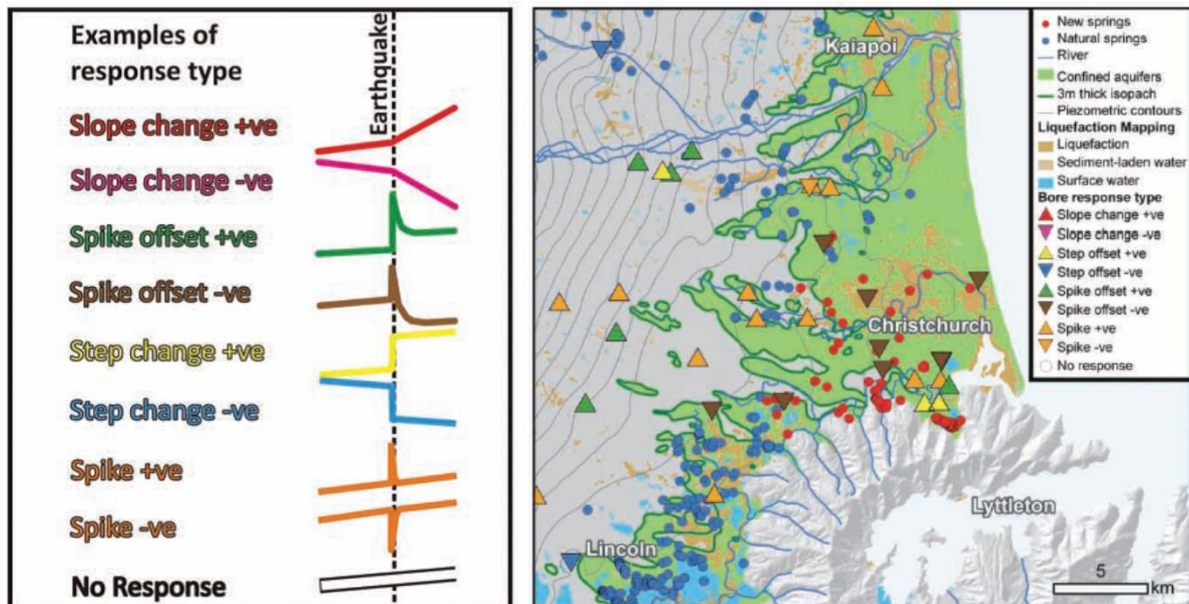


Figure 2.3: Figure showing the type of earthquake related response seen in piezometers proximal to Christchurch during the Darfield earthquake. Also shown are areas of liquefaction and new spring development (modified from Cox et al. 2012)





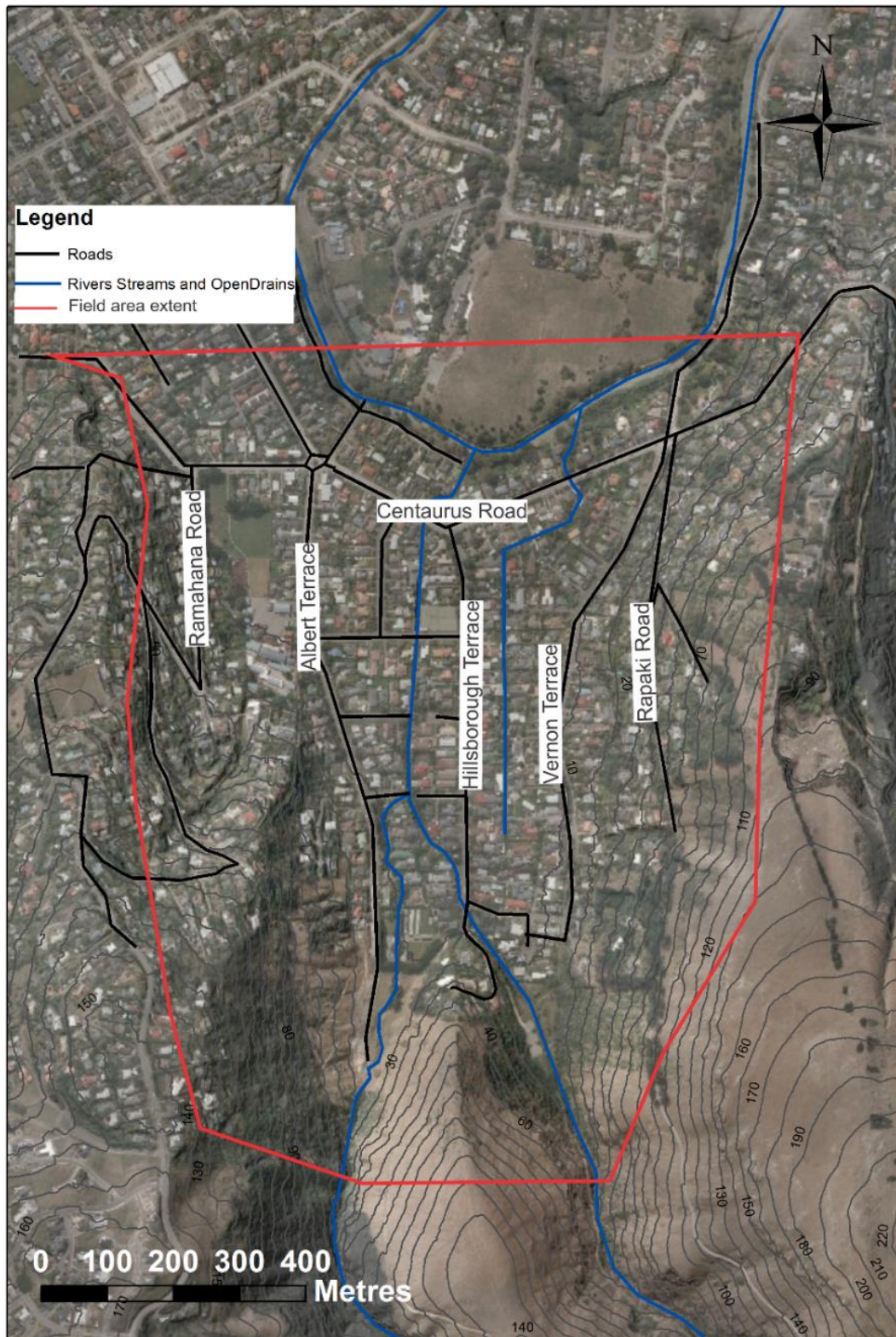


Figure 3.2 Map of the Hillsborough Valley study area with notable roads and waterways shown. Elevation contours are also displayed.

## **3.2 The Geology of Hillsborough Valley**

### **3.2.1 Introduction**

The Hillsborough Valley is located at the boundary between the two key geologies of the Christchurch area; the volcanic rocks and loess deposits of the Port Hills, and the alluvial fan/coastal transgression deposits of the Canterbury Plains. The spring waters of the Christchurch area are intimately related to the composition, morphology and distribution of the associated source aquifers and surficial deposits (Sanders 1986). The geologic units of the Hillsborough Valley which form these aquifer systems, as well as the geomorphology of the valley, influence the source, flow paths and distribution of the recently emergent springs in the valley. The geology of the Hillsborough Valley is documented by Brown et al. (1992) and Forsyth et al. (2008). This has been further explored by field investigations (see Chapter 4) with additional collated geotechnical investigations in the Canterbury Geotechnical Database (CGD) and Environment Canterbury (CERA 2015; Environment Canterbury 2015).

### **3.2.2 The Lyttelton Volcanic Group (11-9.7ma)**

The products of the Lyttelton volcanic complex account for approximately one third of the volume of Miocene volcanics of Banks Peninsula. The Lyttelton Volcanic Group (LVG) rock units form the bedrock for the Port Hills, and consequently, the Hillsborough Valley area. These rocks compose of a mildly alkaline suite of predominantly hawaiite flows, with minor basalt, mugearite and trachyte flows, with numerous dykes, interbedded with clastics, ash and lahar deposits of varying thickness (Brown & Weeber 1992).

#### **Lava Flows**

##### *Morphology*

According to Hampton (2010), lava flows which from Hillsborough Valley are those associated with eruptive packages V and VI, which were erupted from the Governors Bay cone of the Lyttelton volcanic complex. Hawaiian style eruptions have produced thick and extensive hawaiite and mugearites, which typically range in thickness from 0.5m to 10m thick, with rare trachyte flows also occurring in the succession (Sewell 1985). These effusive lavas predominantly range from a'a to blocky type lava flows, with a'a deposits of porphyritic hawaiite outcropping along the flanks and towards the head of the Hillsborough Valley and dipping to the north at an average angle of 8 degrees (Figure 3.3).



**Figure 3.3: Lava flows outcropping along the Rapaki Spur, image is oriented to the east.**

A'a flows are the common lava flow form of the Port Hills suite of alkali volcanic rocks. According to Macdonald (1953), an aa flow is characterised by an exceedingly rough, jagged or spinose top surface and flow front; covered by loose, irregular and rough fragmental material known as flow breccia. Typically, the upper breccia layer grades into a central massive lava, which is only rarely and locally lacking. Underlying this massive layer is a generally thin layer of breccia, which is often less persistent than the upper layer (Figure 3.4). Weathering, overlying regolith deposits and fill obscure the majority of these bedrock features in Hillsborough Valley.

#### *Jointing, pore space and vesicularity*

Jointing in the a'a flows massive centre is highly variable, with both vertically orientated cooling joints and flow orientated platy joints seen in outcrops. Vertical joints are irregular, and spaced between 100- 1500mm apart. Joint apertures are also highly variable, ranging from 0.5 – 5mm. The vesicularity of is generally around 30 percent, although some flows may have up to 50 percent vesicularity. The vesicles are generally irregular and stretched in the direction of flow.



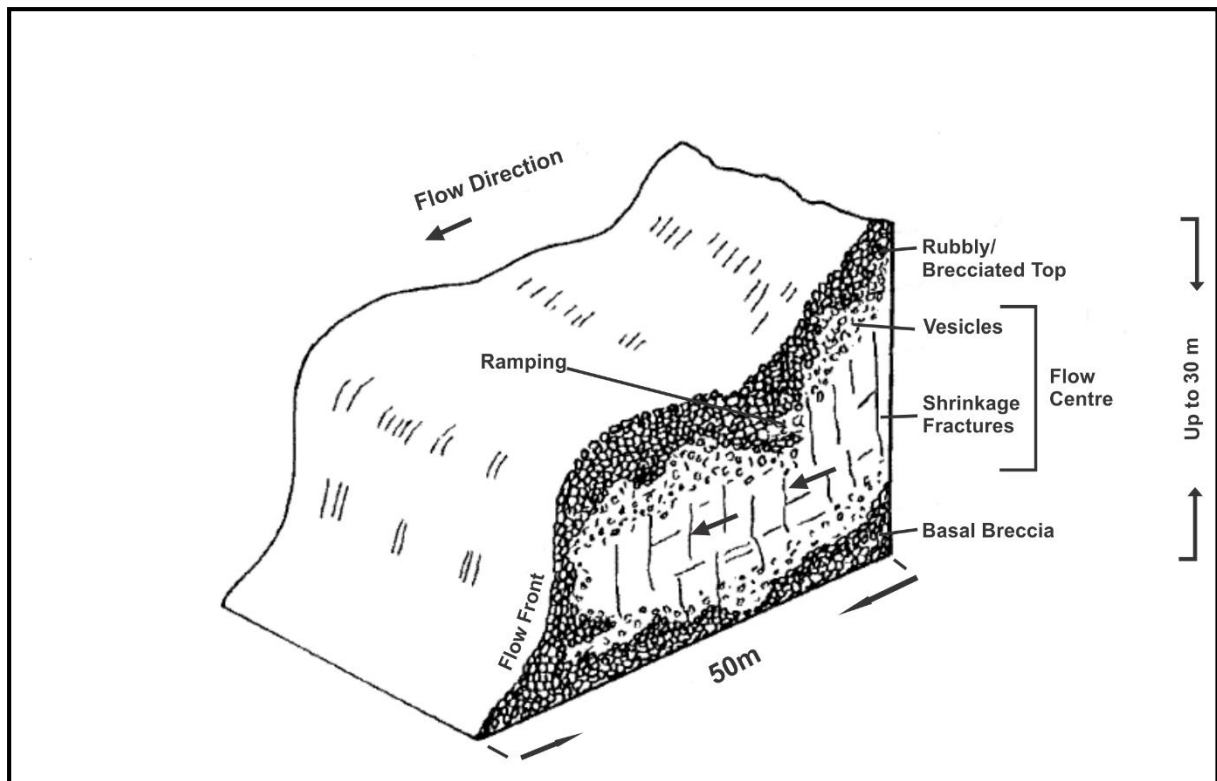


Figure 3.4: Typical aa lava flow morphology of Banks Peninsula. Note the rubbly layers, breccia and cooling shrinkage fractures (after Namjou 1988).



Figure 3.5: Hawaiite flow exposed at the entrance to the Mt. Vernon gorge, Note the irregular and platy cooling joints and fractures.

### *Composition*

Hawaiite is an intermediate rock composed mostly of andesine (plagioclase feldspar with between 50 and 70 percent albite) and pyroxene, usually with some olivine (Figure 3.5). The hawaiite geochemically grades between alkali basalt (rich in alkali feldspar and contains augite), and mugearite (resembles hawaiite but the feldspars are oligoclase plagioclase which is 70 to 90 percent albite). Mugearite geochemically grades into trachyte, composed predominantly of potassium feldspar with minor amounts of opaque minerals (Macdonald et al. 1983). The geochemical composition of these rock types are shown in *Error! Reference source not found.*.

**Table 3.1: Average chemical composition of Hillsborough Valley rock types (in weight percent). (modified from Macdonald et al. 1983)**

	Alkalic basalt	Hawaiite	Mugearite	Trachyte
SiO <sub>2</sub>	46.5	48.6	51.9	61.7
TiO <sub>2</sub>	3	3.2	2.6	0.5
Al <sub>2</sub> O <sub>3</sub>	14.6	16.5	16.6	18
Fe <sub>2</sub> O <sub>3</sub>	3.3	4.2	4.2	3.3
FeO	9.1	7.4	6.2	1.5
MnO	0.1	0.2	0.2	0.2
MgO	8.2	4.7	3.6	0.4
CaO	10.3	7.8	6.3	1.2
Na <sub>2</sub> O <sub>2</sub>	2.9	4.4	5.2	7.4
K <sub>2</sub> O	0.8	1.6	2	4.2
P <sub>2</sub> O <sub>5</sub>	0.4	0.7	0.9	0.2

### *Epiclastic Deposits*

Interbedded epiclastic deposits (volcanic air-fall products including tephra, scoria, ash, blocks and bombs) outcrop along the Rapaki Track, from near the start of the track at 100m above sea level to 1.3km along the track at 190m.a.s.l. The epiclastics overlie weathered basaltic lava flows, and consist of poorly sorted, matrix to clast supported conglomerate, with clasts ranging from lapilli to boulder sized (up to 65cm). The clasts consist of dark grey basalt, grey porphyritic basalt and light cream-green trachyte. The matrix is red-brown, moderately indurated and ranges from fine to coarse lapilli.

### 3.2.3 Regolith Material types and their Distribution

Widespread aeolian loess deposits stratigraphically overlie the Banks Peninsula volcanics, with loess and loess-derived regoliths draping the Lyttelton Volcanics in the Hillsborough Valley. To classify the surficial deposits in the Hillsborough Valley, and to remain consistent with other studies of springs and ground water on Banks Peninsula (Sanders 1986; Namjou 1988; Parker 1989), the classifications made by Bell & Trangmar (1987) are adopted in this study, with idealised distribution and dominant erosional processes illustrated in Figure 3.6.

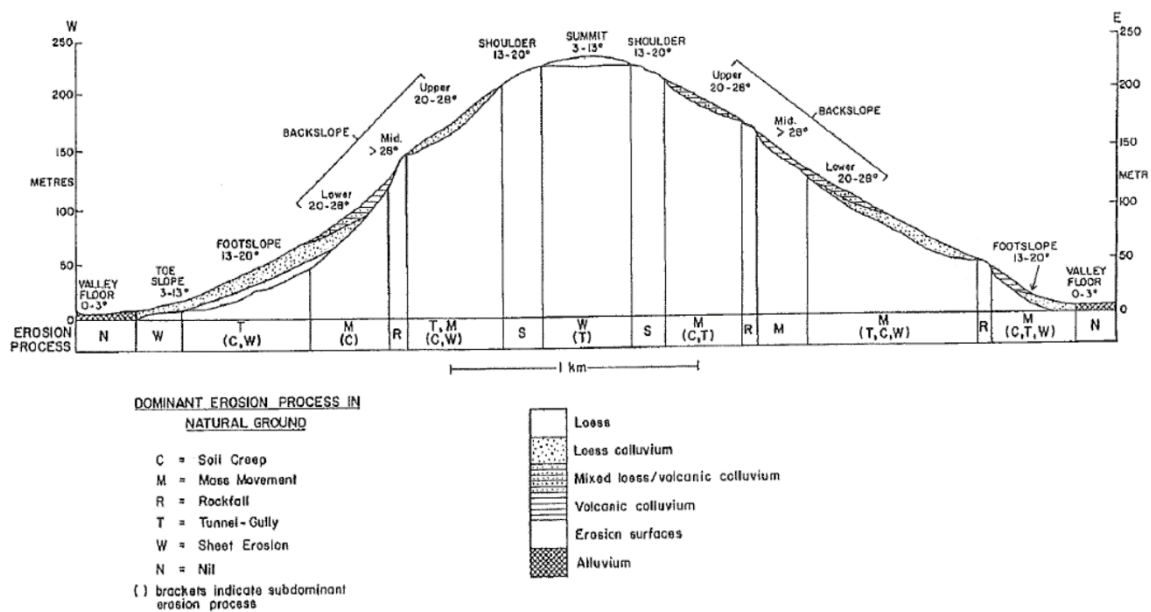


**Figure 3.6: Generalised cross-section of a Port Hills ridge, showing the relationships between landforms, slope, regolith and erosion. (Bell & Trangmar 1987)**

According to Bell & Trangmar (1987), there are five predominant regolith types on the Port Hills, and elsewhere throughout Banks Peninsula, listed as follows:

1. In-Situ (primary airfall) loess.
2. Loess-colluvium
3. Mixed deposits of loess and volcanic-derived colluvium.
4. Volcanic Colluvium
5. Residual regoliths.

## **In-Situ (primary airfall) Loess**

### *Composition*

Two types of Loess deposits are found on Banks Peninsula; the calcareous and coarser grained Birdlings Flat Loess, and the non-calcareous finer grained Barry's Bay Loess. Of the two loess types on Banks Peninsula, only the Birdlings Flat variety occurs in the Hillsborough Valley area. Along the northern margin of the Port Hills, such as the Worsley track (5.1km SE of the study area), the loess is over 12m thick with only minor textural variations; from fine sand to fine sandy loam throughout the sequence. This suggests that the loess was deposited in one continuous period, due to close proximity of the source area, the Waimakariri River flood plain (Griffiths 1973).

In-situ loess facies are composed predominately of quartzofeldspathic minerals with minor accessory minerals (including epidote, tourmaline and zircon), and secondary clay minerals (e.g. illites and vermiculites). The Birdlings Flat Loess also contains various salts, including calcium sulphate, calcium chloride, calcium carbonate, sodium sulphate and sodium chloride. The calcium carbonate is first to precipitate out and is found at higher elevations (up to 270m), while the other salts are only found at lower elevations (Griffiths 1973).

### *Distribution*

In-situ loess of up to 3m mantles the bedrock summits of the Hillsborough Valley along both the eastern and western ridge tops. These summit loess deposits are massive, with little amounts of texture, and overlie the basaltic bedrock of the valley ridges. Buried in-situ loess of up to 8.4m thickness is observed in the BH-VRN-08 borehole drilled by Tonkin & Taylor on the Rapaki Spur slope in Hillsborough Valley, at a depth of 1.5m below mean sea level (see appendix I.). These low altitude loess deposits overlie loess and volcanic colluvium, indicating active erosion occurring prior to and during loess deposition. According to Griffiths (1973), the hillside loess deposits thin with increasing altitude. As a result of this, no in-situ loess deposits are observed in boreholes or at the surface along the valley slopes (backslope).

## **Loess colluvium**

### *Composition*

Loess colluvium forms due to the erosional downslope transportation of previously in-situ loessial deposits. It consists of clay-sand sized reworked loess material, with the addition of up to 10% hillside derived angular volcanic clasts, which vary from sand sized through to ~200mm boulders.

### *Distribution*

Loess colluvium occurs downslope of in-situ loessial deposits, generally at the toe slopes, footslopes and backslopes of ridges. In the Hillsborough Valley, loess colluvium deposits overlie various bedrock, in-situ loess, mixed and volcanic colluvium and alluvium. The colluvial deposits are interbedded with alluvium at the toe slope - valley floor interface.

## **Mixed loess and volcanic colluvium**

### *Composition*

Mixed loess and volcanic (mixed) colluvium deposits are comprised of a mixture of loess colluvium with further inclusion of volcanic material, sourced from upslope weathering of outcropping bedrock. The ratio of loess colluvium to volcanic colluvium in these deposits ranges from 10% to 90%. This results in a highly variable morphology, with the percentage of volcanic colluvium decreasing with distance from the source outcrop of bedrock. The grain size of the volcanics fragments ranges from sand sized particles, through to 2m+ thick boulders which are encountered in multiple borehole investigations in the study area.

### *Distribution*

In Hillsborough Valley, mixed colluvium occurs at the surface on backslopes and upper footslopes, below volcanic rock outcrops. Mixed colluvium is also seen in borehole logs at various depth, underlying loess colluvium and alluvium and overlying in-situ loess, alluvium and bedrock. Measured thicknesses of mixed colluvium range from 1.5 to 16 metres. The deposits are predominately observed on the eastern ridge slope in Hillsborough Valley, with no mixed colluvium observed in boreholes on the western slopes of the valley's Huntsbury Spur ridge slope.

## **Volcanic Colluvium**

### *Composition*

Volcanic colluvium is described as deposits which consist of slightly-moderately weathered volcanic rock fragments set within a matrix of silty clay to clayey loam. This matrix is composed of highly weathered fine-grained material weathered from the volcanic bedrock, with the addition of a small amount (<10%) of loess-colluvium. Clast size of the fragments ranges from fine to coarse gravel, with occasional boulders interbedded.

### *Distribution*

Volcanic colluvium is generally found underlying bedrock outcrops, on moderately steep mid-backslopes. Due to the high rates of erosion at these sites, the volcanic colluvium is highly variable in thickness, typically ranging up to 1.2m thick, and thinning away from bedrock outcrops. Thin, up to 0.5m thick deposits, are observed in boreholes along the toe slopes, overlying mixed-colluvium and bedrock. Volcanic colluvium is displayed as mixed colluvium in the geology map and cross sections for ease of presentation.

## **Residual Regoliths**

Residual regoliths are deposits which have formed from the in-situ weathering of volcanic bedrock outcrops. In areas where residual regoliths occur, with the exception of local pockets between outcrops, the loess cover has been stripped from the hill slopes, initially probably due to freeze-thaw induced downslope movement during the Pleistocene, and later due to post-Pleistocene wind and rill sheet erosion (Griffiths 1973).

### *Composition*

The residual regolith deposits are made up of 5 to 20% sub angular, slightly to highly weathered gravels and stones, which are set in a matrix of reddish-brown silty clay loam or clay loam. The gravels and stones become more numerous and weathered with depth.

### *Distribution*

Deposits of residual regolith occur on erosional surfaces at the summits and shoulders of ridges, usually at altitudes greater than 100 metres. The deposits are usually less than 0.9m thick, merging through a thin (<0.3m) saprolite zone in to the underlying volcanics.

## **Alluvium**

Deposits classified as alluvium in the Hillsborough Valley are comprised of reworked loess and colluvial deposits which have transported by alluvial processes, such as stream flow and slope erosion.

### *Composition*

Alluvial deposits in the Hillsborough Valley are composed of undifferentiated sands, silts, gravels, clays and organic matter. These are derived from heavily reworked loess, volcanics and possible marine deposition due to

### *Distribution*

Alluvium is the predominant sediment in the valley floor area of Hillsborough Valley. Borehole Data shows it underlies the peat deposits in the centre of the valley, and is interbedded with loess and loess colluvium deposits towards the toe slopes of ridges. The exact depth of the alluvial deposits in the valley is unclear, due to lack of geotechnical data, however the boreholes at the toe margins in the valley indicate a minimum depth of 50 metres+, with the depth in the centre of the valley inferred to be deeper than this due to the slope of the bedrock at the valley margins.

## **Peat**

Surface peat deposits of varying extent occur in the Christchurch area, associated with swamps and marshes of both the Christchurch and Springston formation (Brown & Weeber 1992). Peat deposits have formed in the Hillsborough Valley area due to the presence of swampy land as highlighted in the Black Maps of 1856 (**Error! Reference source not found.**).

### *Composition*

Peat is composed of predominantly organic material derived from plants that accumulate in ecosystems where there is an excess of local plant productivity over the respiratory rate of organisms (Moore 1989). Peat deposits in the study area are organic rich, with some silt occurring. The peat deposits are massive, fibrous and most commonly saturated.

### *Distribution.*

Surface peat deposits of varying extent occur in the Christchurch area, associated with swamps and marshes of both the Christchurch and Springston formation (Brown & Weeber 1992). Peat

and organic deposits are observed by geotechnical investigations throughout the Hillsborough Valley floor. This deposit is variable in both extent and thickness, with the thickest deposits of over 4m recorded adjacent to the central flanks of the valley slopes, with the deposit thinning towards the outer margins. The peat grades laterally into trace organics within the alluvium and loess colluvium deposits in the valley floor, and overlies organic silts. Peat may also affect the hydrology of the Valley (Figure 3.7) (Lowry et al. 2009)

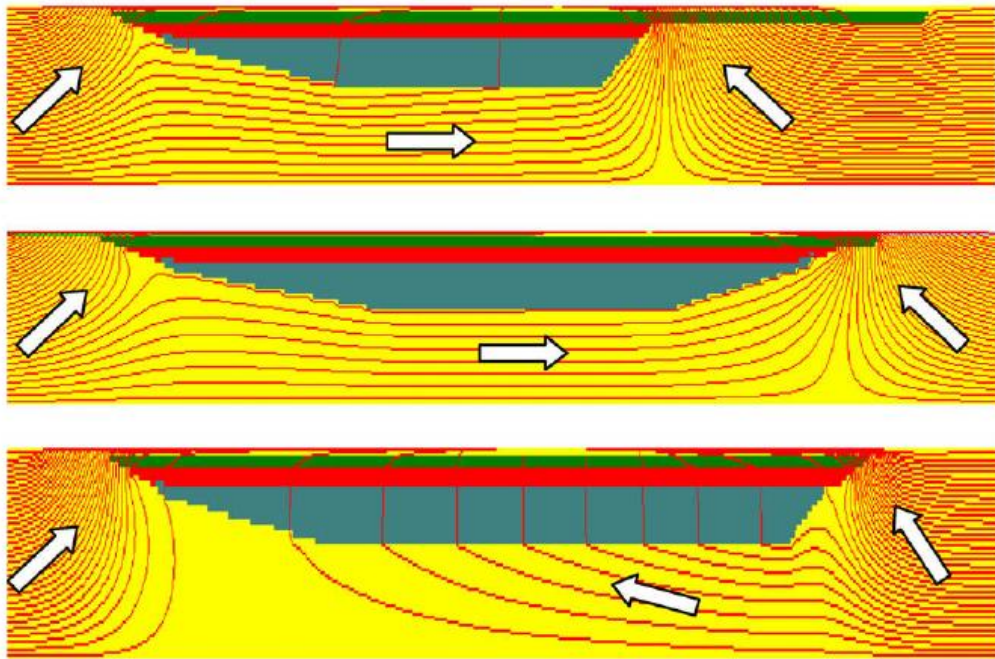


**Figure 3.7: The effects of a shallow subsurface peat deposit. Note the groundwater flow paths. (Lowry et al. 2009)**

The distribution of the various geological units is displayed in Figure 3.8. The peat deposits are seen overlying most of the valley floor area. The contact with the Springston Formation of Christchurch is also highlighted. As discussed by Brown & Weeber (1994), This represents the approximate location of the boundary between the Christchurch Artesian Aquifer System and the Banks Peninsula Volcanic Aquifers. This has implications for the groundwater of Hillsborough. It is also possible that Springston and Christchurch formation deposits are interbedded at depth in the valley alluvium (Brown and Weeber 1992). The depth to bedrock in the centre of the valley is unclear, borehole data only extends to ~16m in the area.



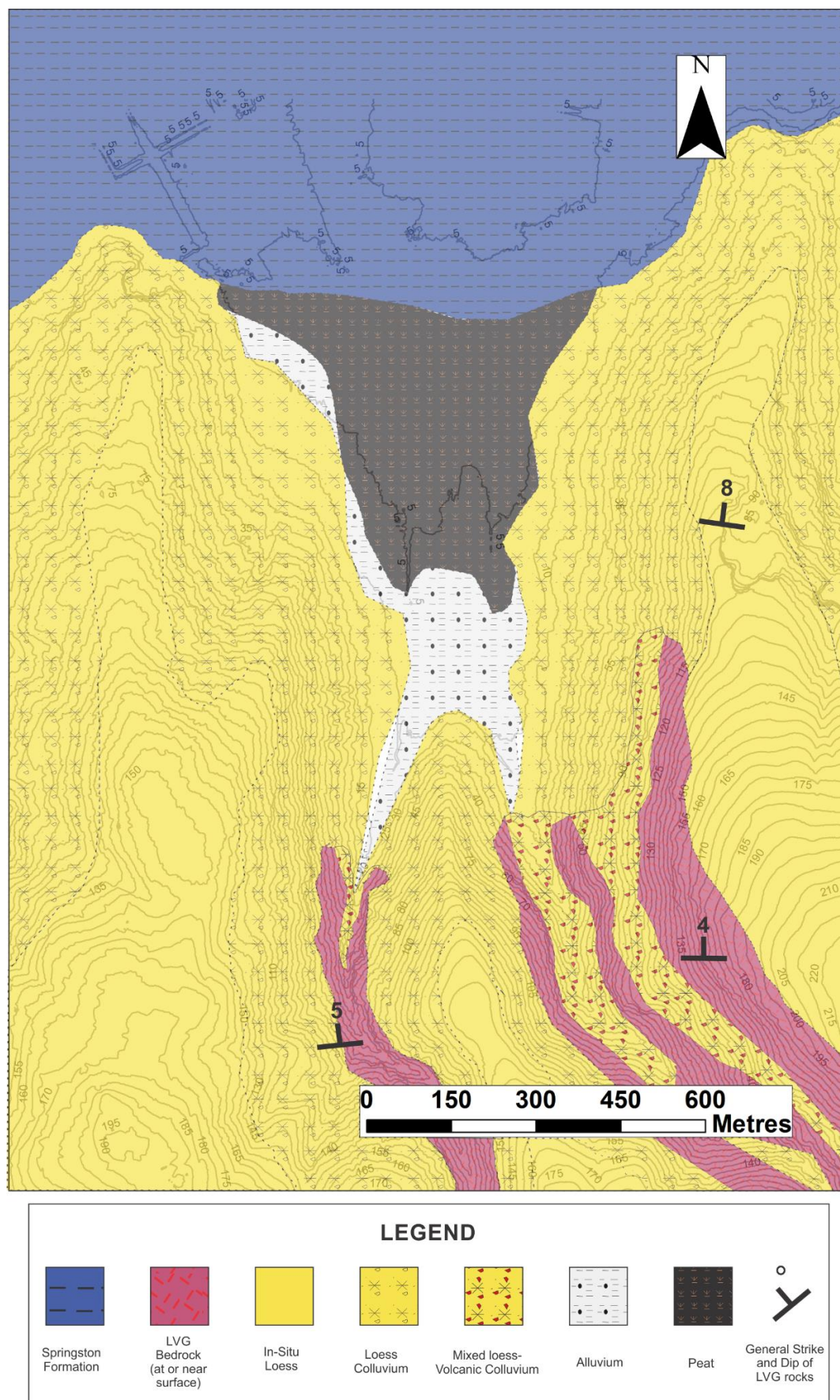


**Figure 3.8: Geological map of the Hillsborough Valley. Note the contact with the Springston Formation at the Valley entrance and the extensive peat deposits in the Valley floor.**

### **3.3 *Geomorphology***

The Hillsborough valleys morphology is defined by the prominent lava flow sequences of the Lyttelton Volcanic Group, which form the Huntsbury Spur (western valley ridge), the Rapaki Spur (eastern valley ridge) and the Vernon Spur (central ridge in valley head). The basin like structure produced by these ridges has allowed the thick deposition of alluvial deposits in what is now the valley floor.

#### **3.3.1 Erosional Geomorphology**

Rainfall and weathering have shaped the present day morphology of the Hillsborough Valley (Hampton 2010). Streams which drain into the valley from Mount Vernon (at the head of the valley) have eroded prominent gully features, especially on the western margin the Vernon Spur, and are likely linked to the process of alluvial deposition in the valley floor.

Six key forms of erosional regolith are identified by Bell and Trangmar (1987):

- 1) Rock and debris falls
- 2) Soil creeps
- 3) Slide-avalanche-flow mass deposits
- 4) Sheet and rill erosion
- 5) Tunnel gully erosion
- 6) Wind erosion

These may all also allow for further loess deposition from the slopes to the valley floor.

Tunnel gullying in loess may also form pipe-like structures allowing the transportation of water through the subsurface as discussed by (Bates 1979).

Anthropogenic geomorphology in the Hillsborough Valley includes the infilling of the marshy land with loess-like fill (Figure 3.9), residential development including the laying of service pipes such as water supply, wastewater and storm water (Appendix VI) and stream concreting.



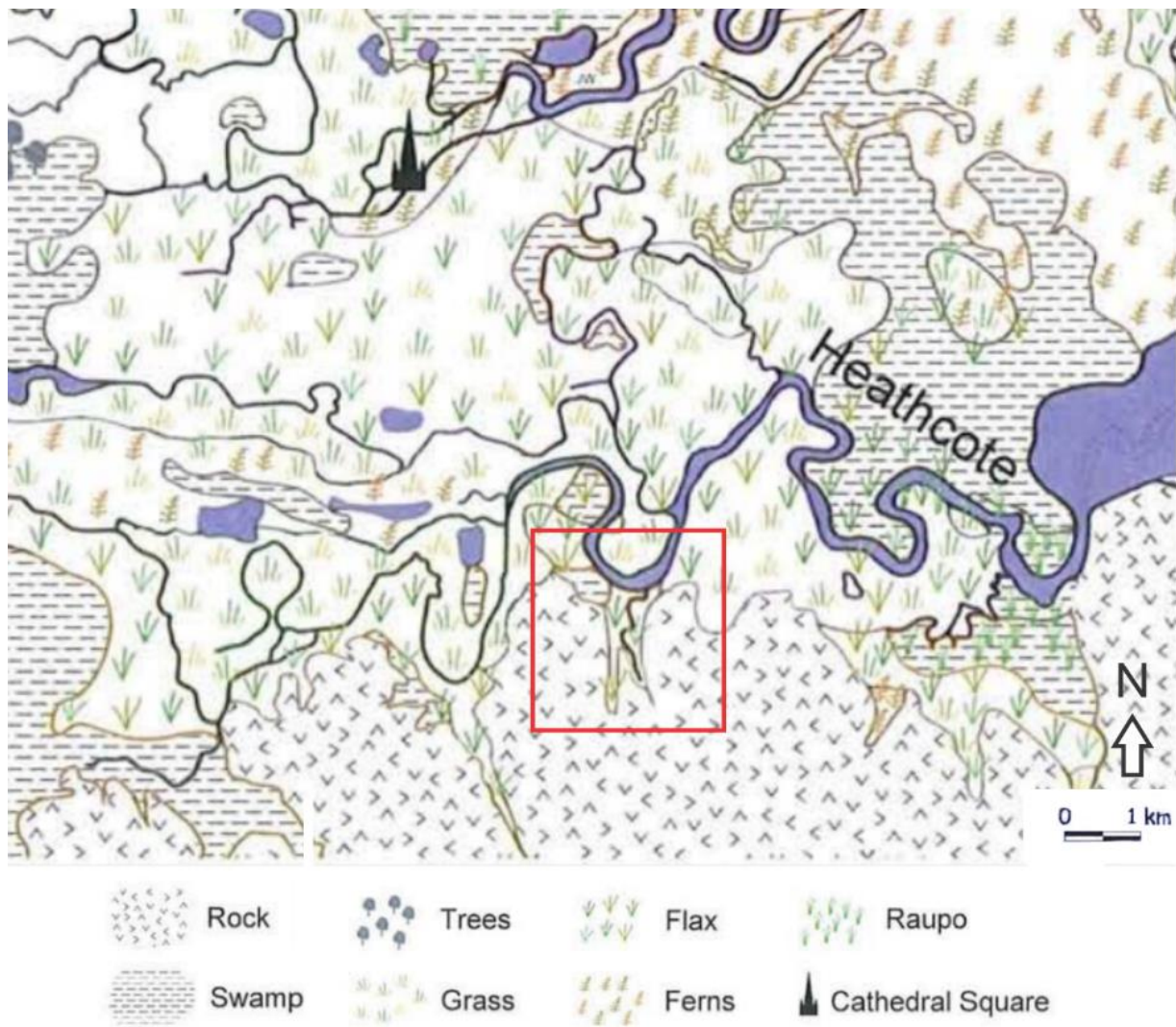


**Figure 3.9: Waterways, wetlands and vegetation cover as detailed in the 1856 Black Maps of the Christchurch area. The Hillsborough Valley study area is highlighted in the red box, note the presence of marshy land at the mouth of the valley (Christchurch City Council 2010).**

### **3.3.2 Earthquake Geomorphology**

Earthquake shaking has produced a series of earthquake related geomorphological features. As discussed by GNS Science (2010) and Stephen-Brownie (2012), these include extension tension cracks (fissuring), compressional features and resulting spring formation.

#### **Fissuring**

Fissure cracks are related to extensional movement of the footslopes. They traverse the Hillsborough Valley lying at approximately 20m high upslope of the valley floor. Of note is the fissure trace which runs along the north-western margin of the valley. This occurs on the valley floor area near Centaurus Road (Figure 3.10)

#### **Compressional Features**

Compressional features are related to the movement of loess downslope of fissures and caused by displacement upslope. Compressional features often form mounds and cracks. They can be found in loess where the slope angle decreases to the toe slope (Figure 3.10). Some compressional features are also found in the centre of the Hillsborough Valley. All compressional features are aligned parallel to the topography.

#### **Spring Formation**

Springs have formed in areas of compression in the valley up to 24 hours after the Darfield earthquake and have exaggerated with subsequent earthquakes. They occur in the toe-slope position of the valley, and not mid-way.

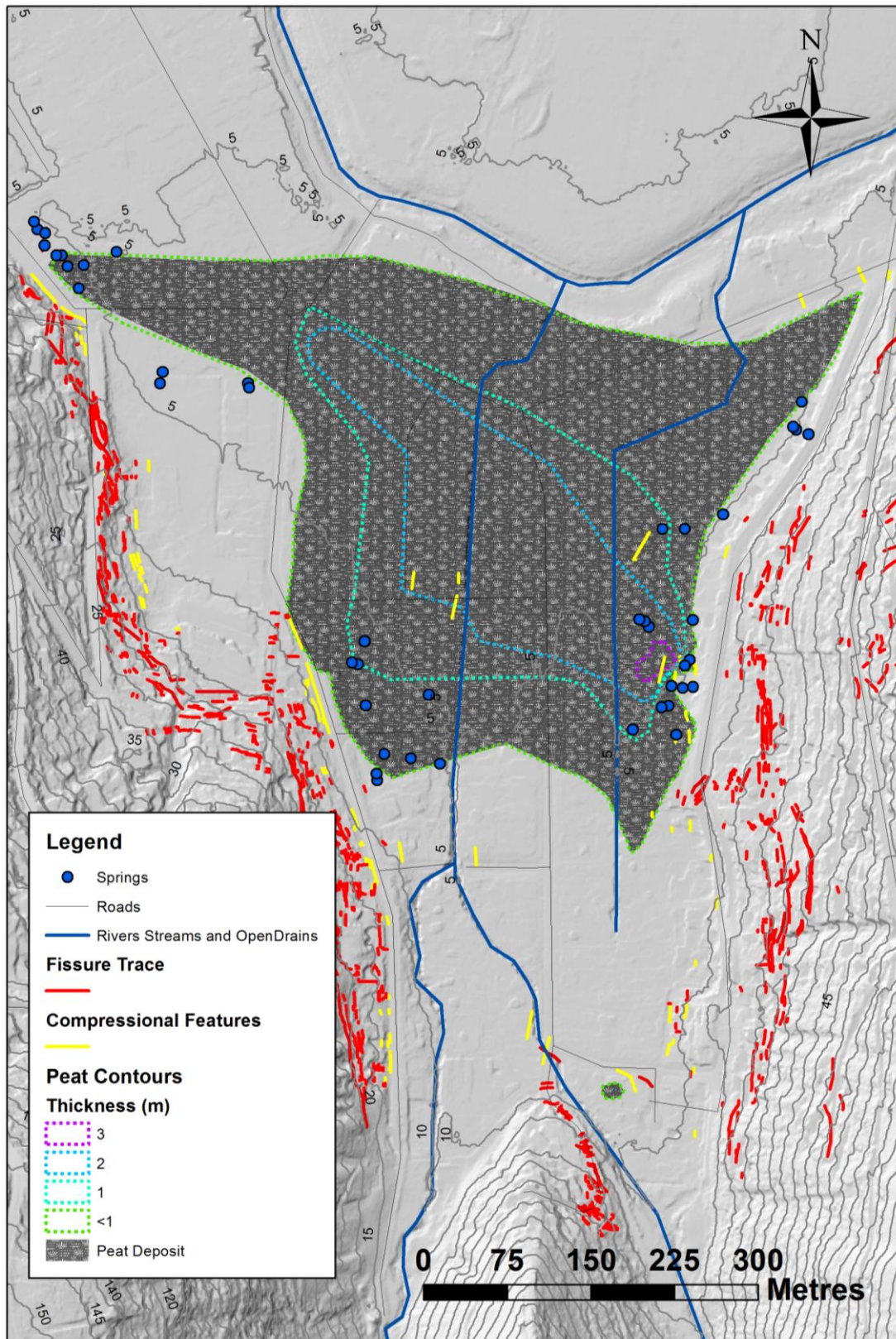


Figure 3.10: Hillshade map of the Hillsborough Valley. Earthquake related springs, fissure traces and compressional feature locations are displayed, as is the extent and thickness of peat deposits in the valley floor. (Data is sourced from CERA 2015)



### ***3.4 Sample Site Locations***

Long-term monitoring of springs and groundwater levels was required for this study within the Hillsborough Valley study area.

Spring and groundwater sampling sites were chosen based on four key criteria:

- **Accessibility:** The water must be accessible in order to be sampled.
- **Measurability:** Springs must have adequate flow in order to be sampled, the diffuse and slow flow of seepages are not viable without significant modification of the area around them.
- **Consent from land-owners:** Most spring water and groundwater issues are located on private land. Consent was required to access the land, perform invasive and non-invasive geotechnical investigations (Hand augering, weir construction), and to retrieve samples.
- **Spatial Distribution:** Earthquake related spring and seepages occur throughout the Hillsborough Valley, in a somewhat circular arrangement. To determine the similarities and/or differences between the different spring features, spring water and groundwater was sampled from relatively evenly spaced sites around the study area, where the above criteria could also be met.

For the interest and respect of land owners privacy, and conditions on data usage collated by 3<sup>rd</sup> parties to this study, the names and numbers of property addresses have been suppressed within this study. As an alternative, and for spatial recognition, selected study sites which meet the criteria set out above have been allocated site codes (Figure 3.).

Six key study are established. These are:

- **Site A:** An occupied property on Centaurus Road
- **Site B.** An occupied property at the northern margin of Vernon Terrace
- **Site C.** An occupied property located in the central area of Vernon Terrace.
- **Site D.** A property located in the central area of Albert Terrace, unoccupied with house removed following extensive earthquake damage.
- **Site E:** An unoccupied property at the Easter edge of Leonard Place.
- **Site F:** Heathcote River southern bank area located along Riverlaw Terrace.

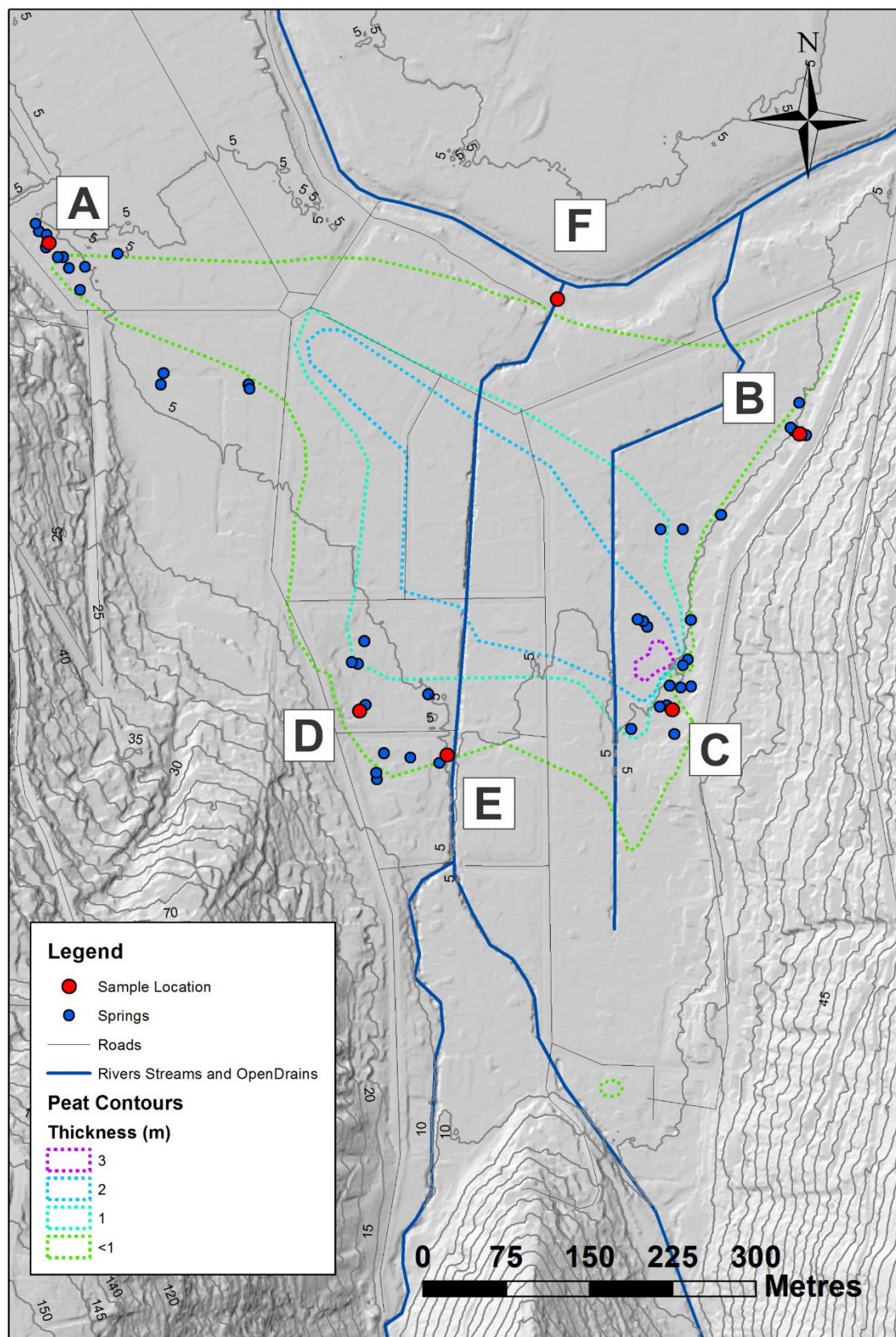
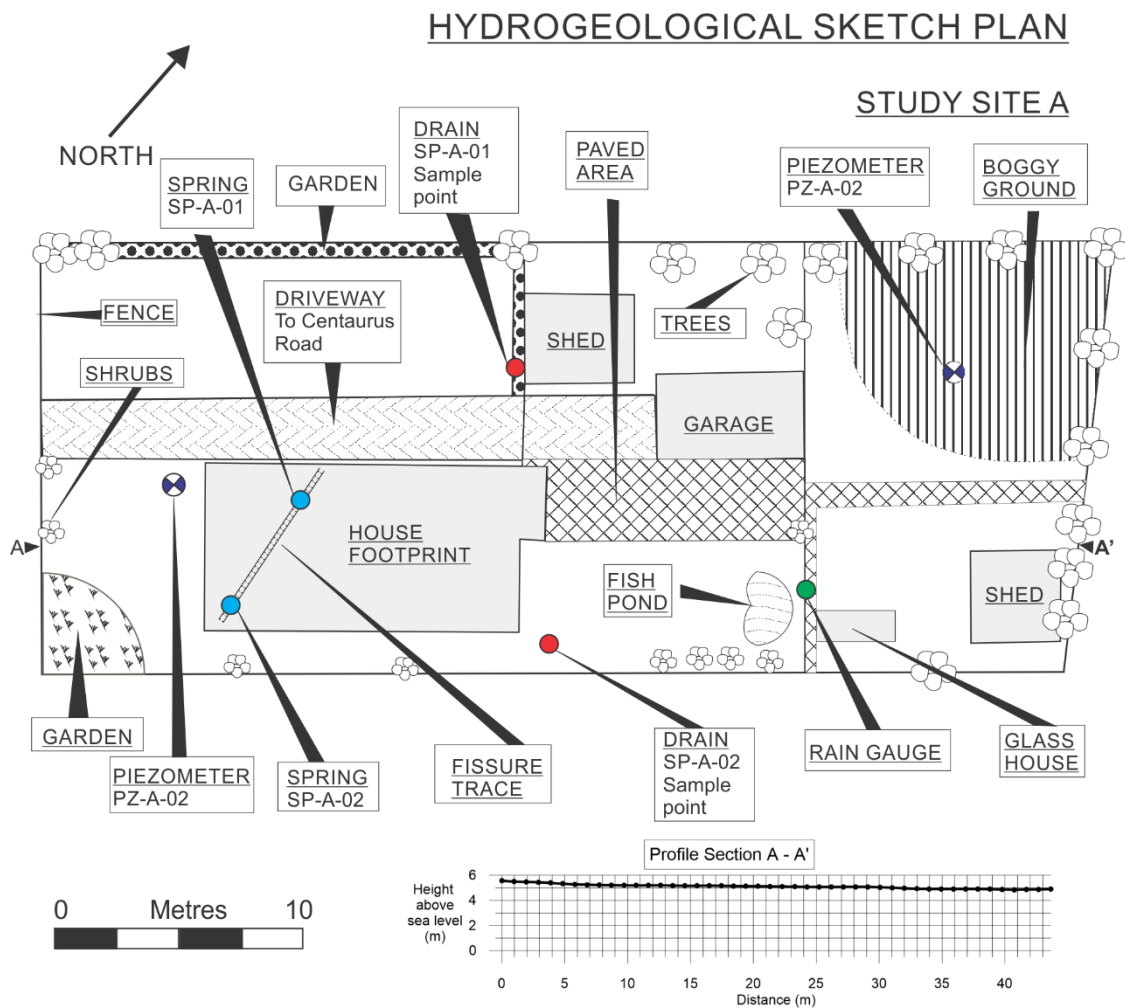


Figure 3.9: LIDAR derived hill shade and contour map of the Hillsborough Valley study area with spring, waterway and site locations displayed. The extent of peat deposits in the valley floor are also displayed.

### 3.5 Study area site plans

#### Study Site A



**Figure 3.10: Hydrogeological sketch plan for the Site A study area.**

Study Site A is located in the North-Western edge of the Hillsborough Valley mouth, along Centaurus Road (Coordinates: 5176681mN, 1572120mE). The property covers 800m<sup>2</sup> and includes an occupied single story dwelling (Figure 3.12). Two spring features formed associated with fissuring underneath the house which were first observed 24 hours following the Darfield 2010 earthquake, with flow exacerbated by following earthquakes (Stephen-Brownie 2012). The under-house springs have since been diverted, with plumbing installed and adjoined to storm water drains behind the property, which can be accessed through drainage pipes located adjacent to north side and rear of the house.



## Study Site B.

### HYDROGEOLOGICAL SKETCH PLAN

#### STUDY SITE B

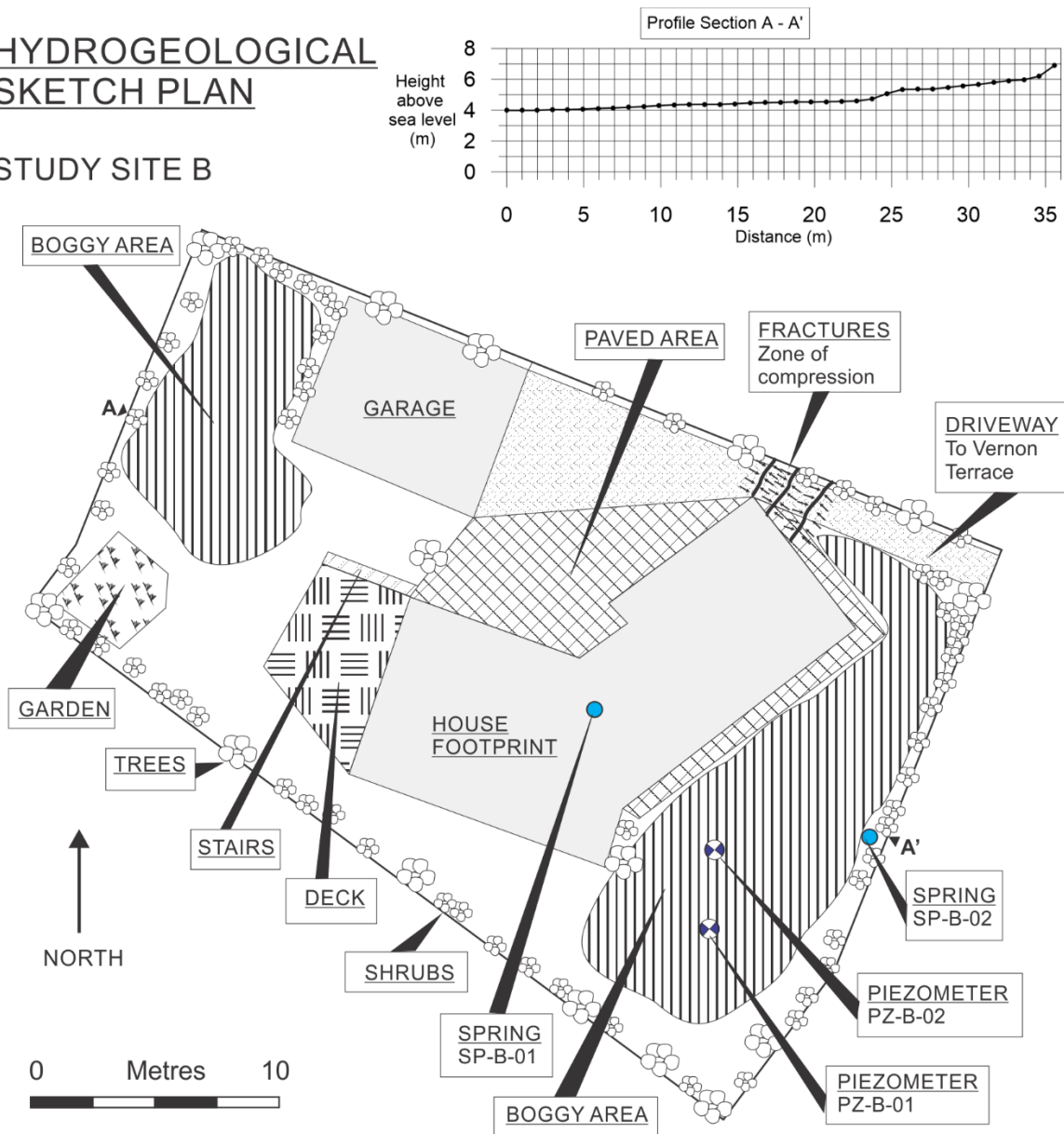


**Figure 3.11: Hydrogeological sketch plan for the Site B study area**

The Site B study area is located at the North-Eastern end of the Hillsborough Valley, on the downslope side of Vernon Terrace (Coordinates: 5176510mN, 1572798mE). The property covers 758m<sup>2</sup> and includes a dwelling that has two floor levels due to the sloped nature of the land (Figure 3.13). As a result of the Canterbury 2010-2012 earthquake sequence, the property was subjected to compression due to extensional movement upslope. This altered and fractured the underlying substrate, allowing the formation of springs, seepages and boggy patches in the area, with the emergence of a constantly flowing spring underneath the house of particular interest. A gauging weir under the house and two constantly monitored piezometers were

installed in 2011 by Aqualinc research. These are the points where data and water samples are collected.

### Study Site C

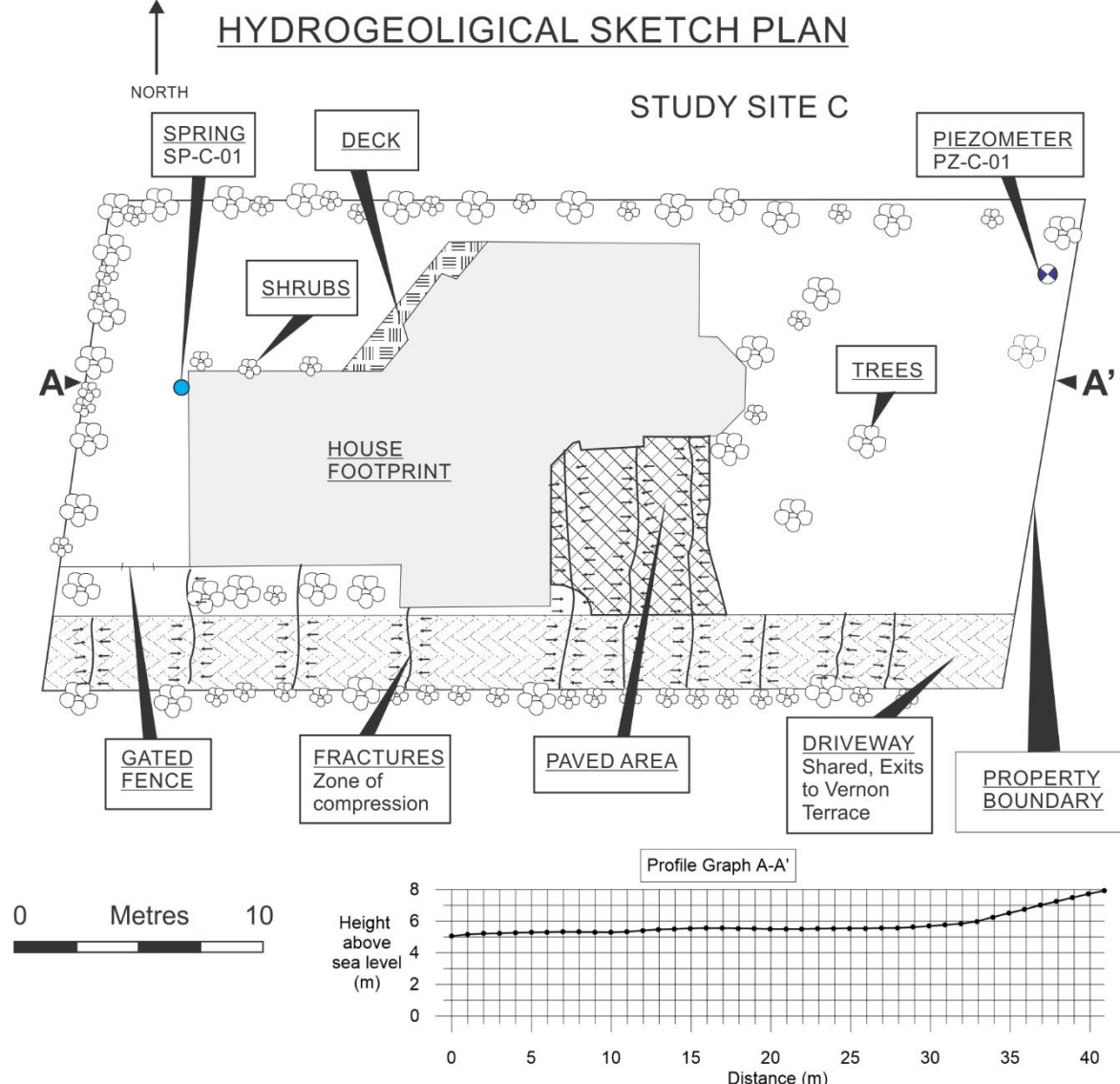


**Figure 3.12: Hydrogeological sketch plan for the Site C study area. Note the presence of compressional zone fractures along hard surfaces such as the asphalt driveway and the paved area at the house entranceway.**

Site C is located in the central-eastern area of the Hillsborough Valley (5176259mN, 1572679mE). The property cover 676m<sup>2</sup> and includes a large and modern single story dwelling. The Site C study area shares similar deformation and water issues as Site B (Figure 3.14). A spring emerges at the rear of the house which has had a reportedly constant flow since the 22<sup>nd</sup> February 2011 Christchurch earthquake. Parallel fractures are evident along the properties driveway, indicating earthquake induced compressional movement of the area. There is also a Tonkin-Taylor Ltd. installed Piezometer upslope of the property which was accessible (PZ-

VRN-05). Neighbouring properties to the north sustained heavy damage as a result of the quakes and have since been demolished.

### Study Site D.

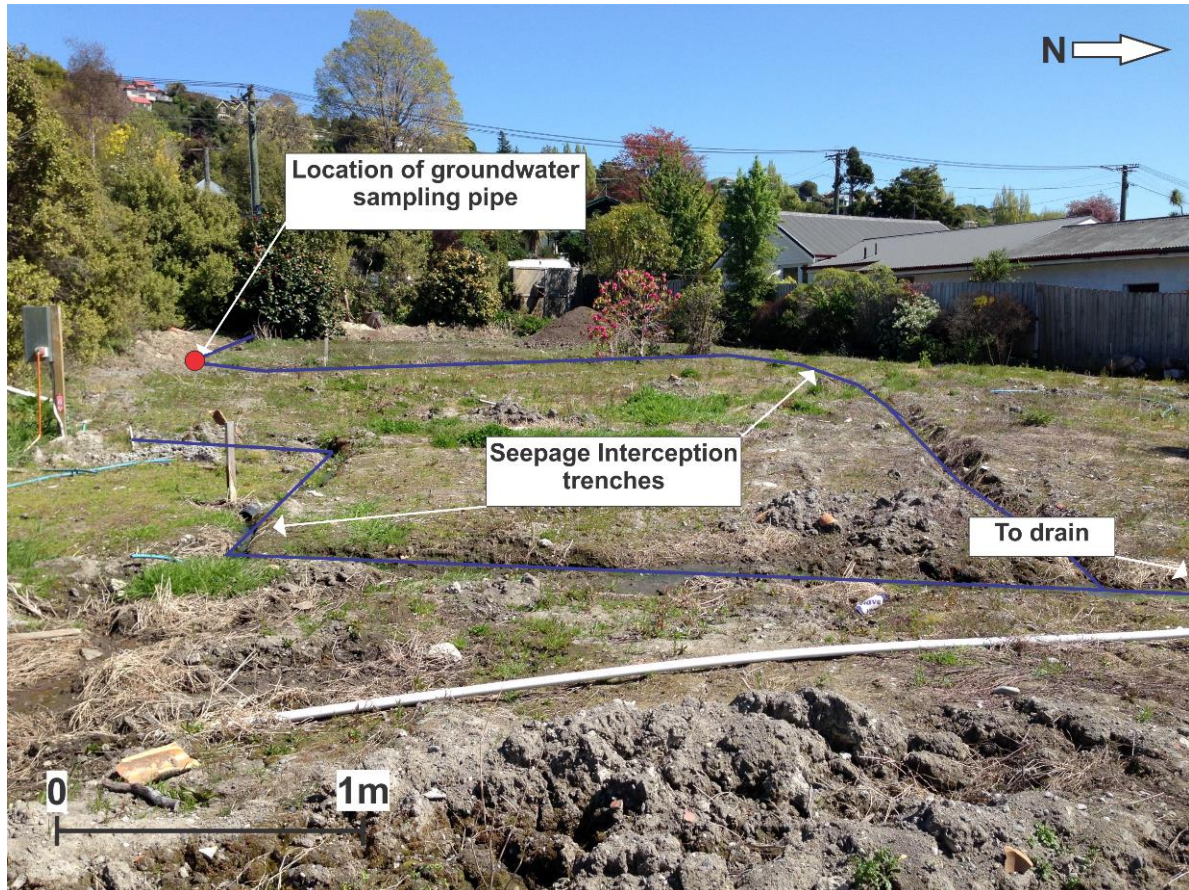


**Figure 3.13:** Site plan for the Site D study area. The pre-existing house has been demolished allowing full access to the site. Note the location of the groundwater sampling pipe and seepage interception trenches.

Study Site D is located towards the central-western area of the Hillsborough Valley (5176262mN, 1572403mE). The property is 885m<sup>2</sup> in area, and at the time of surveying and sampling for this study, was cleared of its dwelling due to earthquake damage (Figure 3.15). Large amounts of the property were affected by groundwater seepages following the earthquakes, and two major seepage interception trenches have been dug in order to drain the property. Due to the possibility of future rebuild work, no piezometers were installed on the site. However, a simple 2cm diameter galvanised steel pipe was driven into the ground in the site to a depth of approximately 3 metres, resulting in artesian water flowing out of the pipe (GW-D-01). The water in the seepage interception trenches was observed to be flowing, however was mostly stagnant. A prominent spring is emerging from a garden in the property two houses north of Site D. This spring was sampled once and is recoded as SP-D-01.

**Study Site's E and F**

A spring at Site E (5176226mN, 1572473mE) had been sampled by Aqualinc research in 2011 (Appendix IV). However this had silted over and had become a seepage feature by the time of sampling. A ground drain emerging from the property was however sampled. Site F (5176649mN, 1572585mE) was the site of Heathcote river water sampling, where samples were collected by hand by dipping a vial into the river flow.



## **Chapter 4. Methodology**

### ***4.1 Introduction***

This chapter outlines the methods used in this thesis study for gathering the physical and chemical hydrogeological aspects of spring water, ground water and rainwater in the Hillsborough Valley study area. Site investigation, mapping methodology and key study sites are outlined. The techniques of piezometer construction and monitoring are also detailed, as are spring discharge monitoring and procedures. Water sampling, stable isotope and anion analysis procedures are also described in this chapter.

### ***4.2 Site Investigation and Mapping***

In order to properly investigate earthquake related springs in the Hillsborough Valley, accurate reconnaissance and site investigation was carried out in order to establish the location of earthquake related ground deformation, spring formation and suitable water sampling study sites. This is achieved by a combination of in-field mapping and review of available Geographical Information System (GIS) data.

#### **4.2.1 Field Investigations**

Site investigation work took place over a three month period from December 2013 through to February 2014 throughout the Hillsborough Valley study area. The aim of this site investigation was to determine the location and details of post-earthquake land damage and groundwater related issues on individual land parcels within the study area. Previous investigation and mapping by Stephen-Brownie (2012) allowed areas of interest to be highlighted. These included areas of confirmed and possible spring activity, seepage and boggy areas, or earthquake related fissuring and compression zones within the study area.

#### **4.2.2 Mapping and LiDAR**

LiDAR data was obtained through the Geography Department at the University of Canterbury. This LiDAR imagery data was collected via Airborne Laser Scanning (ALS) between the 20<sup>th</sup> May and the 30<sup>th</sup> May 2011 from a fixed wing aircraft, and was carried out in order to support the February 2011 earthquake recovery effort as commissioned by the Christchurch City Council. The accuracy of the ALS survey was verified by ground measurement at 1360 test points, where a mean elevation difference of 0.255m was identified throughout the survey data. This difference was manually corrected and edited against other available imagery, further improving the quality of the terrain model.

The data was originally displayed in a 1km by 1km tile format for functionality and ease of display, layout map is located in Appendix VI. LiDAR laser strikes are classified into ground and non-ground points by using a single algorithm over the project area. The corrected LiDAR data is displayed as a bare-earth digital elevation model (DEM) using the laser strikes classified as ground level (AAM 2011). This allows for 3D mapping of the ground surface of the Hillsborough study area, allowing geomorphic and topographic features to be analysed and displayed (Figure 4.1).

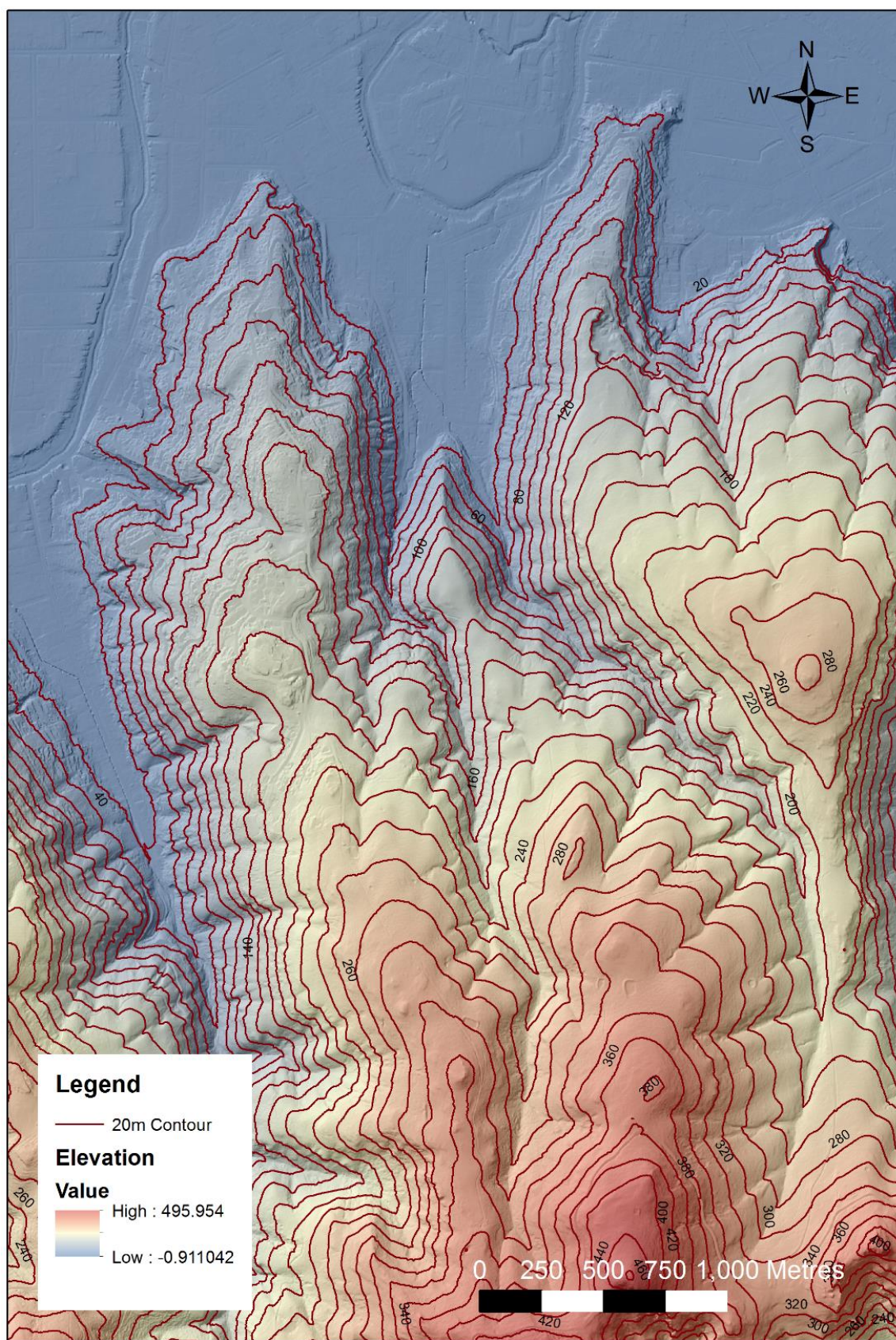


Figure 4.1: Bare-Earth DEM map of the Hillsborough Valley/ Mt. Vernon Area with 20 metre contours shown.

### **4.2.3 Geotechnical Data**

Numerous geotechnical investigations have been carried out throughout the Hillsborough Valley, prior to, during and following the Canterbury 2010-2012 earthquake sequence. Record of these investigations are stored in online databases.

The Canterbury Geotechnical Database (CGD) data was accessed using the Project Orbit program. The CGD is an online GIS-based database built on the Project Orbit platform, established by the Canterbury Earthquake Recovery Authority (CERA) in November 2011. The CGD provides extensive geotechnical investigation data including borehole logs (a selection of which are provided in Appendix 1), hand auger logs, groundwater levels, as well as the locations of spring and ground deformation features. The data is uploaded to the database by various geotechnical, structural and other suitable professionals (CERA 2015).

Access to Environment Canterbury's (ECan's) groundwater well, spring location, historical aerial photography and subsurface infrastructure data was gained through the Canterbury Maps GIS database. The well logs provide details of the subsurface lithology and historical groundwater levels. (Environment Canterbury 2015).

Relevant geotechnical data provided by these databases was collated for the Hillsborough Valley area (Figure 4.2). This data, in combination with topographic analysis using LiDAR data and site investigations carried out by author, allows of detailed overview of the geology, geomorphology and groundwater occurrence of the Hillsborough Valley area.



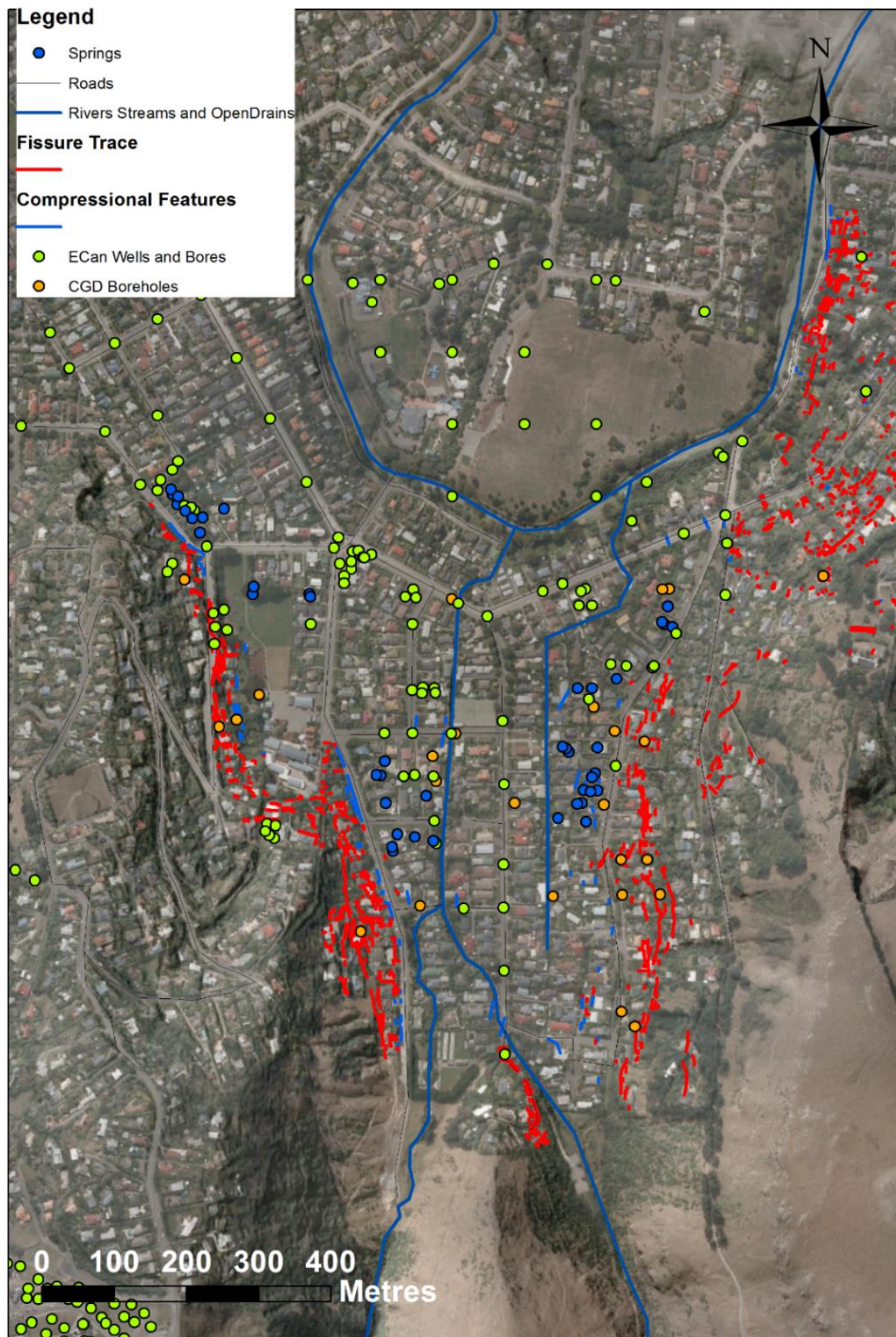


Figure 4.2: Map of the Hillsborough valley with spring, borehole and mass movement features displayed over DEM derived Hillshade map (Data acquired by field observations and from Project Orbit (CERA 2015))

### 4.3 Sampling and Monitoring Schedule

Sampling and monitoring of springs, groundwater and rainfall took place over a 10 month period between January and October 2014. The focus of this study was to determine the source and formation mechanism of earthquake relate springs in a valley aquifer system. The springs in the valley had been reported as being persistent since the earthquake, with little change in flow characteristics reported. Therefore, long term physical and chemical analysis of spring discharge and groundwater sampling was required to determine the typical characteristics of the spring source water, and to determine any seasonal variations in spring flow or spring water chemistry. Also of importance to this study was the impact of groundwater–surface water interactions on the spring discharge, such as rainfall infiltration to the underlying groundwater. Sampling and monitoring frequency was therefore determined from guidelines outlined by Sundaram et al. (2010), as displayed in Table 4.1. Samples and measurements were collected on a monthly basis in an effort to monitor long-term physical and chemical trends of spring water and groundwater, with additional collection during heavy or chemically significant rainfall (e.g. cyclonic rain water with depleted isotope values), or drier periods where spring base flow is most likely to be observed (Kresic & Bonacci 2010).

**Table 4.1: Recommended monitoring frequency for various groundwater monitoring scenarios. For the purpose of this study, the ‘Recharge Process and Rainfall Response category is most applicable (Sundaram et al. 2010).**

PURPOSE FOR MONITORING	GROUNDWATER LEVEL	GROUNDWATER QUALITY INDICATOR (e.g., EC, T)	GROUNDWATER QUALITY PARAMETERS**
Basic Resource Monitoring	Quarterly	Annual	As required
Resource Monitoring at Sensitive Sites (eg. <i>Significant Drawdown, Well Head Protection Zone, Risk of Groundwater Quality Impacts</i> )	Daily	Monthly	Quarterly
Recharge Processes & Rainfall Response	Daily or Hourly	Monthly or Hourly	As required
Measure Aquifer Confinement and Specific Storage	Hourly or 15 minute*	-	-
Point Source Contamination – Potential Impacts^	Quarterly	Quarterly	Half-yearly
Diffuse Source Contamination – Potential Impacts	Half-yearly	Half-yearly	Annual
<p>* Including barometric pressure measurement at the bore site, ≠ NSW Groundwater Quality Protection Policy,  ^ Depending on Groundwater Quality Protection Level.  ** Selection of appropriate water quality parameters for testing depends on the purpose of monitoring, possible contaminants and constraints on the cost of analyses.</p>			

#### 4.4 Piezometer installation and Monitoring

Monitoring of groundwater levels throughout the Hillsborough valley was carried out using five piezometers, located at the study sites A, B and C. The groundwater levels in these piezometers were measured either manually by a dip meter, or automatically by barometric level trolls installed inside the piezometer (Table 4.2).

**Table 4.2: Sampling regime for monitored piezometers throughout the Hillsborough Valley.**

Piezometer	Manually Measured (Dip Meter)	Automatic (Barometric Level Logger)
Site A PZ-A-01	●	
Site A PZ-A-02	●	
Site B PZ-B-01	●	●
Site B PZ-B-02		●
Site C PZ-C-01	●	

The dip meter method allowed rapid analysis of groundwater levels at the time of sampling, whereas, the barometric logger's measure minute scale data over longer timespans. Two types of barometric loggers were used at Test Site B. An In-Situ Inc. Level TROLL 300 in-tube barometric logger was used in PZ-B-01, with an In-Situ Inc. Baro TROLL 500 located adjacent to the piezometer to provide necessary atmospheric pressure data to correct the Level TROLL water level data (In-Situ Inc. 2015). Alternatively, an 'Air-Force HS-40' Gas Bubbler System was used in PZ-B-02 at the site, providing a secondary form of groundwater level measurement at Site B. Data was downloaded from the barometric trolls and following two months of operation. Groundwater levels are recorded every minute over the sampling period. The barometric measuring method used by the Level troll in PZ-B-01 allowed access to the piezometer construction, where groundwater could be sampled and level dipped, whereas PZ-B-02 was inaccessible, due to risk of releasing gas pressure in the Gas-Bubbler system. Both

piezometers and associated data loggers were installed by Aqualinc Research Ltd. The Site C piezometer (PZ-C-01) is a groundwater monitoring piezometer installed by Tonkin & Taylor Ltd (PZ-VRN-05). Permission was granted to access this at a later date than the other piezometers were available to be monitored (02/05/2014) All Tonkin & Taylor borehole and associated Piezometer logs are displayed in Appendix I. They were monitored manually using the dip meter method. Groundwater samples were extracted from study site D from the continuously flowing groundwater sampling pipe (GW-D-01).

### **Piezometer installation at Site A**

Two additional Piezometers were installed as study site A to compliment the previously installed piezometers at Sites B and C. The Piezometers at Site A were installed following the methods recommended for shallow piezometer installation guidelines (Fetter 2001; Sundaram et al. 2010; Heath 1983; Brassington 2007). This method was chosen primarily due to the low water table observed throughout the valley by ECan boreholes (Environment Canterbury 2015), which was confirmed during initial hand augering. The piezometers were constructed using 30mm continuous non-jointed PVC pipe, and were screened towards the base of the piezometer, below the water table. This was an attempt to collect deeper groundwater, where the adjacent fissure springs are thought to be sourced from and where water samples are less likely to be affected by surface pollutants and run-off. Hand Auger and associated piezometer construction logs can be found in Appendix 1, giving insight into the shallow subsurface geology at the Site A study site.

### ***4.5 Spring Discharge Monitoring and Weir Installation***

At Site A, spring discharge is measured by intercepting the water discharging from the spring diversion drainage pipe. The spring water was collected into a large plastic bag over stopwatch timed 10 second intervals, a modification of the jug and stopwatch method outlined in Brassington (2007). The contents of the bag was then carefully poured into a large measuring vessel. This was repeated five times to ensure accuracy of measurement. If values were consistent, then the average amount collected over each 10 second interval is multiplied by 6 to give the litres per minute (L/min) discharge of the spring.

In order to monitor the confined access under house spring at Site B, a 90° sharp-crested V-Notch weir previously used by Aqualinc Research was re-commissioned. The setup was equipped with an automatic-gauging logging float device which monitored the reservoir level



behind the weir. The dimensions of the weir (Figure 4.3) meant that it was classified as a fully-contracted 90° V-Notch weir (U. S. Department of the Interior Bureau of Water. 2001), although the V-notch is not located at the centre of the weir structure. This is due to the shape of the spring drainage channel and the concrete house wall located on the left of the structure. Previous to this study, the weir provided spring discharge data for Aqualinc Research and the University of Canterbury.

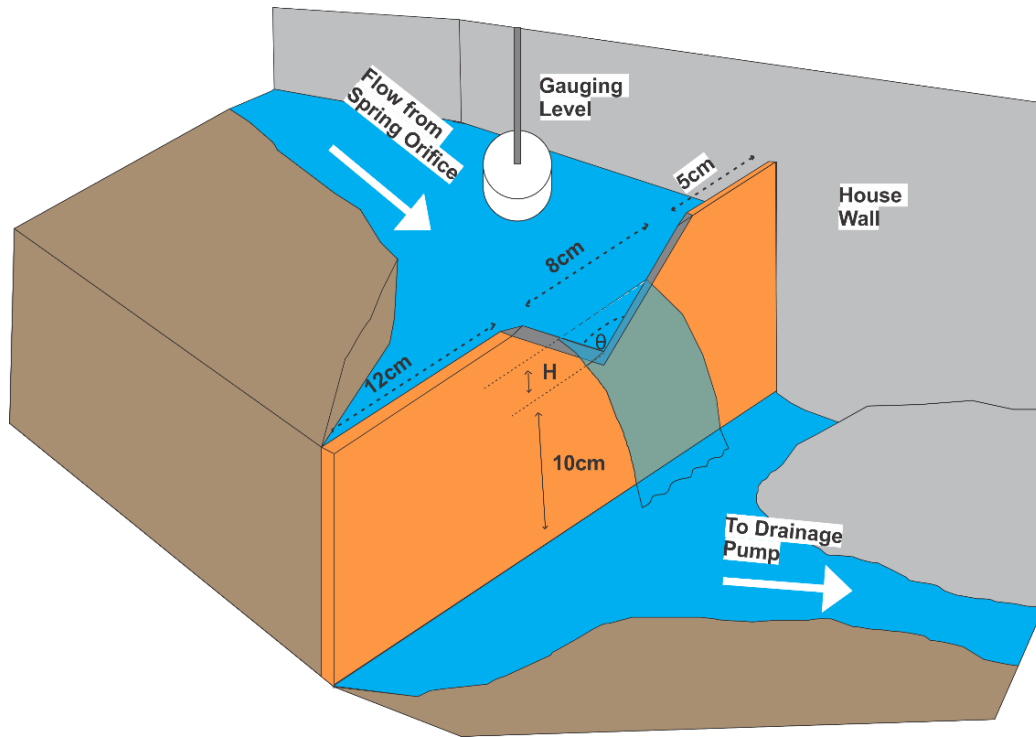


**Figure 4.3: The V-Notch weir installation under the house at Site B. Where:**

**H = Water level head flowing through V- Notch of the weir**

**θ = Angle of the V- Notch (90°)**

Spring discharge in litres per minute was calculated using the calculation for 90 degree weirs outlined in Brassington (2007), given as the equation:

$$Q = 1.342h^{2.48} \quad \text{Eq. 4.1}$$

Where  $Q$  is the spring flow in  $\text{m}^3/\text{s}^{-1}$ , is the discharge coefficient for a 90° v- notch weir,  $h$  is the water level head stage height through the weir in metres, and 2.48 is the head correction factor for a 90° v-notch weir. This data was subsequently converted into litres per minute due to the low flow rate of the spring. This raw data is presented in Chapter 5 and Appendix V.

#### **4.6 Water Sampling Analysis**

A total of 78 filtered water samples were analysed in order to determine their respective  $\delta^{18}\text{O}$ ,  $\delta^2\text{H}$  and anion concentrations. Water extracted out of the Site B and Site C piezometer tubes, using a bailer, was poured into a jug to allow infield measurements or into a sample vial for further analysis, the piezometers at Site A were sampled with a hand operated pump. Both the bailer and hand pumps are rinsed with de-ionised water, followed by sample site water prior to use. Rainfall and rainwater was measured/stored in the installed rain gauge system at test sites A and C, where rain samples were collected from both near the mouth and near the head of the valley to monitor any possible variations in volume. Rainwater samples were collected during or immediately following a rainfall event to prevent evaporation or contamination of the rain water. Water samples were collected from the springs, piezometers and the rain gauges via 50ml threaded cap centrifugal plastic vials. These were filled to the brim with non-stagnant water to ensure freshness of the sample by minimising atmospheric exposure.

Temperature, pH, Conductivity and Total Dissolved Solids (TDS) measurements were collected in-field using a Eutech Instruments pH/conductivity meter. These samples were generally collected monthly, with additional samples taken at times such as during rainfall events where mixing of rainfall may be present; or following persistent drier periods, where during spring base flow recession, the groundwater component of spring discharge is most likely to be observed (Brassington 2007). Filtering of water samples took place upon immediate return from the field area, in the University of Canterbury's Geological Sciences Sedimentology laboratory. Using 60ml syringes, samples were filtered through 0.45 micron (0.45  $\mu\text{m}$ ) syringe filters (using a caulking gun) into fresh 50ml centrifugal vials. All water samples were stored in upright crates and refrigerated to ensure the integrity of the sample until anionic and stable isotope analysis were carried out.

To prepare samples for stable isotope analysis, a 1ml syringe was used to fill 2ml glass sample vials with PTFE caps. These vials had been helium and phosphoric acid flushed before use. Prior to filling the 2ml vials, the syringe was decontaminated by flushing it with de-ionised water and then air dried. Sample water was then drawn from the 50ml sample vials and ejected into a waste-water beaker three times prior to each 2ml vial being fully filled. This process was followed for every water sample.

#### ***4.7 Isotope Testing***

The Hydrogen and Oxygen stable isotope analysis was carried out at the University of Canterbury's Stable Isotopes Facility (UCSIF) using the UCSIF's Thermo Scientific TC/EA (Thermo-Combustion Elemental Analyser). Samples were analysed using a Piccaro L-2120-I in order to determine the  $\delta D$  and  $\delta^{18}O$  isotopic composition of each water sample collected. The complete isotope sampling dataset can be found in Appendix III. The Piccaro analyser simultaneously measures values for  $\delta^{18}O$  and  $\delta D$  from the optical spectra of specific stable isotopologues of water ( $H_2^{16}O$ ,  $H_2^{18}O$ , and  $HDO$ ) using a time-based optical measurement technique called Cavity Ring-Down Spectroscopy (CRDS). The CRDS technique quantifies the optical absorption by measuring the rate of decay (the ring-down) of laser light in a cavity containing a gaseous sample (Piccaro 2010). Isotope samples were calibrated against the world standard for defining isotopic composition, the Vienna Standard Mean Ocean Water (V-SMOW).

#### ***4.8 Anion Testing***

Anion testing was undertaken using the Ion Chromatograph in the Sabre lab at the University of Canterbury's Department of Geological Sciences. The 78 filtered water samples ionic concentrations of fluoride ( $Fl^-$ ), chloride ( $Cl^-$ ), bromide ( $Br^-$ ), nitrate ( $NO_3^-$ ), sulphate ( $SO_4^{2-}$ ) and phosphate ( $PO_4^{3-}$ ) were analysed using a DIONEX ICS-2100 reagent free ion chromatograph. The raw data is provided in Appendix IV.

Each sample was prepared by pouring water samples from 50ml vials into sterile 6ml plastic tubes, which were then capped with plastic cap. Calibration standard solutions were required to be run with each sample cycle, made to the ratio of  $1Fl^- : 30Cl^- : 1Br^- : 1NO_3^- : 10SO_4^{2-} : 1PO_4^{3-}$ . The standard solutions were made in concentrations of 3mg/L, 15mg/L, 30mg/L, 150mg/L and 300mg/L (based on the levels of Chloride in each standard solution with other anions adjusted accordingly), and made in bulk from a concentrate and diluted with deionised and SITE C treated water.

The samples were then manually calibrated using the Chromeleon (c) Dionex 1996-2009 v7.1.0.898 software program to determine relative anion concentrations within each of the water samples being tested.



## **Chapter 5. Hillsborough Valley Physical Hydrogeology**

### ***5.1 Introduction***

The understanding and interpretation of springs and groundwater systems requires knowledge of the characteristics of the spring discharge, groundwater levels and the hydrogeological properties of the underlying aquifer systems (Trček & Zojer 2010). Following site mapping and geotechnical investigations, more than 40 earthquake related spring and seepage features were identified in the Hillsborough Valley study area.

### ***5.2 Groundwater in the Hillsborough Valley***

Piezometric analysis using data from boreholes throughout the Hillsborough Valley shows that the groundwater table is relatively shallow (<1m) throughout the valley floor. This is shown by shallow saturated deposits observed during geotechnical investigations (CERA 2015). Evidence that this shallow groundwater table existed prior to the earthquakes is shown by geotechnical investigations carried out by Environment Canterbury, which show saturated deposits occurring close to the ground surface in numerous locations throughout the valley (Figure 5.1).

The groundwater table is not a simple unconfined surface throughout the valley as evidenced by flowing artesian heads in piezometers located at the valley entrance on both BH-VRN-07 (Appendix 1) and SCIRT monitored boreholes. The artesian heads are caused by confining sediments over a more permeable aquifer system that is clearly under pressure.

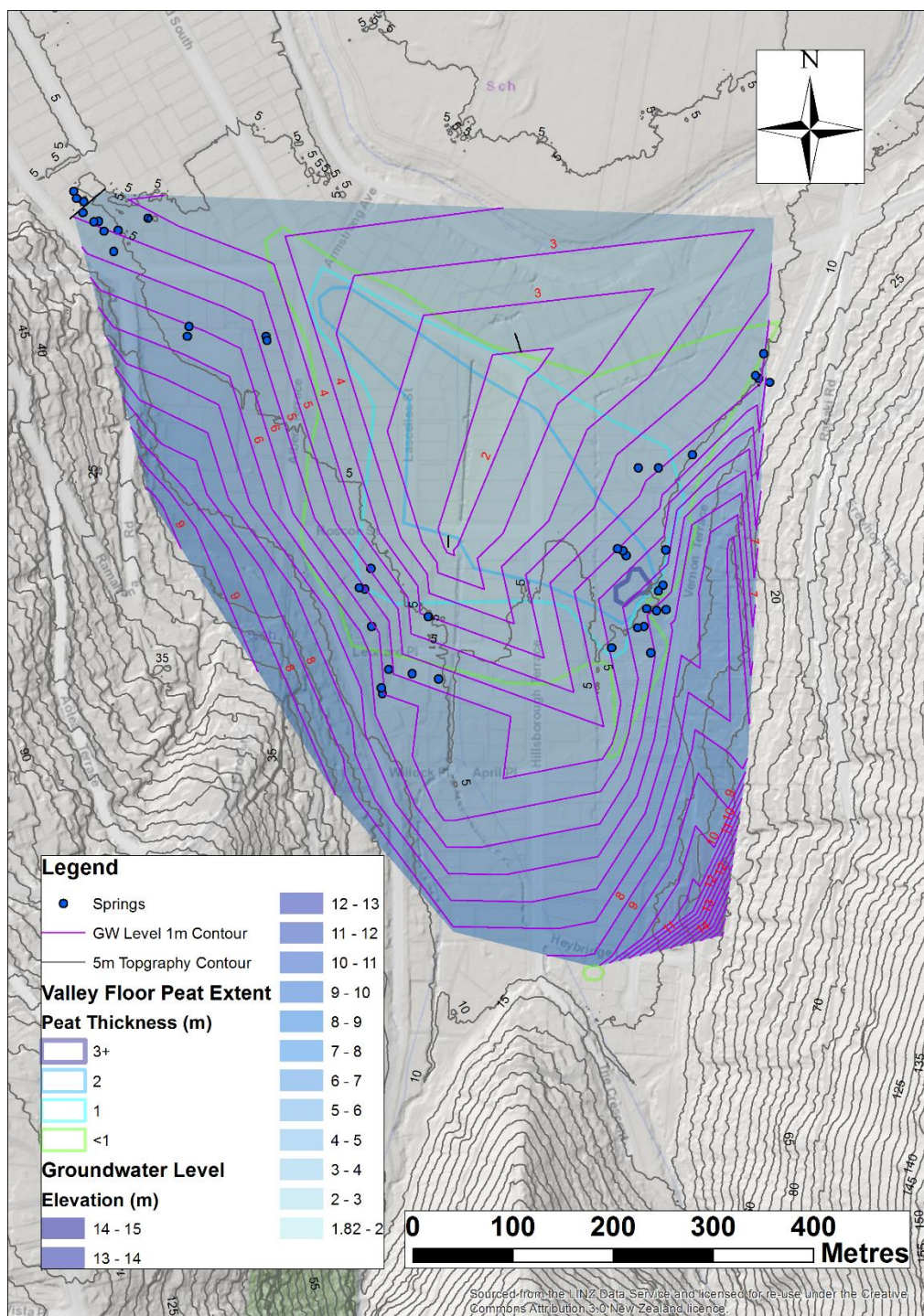


Figure 5.1: Contours of the groundwater table compared to the ground surface contours. Note the 6m groundwater potentiometric surface often crosses the 5m

### 5.2.1 Earthquake response

Cox et al. (2012) and Gulley et al. (2013) showed that there was a range of hydrological responses to the earthquakes of the CES. These ranged from near instantaneous fluctuations in groundwater levels in piezometers to slow response times.

A ground water earthquake response was recorded in Hillsborough Valley borehole monitored by Tonkin and Taylor. The boreholes show a ‘spike positive’ - a rapid increase in groundwater level with no correspondence with rainfall (Figure 5.2). This may be showing how springs initially form from rapid groundwater increases due to increased pore pressures during an earthquake event (Cox et al. 2012).

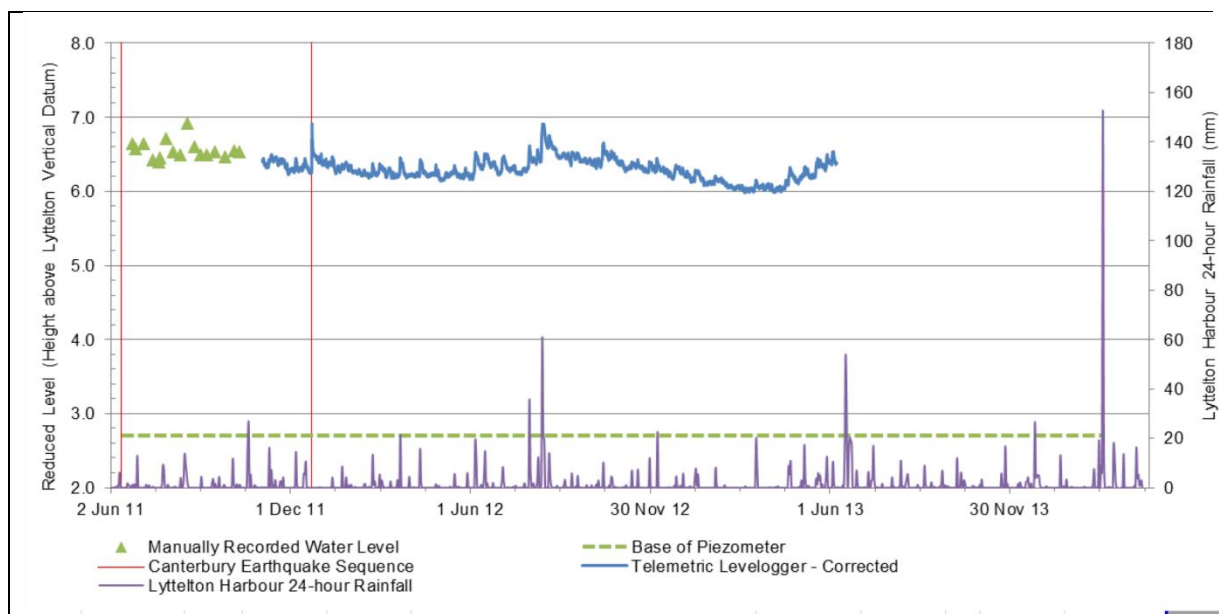


Figure 5.2 Hillsborough Valley borehole monitored by Tonkin and Taylor (Cox et al. 2012).

### 5.3 Spring Distribution and Classification

Field investigation of the morphology and distribution of earthquake related springs in the Hillsborough Valley shows that they resemble spring features classified by (Bryan 1919).

### 5.3.1 Spring Features

Two key spring types have formed as a result of the Canterbury Earthquake Sequence in the Hillsborough Valley (Figure 5.3). Springs which have formed on the toe slopes of the valley appear to be due to water table intersection on the hillslope land surface, which resemble depression gravitational type springs. These include the springs at Sites B, C and D. These springs all form in areas of compression identified by Stephen-Brownie (2012); GNS Science (2010).

Gravitational springs occur at toe slope locations where the descending land surface intercepts the relatively flat groundwater table in the Valley. Examples of these springs are those at study Sites B and D. Seepages occurring adjacent to these springs along the valley ridge slopes may also be gravitational springs, with diffuse type flow without a distinct orifice spreading the spring discharge over a wider area.

Artesian springs occur in both areas of toe slope compressed ground and where extensional fissures occur in the valley floor, such as at Site A. The Site A spring is known to be artesian and not gravitation according to Aqualinc research. They attempted to intercept the spring by trenching along Centaurus Road (between the Site A and the hillside). Aqualinc were unable to find any ground water to a depth of 3m. Artesian seeps occur along the hillside road cutting on the lower slope of Centaurus Road (near Ramahana Road) where fissure traces intersect the ground surface.

Subsurface artesian pressures have been recorded in boreholes throughout in the valley, especially towards the valley entrance. Artesian pressures may be the results of increased pore pressures due to earthquake induced ground flow distribution under the peat layer in the valley or fault derived upwelling due to the proximity of the Port Hills blind fault. Where springs have emerged they appear to take advantage of permeable ‘vent’ structures in the subsurface such as compressional fractures, extensional fissures and house foundations.



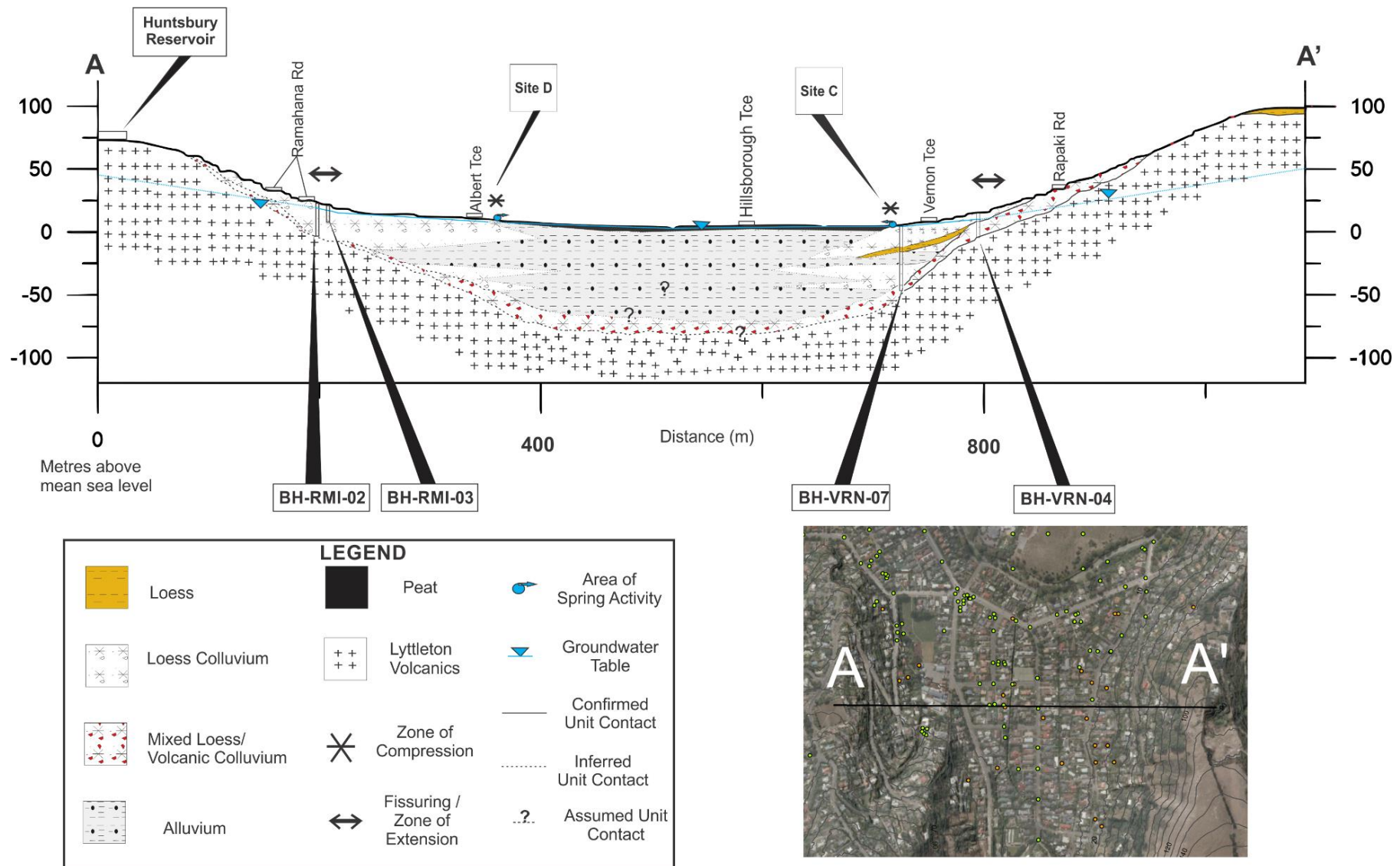


Figure 5.3: Cross-Section #1 through the Hillsborough Valley. Data was obtained via deep boreholes drilled by Tonkin & Taylor Ltd (CERA 2015), and deeper valley fill units have been inferred based on Port Hills Valley morphology presented in previous research (Namjou 1988; Parker 1989; Sanders 1986; Brown & Weeber 1994). Borehole log data is located in appendix 1.

## 5.4 Spring Discharge and Piezometric Investigation results

The physical measurements of quantitative data are discussed in Section 4.1. This includes spring discharge expressed as a quantity in litres/minute or as a stage height through a V-notch weir and groundwater level, displayed as metres below the ground surface or below top of casing.

### 5.4.1 Spring Discharge

In total, 15 samples were collected at Site A across an 8 month period. On each collection date, spring discharge was measured, in addition to infield water testing, water sample collection for anion and isotope testing (see Chapter 4 for methodology), and a combination of infield and third-party rainfall analysis collected from the Kyle Street EWS weather station operated by NIWA (NIWA 2015). Site A spring discharges ranged between a high of 14.4 L/min, recorded during the Ex-Tropical Cyclone Lusi rainfall event, and a low of 4.2 L/min during spring, 2014. Spring discharge for the Site A spring is displayed as litres/minute as per the time of collection (**Error! Reference source not found.**).

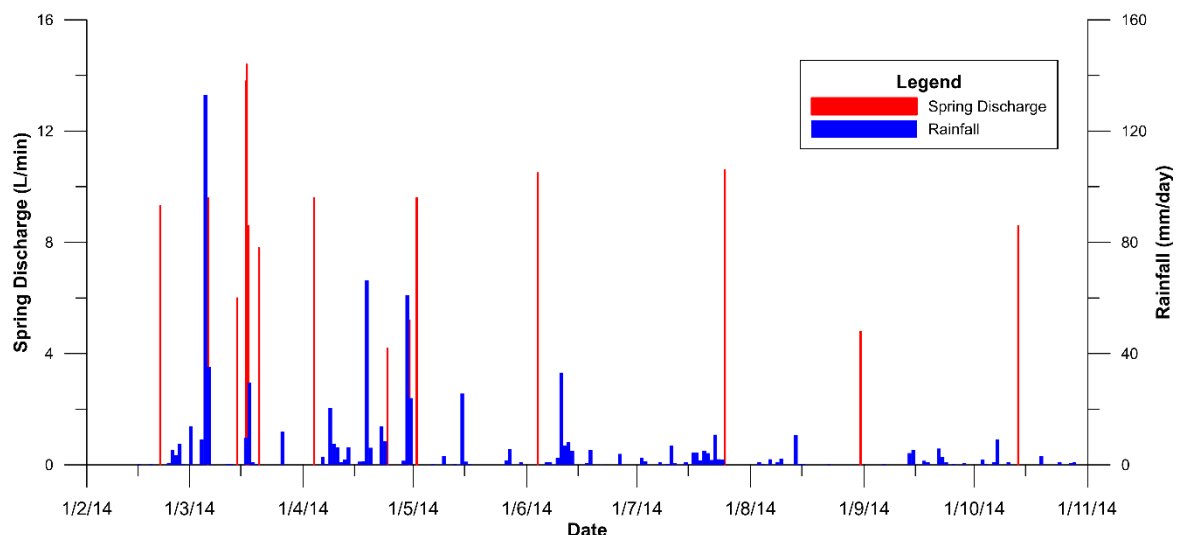
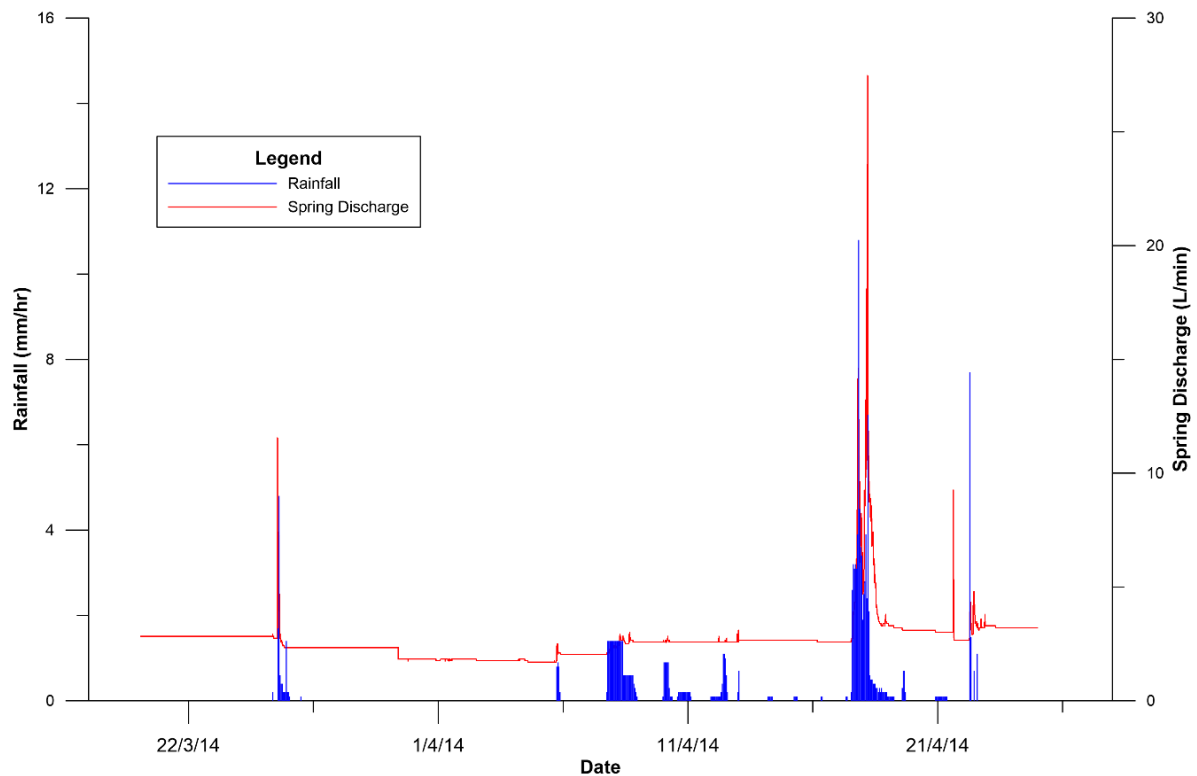


Figure 5.4: Site A Spring Discharge and Daily Rainfall (Spring SP-A-01).

In contrast to the Site A, the electronic gauging weir monitoring system installed at the Site B provides a continuous record of spring discharge over a 40 day period (Figure 5.5). Minute-scale water stage height through the 90° V-notch weir data was converted following V-notch weir methodology (see Chapter 4).



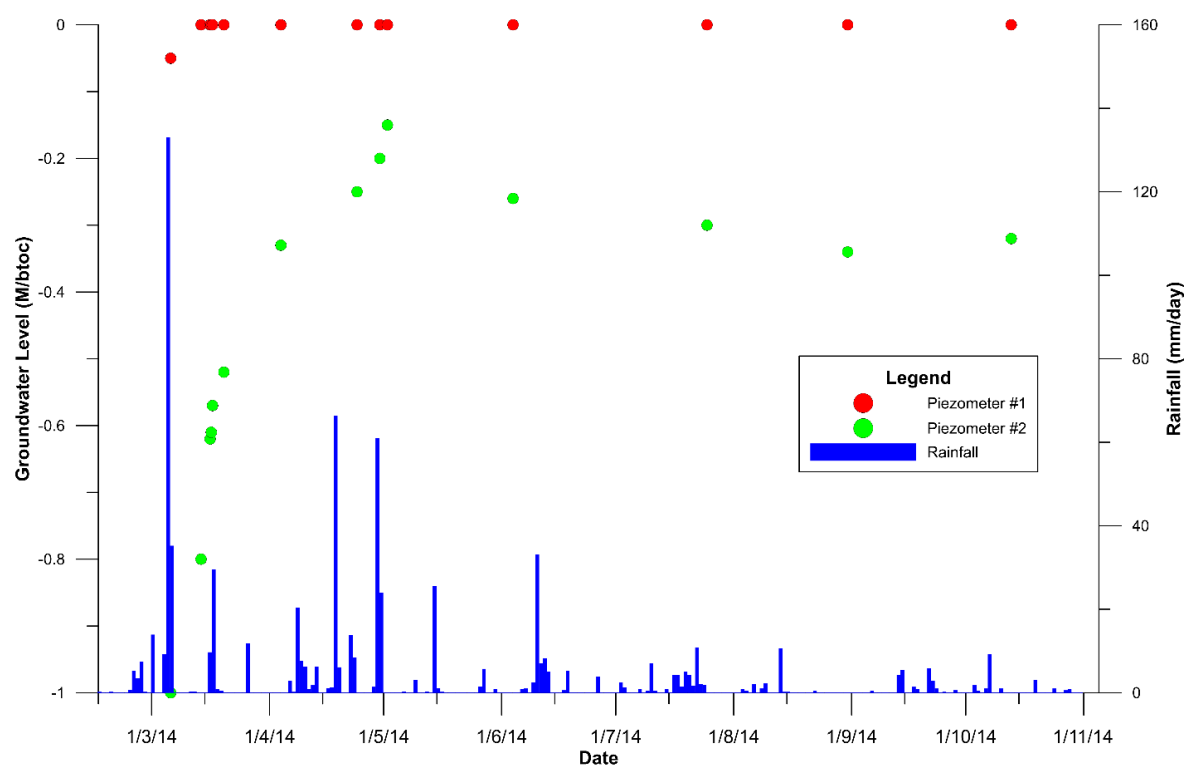
**Figure 5.5: Site B Spring #1 Discharge and Hourly Rainfall**

#### 5.4.2 Groundwater Levels

Monitoring for groundwater levels in the study area was achieved by measuring depth to water in the piezometers installed at each site (see chapter 3 for details). Water depth was measured by dip meter at the two piezometers installed at the Site A. Water levels range from a high of 5cm above the ground level and low of 1.1m (**Error! Reference source not found.**). The water level in PZ-A-01 (5cm above ground surface) rose to the top of casing soon after installation and remained at this level for the duration of this study. Water levels in PZ-A-02 are more variable, initially measuring at 1.1m below casing before slowly rising over the following two months to 0.15m below casing (0.08m/bgl) on the 02/05/2014. Water levels subsequently dropped during the winter months before climbing again following periods of rainfall in the spring.



Figure 5.6: Site A Piezometer monitoring levels and daily rainfall



Water levels in the piezometers at Site B were monitored using automatic pressure loggers, which were installed in two different forms. PZ-B-01 is monitored using a barometric logging

troll (Level Troll 300) while PZ-B-02 is measured using a logging gas bubbler system (Air force Model HS-40), for details see Chapter 4.

Minute resolution water levels for Site B Piezometer PZ-B-01 are shown in Figure 5.7. Water levels clearly spike during rainfall events then gradually subside. Lowest water levels of -0.45m below the ground surface occur during drier periods, and the highest water level spikes bring groundwater to -0.1m/bgl. Groundwater levels were confirmed by manual dip measurements, where following water samples are seen to rapidly decrease water levels in the piezometer before rapidly equilibrating over the following days.

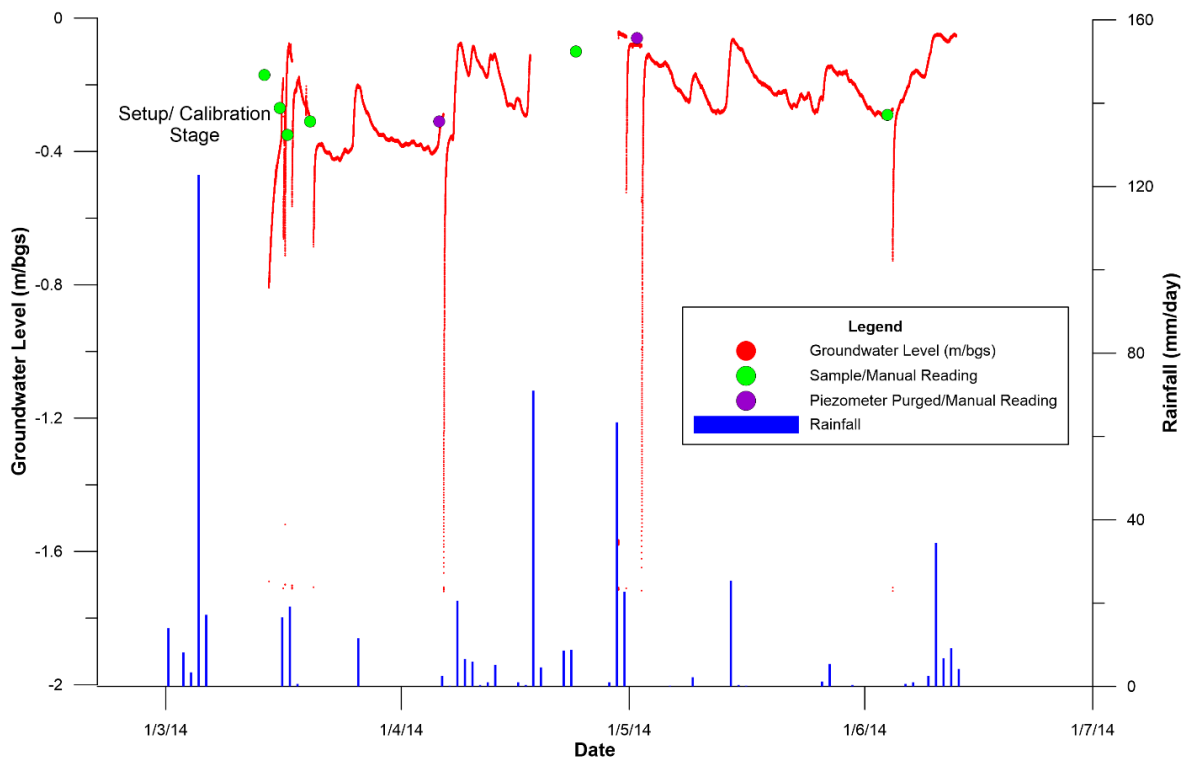
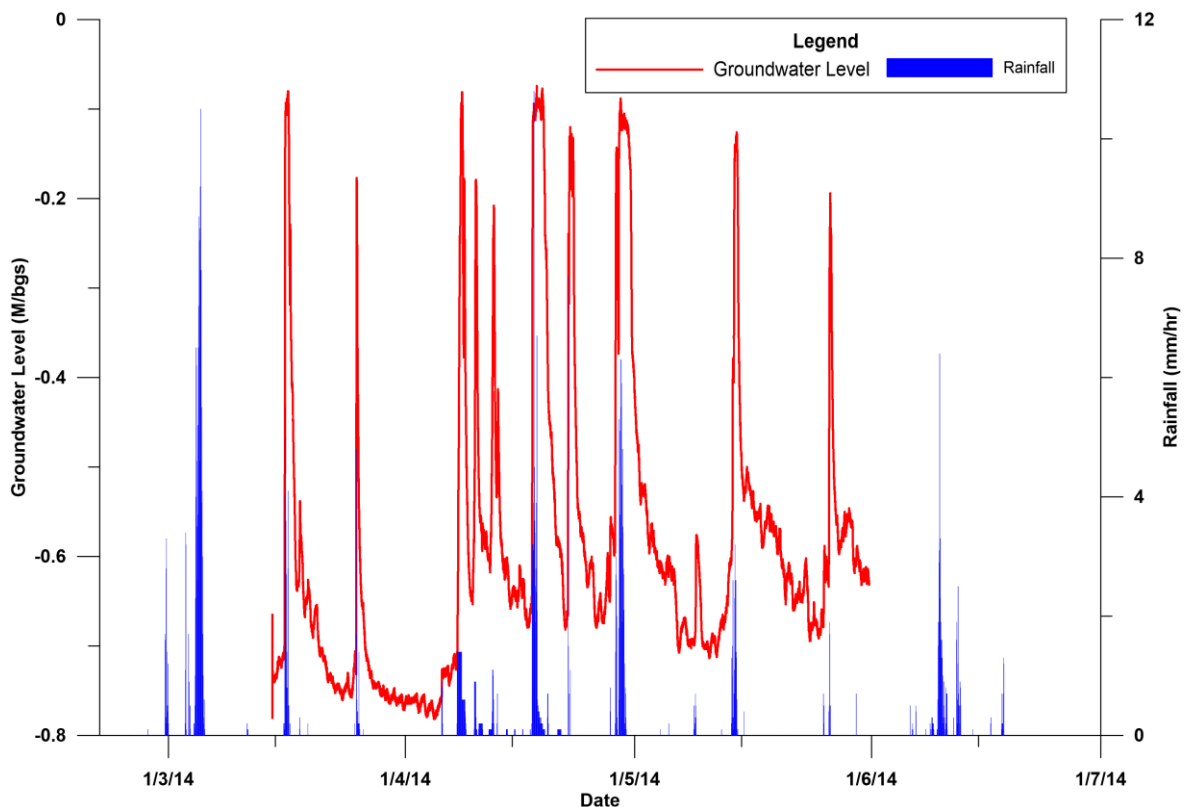


Figure 5.7: Groundwater levels and daily rainfall for Site B Piezometer #1 (PZ-B-01).

The two piezometers installed at the Site B show markedly different results, despite being in close proximity to each other and screened at similar depths (between 2.5-3m below the ground

surface) (Figure 5.7 & 5.8). PZ-B-2 is showing a lower overall groundwater level of between -0.6 to -0.8m/bgl at its position 1 metre downslope of Piezometer #1. Interestingly, groundwater level spikes during rainfall events seen in Piezometer #2 coincide with or are higher than water levels seen in PZ-B-01 at the site, spiking to levels of -0.08m/bgl. Also of note is that due to the construction of the gas bubbler system inside PZ-B-02, frequent manual water level dips could not be collected, apart from calibration measurements during setup. Therefore, rapid drops in the water level are not seen as compared to Piezometer #1 when it was sampled and/or purged.



**Figure 5.8: Groundwater levels and hourly rainfall for Site B Piezometer #2.**

Access was gained to the piezometer at Site C at a later stage of testing (2/05/2014) and was also measured by dip meter from the top of casing. Water levels for this piezometer are given in Figure 5.9 below. All Water levels are given as meters below ground surface. See Pz-VRN-07 for piezometer construction details. This piezometer is measuring deeper groundwater

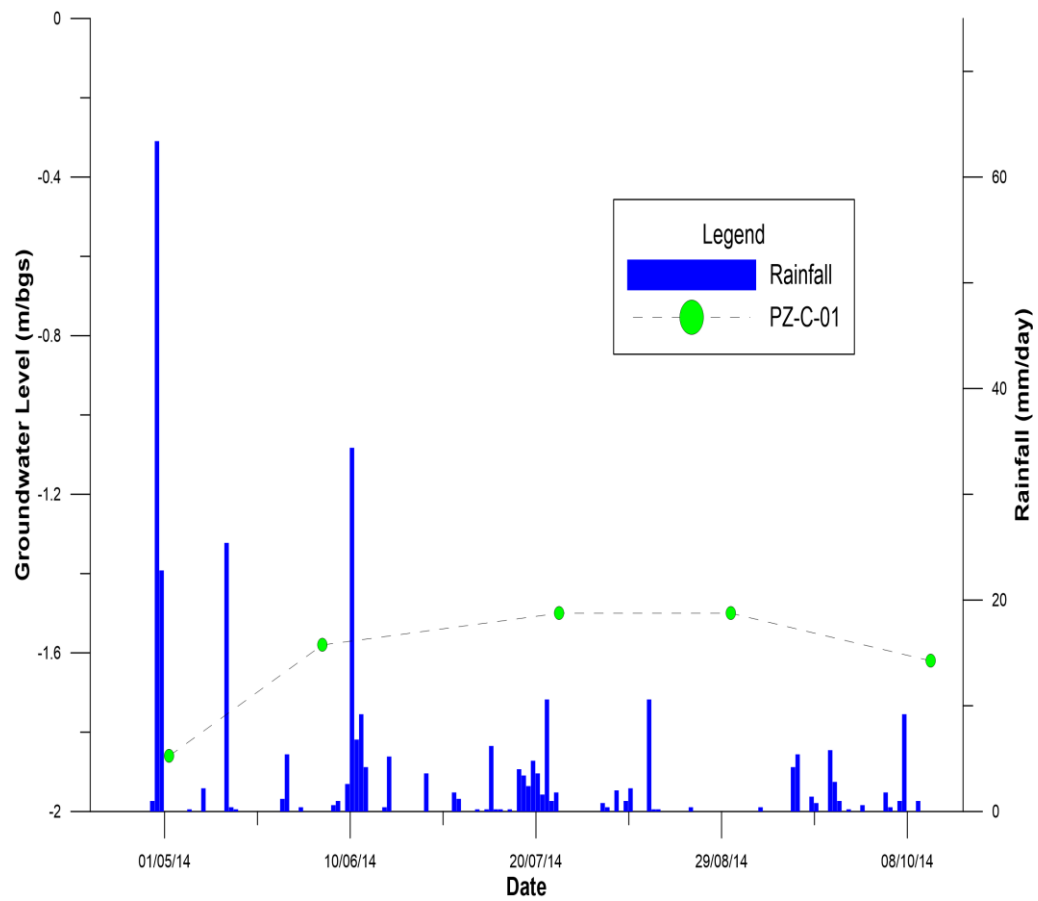


Figure 5.2: Groundwater levels for Site C (PZ-C-01) plotted against rainfall

## **Chapter 6. Hillsborough Valley Chemical Hydrogeology**

### ***6.1 Introduction***

The primary goal of this thesis is to determine the source and hydrogeological mechanism of newly emergent, earthquake-related springs in Hillsborough Valley. With no distinct aquifers recognised in the valley sedimentary strata by geotechnical investigations, chemical analysis of the spring and ground waters in the Hillsborough Valley was carried out in order to determine the source of the spring water. A total of 78 spring water, groundwater and rainwater samples were collected between January and October 2014. These samples were analysed for their isotopic composition and anion concentration; which allows for temporal water data results to be evaluated for both short term (hours) and long term (months) fluctuations and seasonality. Isotope data is also compared to the Global Meteoric Water Line (GMWL) to further constrain the source of the water. Five samples of spring water collected by third party investigations in the study area have also been examined, which include thorough chemical analyses that are used to compare the Hillsborough Spring water with other spring and ground waters in the Christchurch and Banks Peninsula area.

### ***6.2 Hydrogeological Geochemistry***

Natural waters contain a number of ionic species. The most common cations in spring waters are Calcium ( $\text{Ca}^{2+}$ ), Magnesium ( $\text{Mg}^{2+}$ ), Sodium ( $\text{Na}^+$ ) and Potassium ( $\text{K}^+$ ), while the most common anions are Bicarbonate ( $\text{HCO}_3^-$ ), Sulphate ( $\text{SO}_4^{2-}$ ) and Chloride ( $\text{Cl}^-$ ). These together form the basis for the chemical classification of natural waters, such as spring water, groundwater and rain water (White 2010). For example, the comparison between fresh and seawater chemistry is evident when displayed on a piper plot (Figure 6.1).





### 6.3.1 Composition of Banks Peninsula Water.

Geochemical studies carried out on Banks Peninsula (Sanders 1986; Namjou 1988; Parker 1989; Brown & Weeber 1994) have found that spring water from Banks Peninsula  $\delta^{18}\text{O}$  V-SMOW values range from  $\sim -7.1$  to  $-8.0$  and  $\delta^2\text{H}$  values range from  $\sim -47.9$  to  $-52.4$  V-SMOW (Figure 6.2). These values plot on or close to the Global Meteoric water line and are therefore deduced to be of meteoritic origin. Comparisons with spring elevation and proposed  $\delta^{18}\text{O}$  vs  $\delta^2\text{H}$  rainfall altitude shows that the recharge site for low level springs was often significantly higher upslope (Sanders 1986).

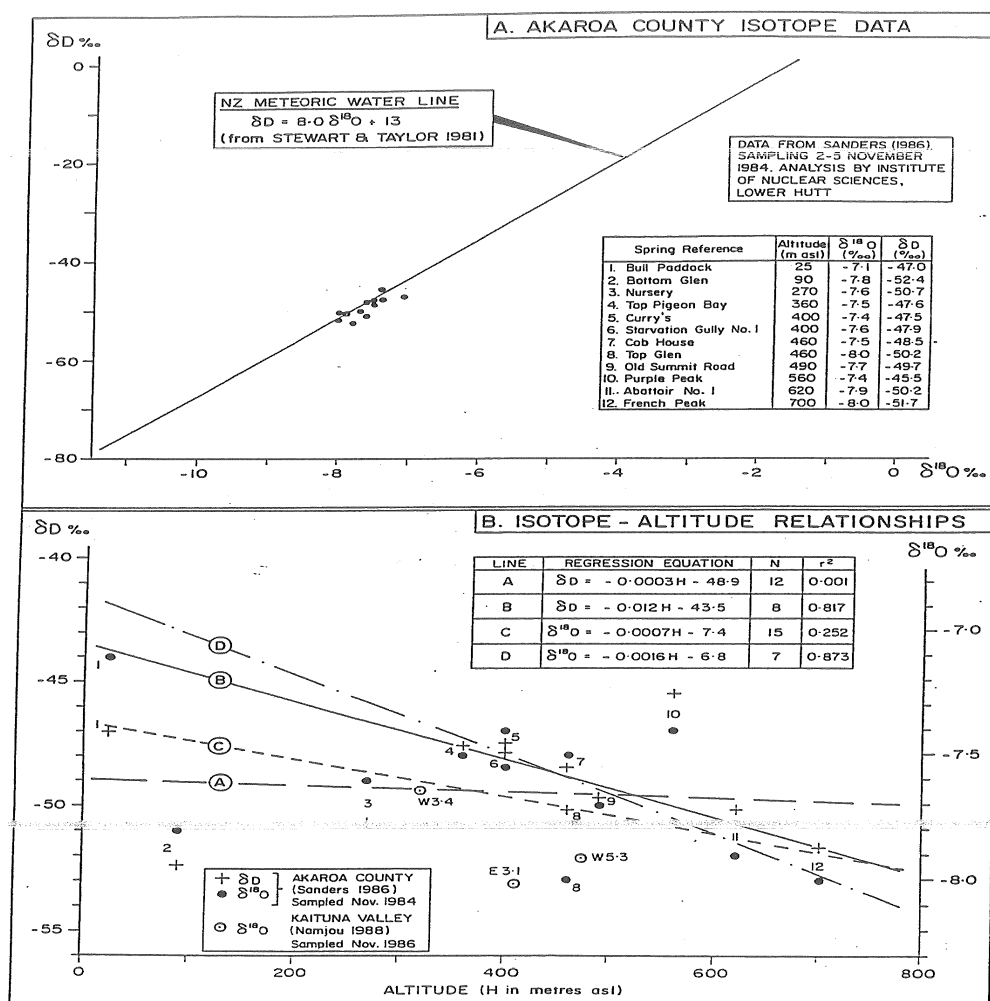


Figure 6.2: Stable isotope values from springs in Akaroa County plotted against the GWML and displayed with isotope-altitude relations.

Table 6.1: Chemical Analysis of Various Banks Peninsula and Christchurch Ground and Spring waters

Locality:	Purau Bay <sup>1</sup>	Lyttelton <sup>1</sup>	Mt Pleasant <sup>2</sup>	Charteris Bay <sup>1</sup>	Ferrymead <sup>2</sup>	Heathcote Valley <sup>1</sup>	Cass Bay <sup>2</sup>	Rapaki Bay <sup>2</sup>	Ataahua <sup>3</sup>
Grid reference	N36/902295	871341	869391	865269	864382	856376	851335	845333	811162
CRC no.*	N36w/30	M36w/3678	—	M36/w3101	M36/w3677	M36/w2591	M36/w3679	M36/w3680	M36/w4349
Total depth	Thermal spring	Thermal spring	Thermal spring	106 m	Thermal spring	29 m	Thermal spring	Thermal spring	63 m
Year sampled	1988	1979	1987	1985	1987	1986	1987	1987	1991
Temperature °C	18.0	20.0	13.2	16.0	16.0	19.86	27.5	27.5	14.3
pH	7.4	7.2	8.1	6.8	8.6	7.1	8.2	8.4	8.1
Conductivity (mS/m)†	61			80		1450			65
NO <sub>3</sub> -N	<0.05	7.3		<0.05		1.7			0.7
NO <sub>2</sub> -N	<0.005			<0.05					
NH <sub>4</sub> -N	<0.04	<0.001		<0.04					<0.005
Na	47	180	80	93	2470	190	425	440	77
K	8.7	21.5	9.3	2.5	113.0	11	183	165	1.8
Ca	51	152	28	56	108	54	11	10	21
Mg	29	108	29	25	395	64	13.0	8.5	22
SO <sub>4</sub>	14	140	48	25	620	86	40	10	16
Cl	82	605	482	130	4704	650	263	237	124
HCO <sub>3</sub>	260	340	130	280	87	192	863	961	
CO <sub>2</sub>	17	34		45		23			2
Fe	1.6	<0.04		2.3		0.12			<0.16
Total hardness	250	830		240		398			143
SiO <sub>2</sub>	78	65	34	37	10	33	96	100	28
Mn	0.07			0.07		1.4			<0.03
Rb			0.010		0.33		<0.05	<0.05	
Cs			<0.002		0.004		<0.05	<0.05	
Li	0.02		0.02	0.02	0.05		<0.05	<0.05	
B	<0.2		0.2	<0.2	1.3		2.1	2.3	
Br	0.35			0.26					
Fl	0.2			0.31					
As	<0.01			<0.01					
Sb	<0.01			<0.01					
Cd	<0.005			<0.005					
Cr	<0.02			<0.02					
Cu	<0.02			<0.02					
Pb	<0.05			<0.05					
Ni	<0.05			<0.05					
Se	<0.005			<0.005					
Sr	0.24			0.55					
Zn	<0.02			<0.02					
Soluble P	<0.06	0.067		<0.06					
Reactive Al	<0.04		<0.02	<0.0					
Chemical O <sub>2</sub> demand	<4			<4					

Locality:	St Martins <sup>3</sup>	Halswell <sup>1</sup>	Ladbrooks <sup>1</sup>	Motukarara <sup>2</sup>	Motukarara <sup>2</sup>	Motukarara <sup>2</sup>	Spreydon <sup>1</sup>	Bexley <sup>1</sup>	
Grid reference	827383	751348	752308	770216	769201	775195	771392	M35/869440	
CRC no.*	M36/w4135	M36/w809	M36/w3853	M36/w3769	M36/w3652	M36/w1467	M36/w1058	M35/w6038	
Total depth (m)	≥55.2	86.0	89.5	51.5	Thermal spring	57.9	120	400–430 m	Sea water <sup>4</sup>
Year sampled	1990	1981	1987	1987	1987	1975	1982	1989	
Temperature °C	20.0		15.7	16.7	28	24.5		19.2	
pH	7.9	9.9	7.8	8.3	8.4	8.6	7.7	8.9	
Conductivity (mS/m)†	51.7	9.2	68				11.2		
NO <sub>3</sub> -N		0.04	0.44					<0.05	
NO <sub>2</sub> -N	0.44		<0.005					0.006	
NH <sub>4</sub> -N	<0.005	0.114	<0.04				0.29	0.16	
Na	65	10.4	82	102	100	108	7.2	39	10 500
K	3.7	0.7	4.2	2.0		2.8	<0.7	0.4	380
Ca	22	6.5	34	49	18.0	13	13.0	4.7	400
Mg	10	0.25	24	31	12.0	10	1.6	0.4	1350
SO <sub>4</sub>	17	0.8	20	23	20	18	3.3	1.8	2700
Cl	92	17.5	140	214	117	110	4.5	8.3	19 000
HCO <sub>3</sub>	130	7	180	174	174	159	59		140
CO <sub>2</sub>	3		6				0		
Fe	0.07		<0.05	0.14			0.71	0.9	0.002–0.02
Total hardness	96	17	180	275			39	13	
SiO <sub>2</sub>	34	0.35	47	33	35	35		14	0.04–8.6
Mn	0.02	0.09	<0.01	<0.05			<0.001	<0.01	0.001–0.01
Rb				0.04	<0.05	<0.05			0.2
Cs				<0.02	<0.05	<0.05			<0.002
Li		0.02	0.01	0.005	<0.05	<0.05		<0.01	0.1
B			<0.2	0.2	<1.0	0.51			4.0
Br			0.42					<0.06	65
Fl			0.21					0.2	1.4
As			<0.01						0.003–0.024
Sb			<0.01						
Cd			<0.005						
Cr			<0.02					<0.03	
Cu			<0.02					<0.02	0.001–0.09
Pb			<0.05					<0.05	0.004–0.005
Ni			<0.05					<0.05	0.0001–0.0005
Se			<0.005						0.004
Sr			0.18					0.04	13
Zn			<0.02					<0.02	0.005–0.014
Soluble P	0.032		<0.06					<0.06	0.001–0.10
Reactive Al			<0.04					0.09	0.16–0.19
Chemical O <sub>2</sub>								<4	

Alluvial aquifers in Banks Peninsula such as those in Kaituna Valley and show slightly are relatively mineral deficient (Namjou 1988; Parker 1989), however springs derived from deeper circulating meteoric water throughout Banks Peninsula have much higher concentrations of cations and anions due to water-rock interactions longer exposure to Banks Peninsula bedrock. (Weeber 1994).

### 6.3.2 The Christchurch Artesian Aquifers.

Values for the chemical composition of the CAAS are shown in Table 6.1. These show that Christchurch groundwater is less mineralised than the Banks Peninsula water, with higher ratios of Calcium and Bicarbonate compared to other ions (Brown and Weeber 1992).

**Table 6.2: Groundwater chemistry data for wells in the Christchurch Artesian Aquifer System and groundwater adjacent to the Banks Peninsula (Heathcote Valley and Lyttelton Tunnel).**

Well Number	M35/w1476	M35/w1925	M35/w2276	M35/w2587	M36/w981	M33/w1159	Tunnel
Locality	Papanui	Aranui	New Brighton	Linwood	Spreydon	Heathcote V.	Lyttelton
Aquifer depth (m)	41	62	89	129	178	34	
pH	7.3	7.7	7.8	7.8	7.7	7.2	7.1
Conductivity (mSm <sup>-1</sup> )	9.8	13.4	10.6	10.2	12.1	204	208
Nitrate nitrogen	0.50	0.2	0.2	0.10	0.14	<0.1	6.4
Ammoniacal nitrogen		<0.01	<0.01	<0.01	<0.01		<0.01
Sodium	5.6	10	8.1	7.4	8.7	167	162
Potassium	0.7	1.0	<0.7	0.5	<0.7	9.6	18
Calcium	12.0	17.0	10.9	12.0	14.0	97.3	144
Magnesium	1.6	2.0	2.4	1.5	1.8	134.4	110
Sulphate	4.8	3.5	5.0	5.5	3.2	80	110
Chlorine in chlorides	3.0	5.5	5.4	3.5	4.3	730	520
Bicarbonate	51	68	52	53	68	62	349
Carbon dioxide	4	2	0	1		11	6
Iron		<0.03	<0.03	<0.03	<0.03	<0.01	0.29
Total hardness (as CaCO <sub>3</sub> )	37	51	37	38	42	796	5
Silica	19.0	21.0	19.0	19.0		24	4
Manganese		<0.001	<0.001	<0.001	<0.001	0.06	
Boron						0.03	
Lithium						0.0038	
Zinc						0.02	

A community supply well at Palatine Terrace shows higher ion content and is possibly showing mixing between the Banks Peninsula groundwater Christchurch Artesian groundwater (Appendix IV)

### 6.4 Aquifers of the Hillsborough Area

The chemical composition of groundwater and springs in the Christchurch area is highly variable, as discussed in Chapter 2 of this thesis. This is a result of the various source aquifers in the region, most importantly, the layered aquifer sequence of the Christchurch Artesian

Aquifer System and the Banks Peninsula Bedrock Aquifers. The Hillsborough Valley covers the boundary between these two aquifer systems as discussed by Brown & Weeber (1994). The contact between the Lyttelton Volcanic groups aquifers and the Christchurch Artesian Aquifer system lies adjacent to the northern margin of the study area (Figure 3.8). As a result of this, there may be mixing of groundwater in the area, especially towards nearing the entrance to the valley. Groundwater located within the valley sedimentary fill may also have a different chemical composition. Piezometric investigations show that there is an extensive cap of peat deposits within the valley, which may influence groundwater flow and chemical composition.

## 6.5 Hydrochemistry of the Hillsborough Valley

Natural waters contain variable isotopic compositions and ionic concentrations, allowing the waters to be differentiated and categorised. A combination of groundwater, spring water and rainwater samples have been collected and analysed from the Hillsborough Valley in an effort to establish the source of the post-earthquake springs in the area. Ionic analysis data collected by Aqualinc Research Ltd and Griffin (2015) are displayed in **Error! Reference source not found..** Aqualinc Research have been investigating the changes to the Hillsborough Valley groundwater following the earthquakes with spring water samples collected in 2011 (Site E) and 2012 (Site B), whereas Griffin is conducting a widespread study on Banks Peninsula springs, with samples collected in May 2015 for Sites A and C. Full results of these studies are available in Appendix IV. The results of these analyses show that the spring waters are variable in ionic composition and temperature within the Hillsborough Valley.

**Table 6.3: Chemical Analysis of the Site A, Site B, Site C and Site E springs from the Hillsborough Valley. Courtesy of Aqualinc Research and Griffin (In Prep.)**

Locality	Site A	Site B	Site C	Site E
Sample	SP-A-01	SP-B-01	SP-C-01	SP-E-01
Grid reference	1572116.55mE 5176676.7mN	1572790.595mE 5176514.277mN	1572671.798mE 5176263.452mN	1572473.755mE 5176212.737mN
Temperature (°C)	18.3	15.5	14.7	-
pH	7.5	7.4	7.7	6.8
Conductivity (mS/m)	101.7	93.8	119.4	77.1
Ca (mg/L)	35.9	42.0	49.9	43.0
Mg (mg/L)	25.0	22.0	30.8	14.4
Na (mg/L)	115.0	103.0	151.6	84.0
K (mg/L)	3.5	4.9	4.5	4.2
Cl (mg/L)	221.5	200.0	241.6	134.0
HCO <sub>3</sub> (mg/L)	48.6	161.0	106.6	184.0
SO <sub>4</sub> (mg/L)	35.2	31.0	44.9	22.0

A summary of the mean values from the infield testing, anion and isotopic analysis of spring water, groundwater and rainwater collected for this study is presented in **Error! Reference source not found.** The full results are available in Appendixes III and IV. Additional one-off sample collection results are displayed in **Error! Reference source not found.** Both spring and groundwater samples are mineralised and isotope depleted when compared to rainfall samples which were collected during testing. This data is analysed in the following section, with a focus on the major cation and anion concentrations, and isotopic composition. Variations are also observed in the temperature and pH levels of the water samples, both geospatially and by sample type. Sample locations are detailed in Chapter 3 (Figure 3.)



**Table 6.4: Summary of average values for results of water analysis from present study. Site locations are shown in Figure 3..**

	Site A Spring (SP-A-01)	Site A Piezometer (PZ-A-01)	Site A Piezometer (PZ-A-02)	Site B Spring (SP-B-01)	Site B Piezometer (PZ-B-01)	Site C Spring (SP-C-01)	Site C Piezometer (PZ-C-01)	Site D Groundwater (GW-D-01)	Rainwater
<b>Grid Reference</b>	1572116.55 E 5176676.7 N	1572110.616 E 5176673.292 N	1572134.693 E 5176697.898 N	1572790.595 E 5176514.277 N	1572798.534 E 5176507.927 N	1572671.798 E 5176263.452 N	1572691.8 E 5176400.2 N	1572396.102 E 5172396.366 N	-
<b>Screen Depth (m)</b>	Spring	2.8-3	2.8-3	Spring	3-3.5	Spring	10.0-12.0	3.0	Rainfall
<b>Temperature (°C)</b>	17.0	-	-	15.5	14.4	14.7	14.0	-	-
<b>pH</b>	7.0	-	-	7.4	6.6	6.9	7.1	-	-
<b>Conductivity (µS/m)</b>	1059.3	-	-	1153.0	1168.8	1246.4	854.4	-	-
<b>Total Dissolved Solids (mg/L)</b>	529.2	-	-	577.5	584.3	622.9	427.2	-	-
<b>Oxygen 18 (δ18O) (V-SMOW)</b>	-8.4	-8.2	-8.3	-8.4	-8.2	-7.9	-8.0	-8.2	-5.4
<b>Deuterium (δD) (V-SMOW)</b>	-57.3	-55.7	-56.8	-56.5	-55.8	-54.2	-55.9	-55.6	-33.1
<b>FI<sup>-</sup> (mg/L)</b>	0.3	0.7	0.9	0.2	0.3	0.3	1.6	0.2	0.0
<b>Cl<sup>-</sup> (mg/L)</b>	227.6	251.4	134.2	214.8	208.3	224.4	23.6	174.7	7.4
<b>Br<sup>-</sup> (mg/L)</b>	0.5	0.7	-	0.6	0.6	0.6	-	-	0.0
<b>NO<sub>3</sub><sup>-</sup> (mg/L)</b>	4.0	1.4	1.3	3.7	0.4	5.2	1.4	2.3	0.0
<b>SO<sub>4</sub><sup>-</sup> (mg/L)</b>	37.3	0.2	1.6	37.9	14.3	46.3	19.7	35.7	1.2
<b>PO<sub>4</sub><sup>-</sup> (mg/L)</b>	0.5	0.9	-	0.4	0.3	0.8	1.4	0.9	1.4

**Table 6.5: Additional single sample anion data collected in relation to Hillsborough Valley waters**

Sample Name	Site A Tap Water	Site C Tap Water	Site D Spring #1	Site E Drainage Pipe	Site F Heathcote River Water
Date	6/04/2014	2/05/2014	30/04/2014	4/06/2014	4/06/2014
$\delta^{18}\text{O}$ (V-SMOW)	-8.97	-8.86	-7.81	-7.80	-8.45
$\delta^2\text{H}$ (V-SMOW)	-61.62	-61.04	-53.31	-52.95	-59.23
Fluoride (mg/L)	0.04	0.03	0.28	0.41	0.00
Chloride (mg/L)	7.67	8.21	156.09	333.88	23.31
Bromide (mg/L)	0.00	0.00	0.42	1.30	0.00
Nitrate (mg/L)	7.29	9.75	1.51	1.69	9.90
Sulphate (mg/L)	9.31	10.56	43.29	47.70	20.23
Phosphate (mg/L)	0.15	0.00	0.44	0.87	1.11

## 6.6 Stable Isotope Analysis

### 6.6.1 Oxygen-18

$\text{D}^{18}\text{O}$  values average between -7.80 and -8.4 V-SMOW throughout the Hillsborough Valley spring and groundwater samples. These values fall between the average  $\delta^{18}\text{O}$  compositions found for Banks Peninsula (~-8.0 V-SMOW) and the CAAS (~-9.0 V-SMOW) as shown in various tap water samples (Brown & Weeber 1994), however have more similar compositions to the Banks Peninsula spring and groundwater. Rainfall samples that were collected in the Hillsborough Valley during major rainfall events have the least depleted  $\delta^{18}\text{O}$  values with a mean of -5.4 (V-SMOW). Sampling by Tutbury (2015) over the course of this study recording  $\delta^{18}\text{O}$  rainfall values ranging between -0.61 and -14.39 (V-SMOW), with an overall mean  $\delta^{18}\text{O}$  (V-SMOW) composition of -5.58.

The  $\delta^{18}\text{O}$  (V-SMOW) results are plotted in **Figure 6**. The plot shows that the  $\delta^{18}\text{O}$  values remain relatively stable over the collection period for both spring waters and ground waters. However rainwater is clearly much more variable. The  $\delta^{18}\text{O}$  values in groundwater and springs spike during periods of rainfall, especially when rain water is more  $\delta^{18}\text{O}$  enrich such as during the extra tropical cyclone Lusi event on the weekend of the 15<sup>th</sup>-16<sup>th</sup> March. There also appears to be a lag time for the groundwater's response to rainwater when compared to that of the spring waters. This is especially evident in the groundwater sampled in Site B piezometer #1, which spikes in  $\delta^{18}\text{O}$  at a much slower rate and less prominently than in spring water observed throughout the valley. The groundwater then continues to become gradually more enriched in  $\delta^{18}\text{O}$  over the following day and to a lesser extent, months, in comparison to the spring waters, which quickly become more  $\delta^{18}\text{O}$  depleted.

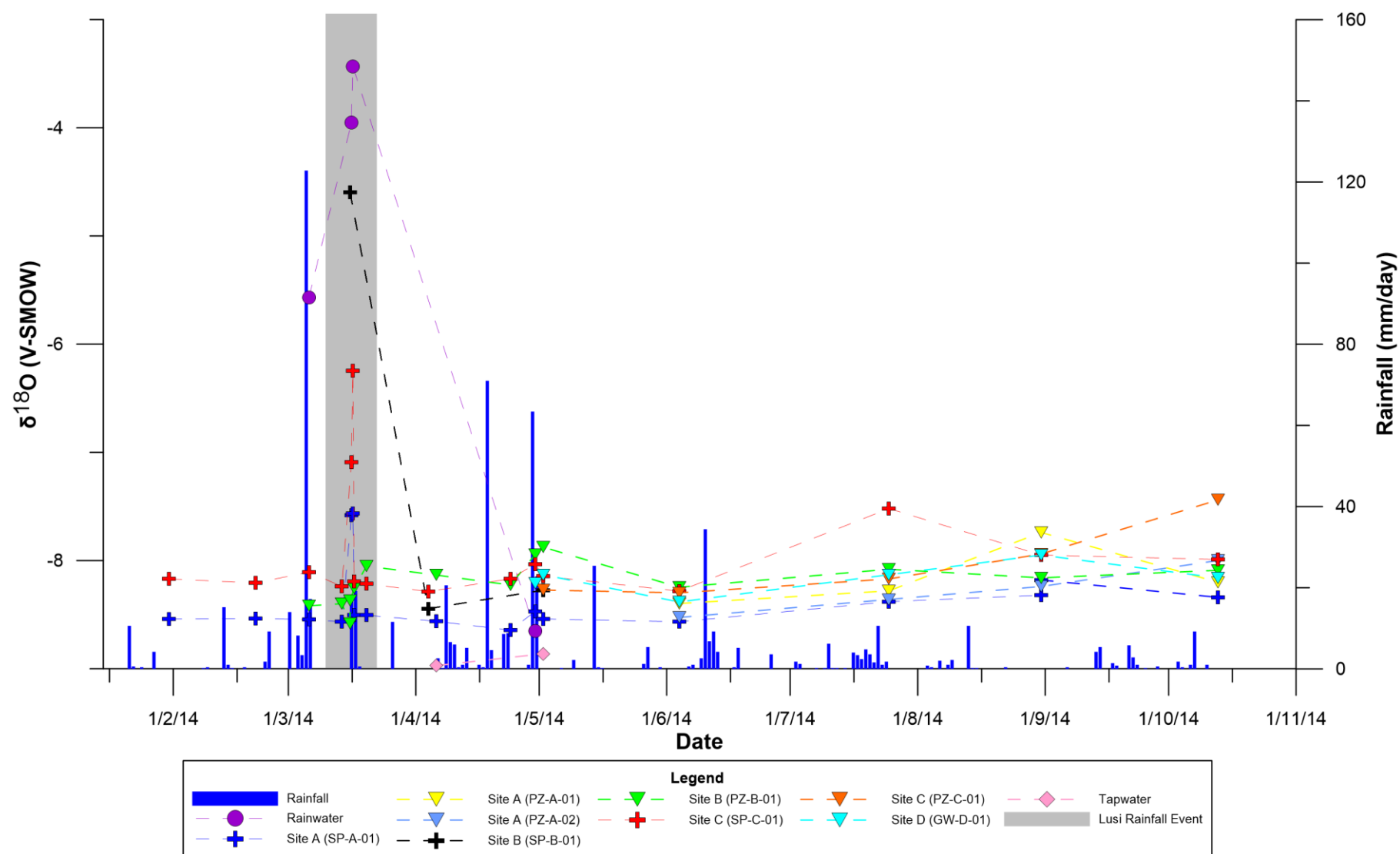


Figure 6.3: Plot of  $\delta^{18}\text{O}$  (V-SMOW) values and Daily Rainfall

### 6.6.2 Deuterium

Deuterium ( $\delta^2\text{H}$  V-SMOW) values are displayed in Figure 6. show a similar geospatial trend as the  $\delta^{18}\text{O}$  compositions throughout the valley, with mean values ranging between -54.2 and -57.3 for the Hillsborough Valley spring and ground waters, a 5.7 percent variation. The mean  $\delta^2\text{H}$  (V-SMOW) observed in rainfall was also more enriched with a value of -33.1 when compared to spring and groundwater. Again, this rainfall deuterium composition correlated with those measured by Tutbury (2015) who found a -35.13 (V-SMOW) average rainfall composition.

The temporal sampling results for  $\delta^2\text{H}$  (or  $\delta\text{D}$ ) are shown in Figure 3.12. These results show similar, trends as those for the  $\delta^{18}\text{O}$  analysis, as would be expected for meteorically derived groundwater waters. Slight variations can be observed in the trends however, particularly in the water samples from the Site B during mid-march and in the water from the Site A spring in the beginning of May 2014.

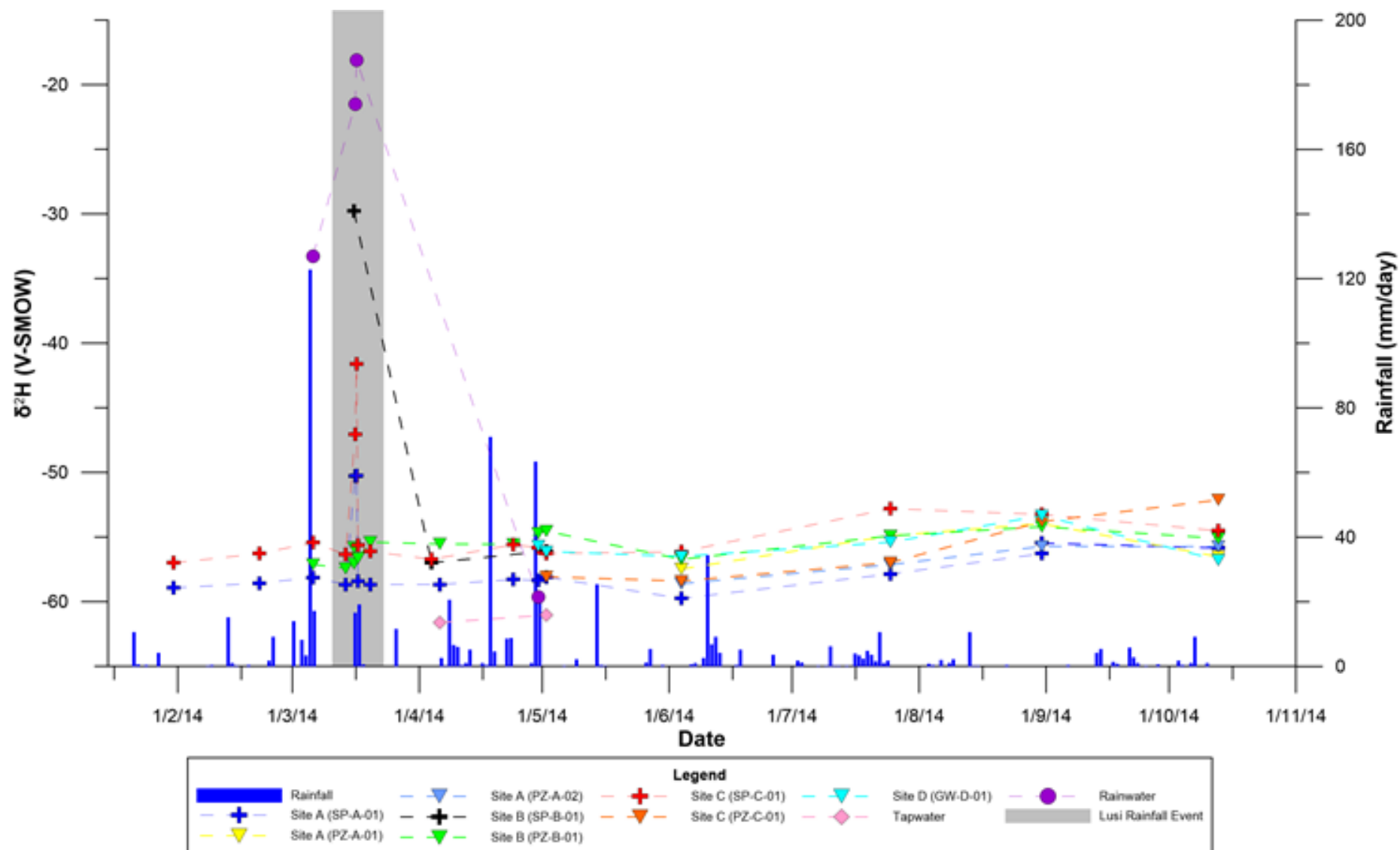


Figure 6.4: Plot of  $\delta^2\text{H}$  (V-SMOW) and Daily Rainfall for Hillsborough Valley water samples.

### 6.6.3 Stable Isotope samples compared with the Global Meteoric Water Line

The relationship between the isotopes of  $^{18}\text{O}$  and  $^2\text{H}$  when compared to the Global Meteoric Water Line (GMWL) is useful for determining the source of waters (Figure 6.5). If the  $\delta$  values plot along the GMWL the water is meteorically derived. If excessive evaporation has occurred, the ratio of  $\delta^{18}\text{O}$  compared to  $\delta\text{D}$  will not plot on the GMWL and will be more enriched in  $\delta^{18}\text{O}$  (Gat 2010)

Waters from the Hillsborough field area plot at near -8 ( $\delta^{18}\text{O}$ ), while Christchurch aquifer waters plot closer to -9 ( $\delta^{18}\text{O}$ ) along the GMWL. There is no evidence for evaporative modification of the Hillsborough Valley waters as all samples plot on, or close to, the GMWL.

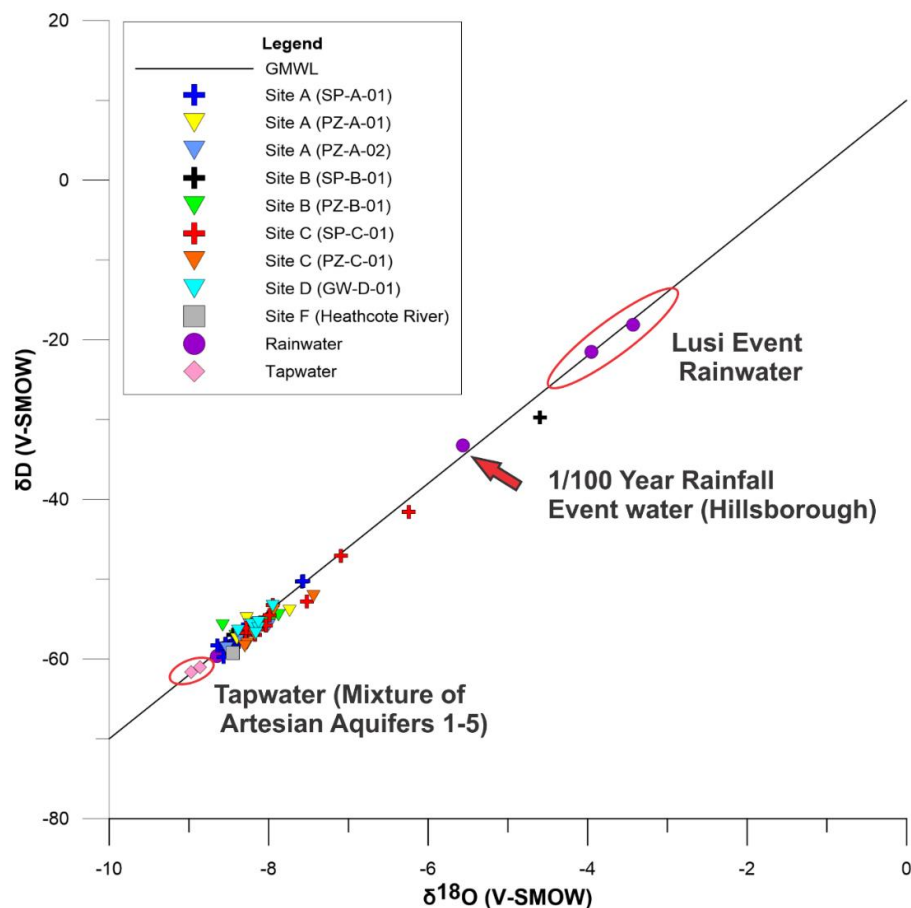


Figure 6.5:  $\delta\text{D}$  vs.  $\delta^{18}\text{O}$  plotted against the Global Meteoric Water Line (GMWL). Tap water collected at the Hillsborough Valley sites plots towards the lower end along the GMWL with more depleted stable isotope values compared to the springs and groundwater of the area. Both the Ex-Tropical Cyclone Lusi rainwater and 6th March 2014 1/100 year rainfall deluge waters are highlighted, these were collected in the rain gauge at the Site A. Rainwater collected the 29th April 2014 at Matipo Street plots closer toward the more negative  $\delta$  values of the Christchurch tap water.



## **6.7 Ionic Analysis**

Physical spring and piezometric monitoring described in Chapter 5 identified numerous fluctuations in spring discharge and groundwater. Short term fluctuations appeared to be due to rainfall events, with rapid spring discharge and groundwater level fluctuations recorded by data loggers at study sites A and B in Hillsborough Valley.

This section presents the results of the anionic analyses of the shallow ground waters collected in the Hillsborough Valley area. Cation values include those for Calcium, Magnesium, Sodium, and Potassium. The anions measured include Fluoride, Chloride, Nitrate, Sulphate and Phosphate. Anion data was analysed during the sample period and is displayed temporally to highlight short-term and long term fluctuations. The Ex-Tropical Cyclone Lusi rainfall event is also highlighted on the graphs. During this storm event, high frequency sampling was carried out, where the short term effects of a rainfall event on the spring and groundwater chemistry was analysed. The high frequency sampling carried out during this rainfall event is discussed later in this chapter.

### **Calcium (Ca)**

Calcium values for the spring waters are variable between the test sites. Site C spring (SP-C-01) has the highest levels with 49mg/L recorded, which is ~50% higher than the Sites A and B springs. Alternatively, Site A has the lowest recorded Calcium readings of 35mg/L. The most likely source of calcium in the water samples is due to the breakdown of calcium rich plagioclase feldspar in the basalts of the Banks Peninsula aquifers (Hem 1985). High levels of calcium are seen in the Banks Peninsula Spring waters (Weeber).

### **Magnesium (Mg)**

Magnesium concentrations in the spring waters are relatively lower than that of Calcium. Again, the highest concentrations of Mg were observed at Site C, whereas in contrast, the lowest concentration are seen in the Site E spring water. Magnesium is a major cation found in basalt, particularly olivine. Therefore a Banks Peninsula Aquifer source is most likely (Hem 1985). High concentrations of magnesium are observed in the Banks Peninsula Spring waters (Weeber).

### **Sodium (Na)**

Sodium is the most abundant cation in the Hillsborough spring waters, ranging from the lowest concentrations found at Site E (SP-E-01) of 84mg/L through to 151.6mg/L in the Site C (SP-C-01) spring water. Sodium in water has a wide range of source such as the dissolution of albite and is a constituent of NaCl which is sourced from seawater. (Hem 1985).

### **Potassium (K)**

Potassium is the least abundant cation in the Hillsborough Valley spring waters.

Concentrations range from 3.5mg/L (SP-A-01) through to 4.9mg/L in the SP-B-01 spring waters. Potassium is less common in igneous rocks but is found in and is more commonly a constituent of sedimentary rocks and will (Hem 1985).

### **Fluoride (F)**

Fluoride concentrations are variable (Figure 6.6), ranging between 0 and 1.7mg/L. Levels below the detectable limit for the test calibration occur in rainwater and groundwater during testing in mid-June at Site B and Site D. High levels of Fluoride (1.7mg/L) are seen in water collected from the groundwater at the Site C, and levels are relatively consistent over the 5 month period that its waters were tested. Also of interest is the similarity of the springs at Site A which is in the north-western mouth of the Valley and Site C which is on the south eastern section of the valley interior. Despite their very different locations within the Hillsborough Valley, the waters have similar and consistent fluoride levels of ~0.3mg/L. The waters with the most variable levels of Fluoride measured are those measured in Piezometer #2 (PZ-A-02) at the Site A and PZ-B-01 at the Site B. This may be due to variable amounts of waste water input into the subsurface at these locations from potentially leaky pipes which are situated within close proximity to both piezometers as shown in the Environment Canterbury map in Appendix IV (Figure IV.3). Fluoride is common found in apatite rich alkali rocks and is also found in wastewater (Hem 1985).

### **Nitrate (NO<sub>3</sub>)**

Nitrate concentrations in the Hillsborough water data exhibit marked variability both spatially and temporally (Figure 6.7 below). The high concentrations are seen in the spring waters of Site A and the highest overall concentrations were observed in samples collected from the Site C spring. Concentrations increased during rainfall in mid-March 2014 at Site A and PZ-B-01 at Site B but decreased for the spring water at Site C during this same period. There is also an

increase from nitrate concentrations of ~0 to 2.7mg/L for PZ-A-01 at Site A in the July 2014 samples, which subsequently receded to a low concentration ~0.1 in water samples collected in September 2014, in contrast to Piezometer #2 at the site which also has a marked increase in Nitrate in July 2014 and maintains higher concentrations of greater than 1mg/L for the subsequent sampling, despite the sample sites being located in close proximity to each other. Nitrates are common on the ground surface due to their presence in fertiliser. Nitrates are also common in peat due to the breakdown of organic matter (Hem 1985). Nitrates in the spring water may therefore indicate interactions with the underlying peat deposits in the Hillsborough area. .

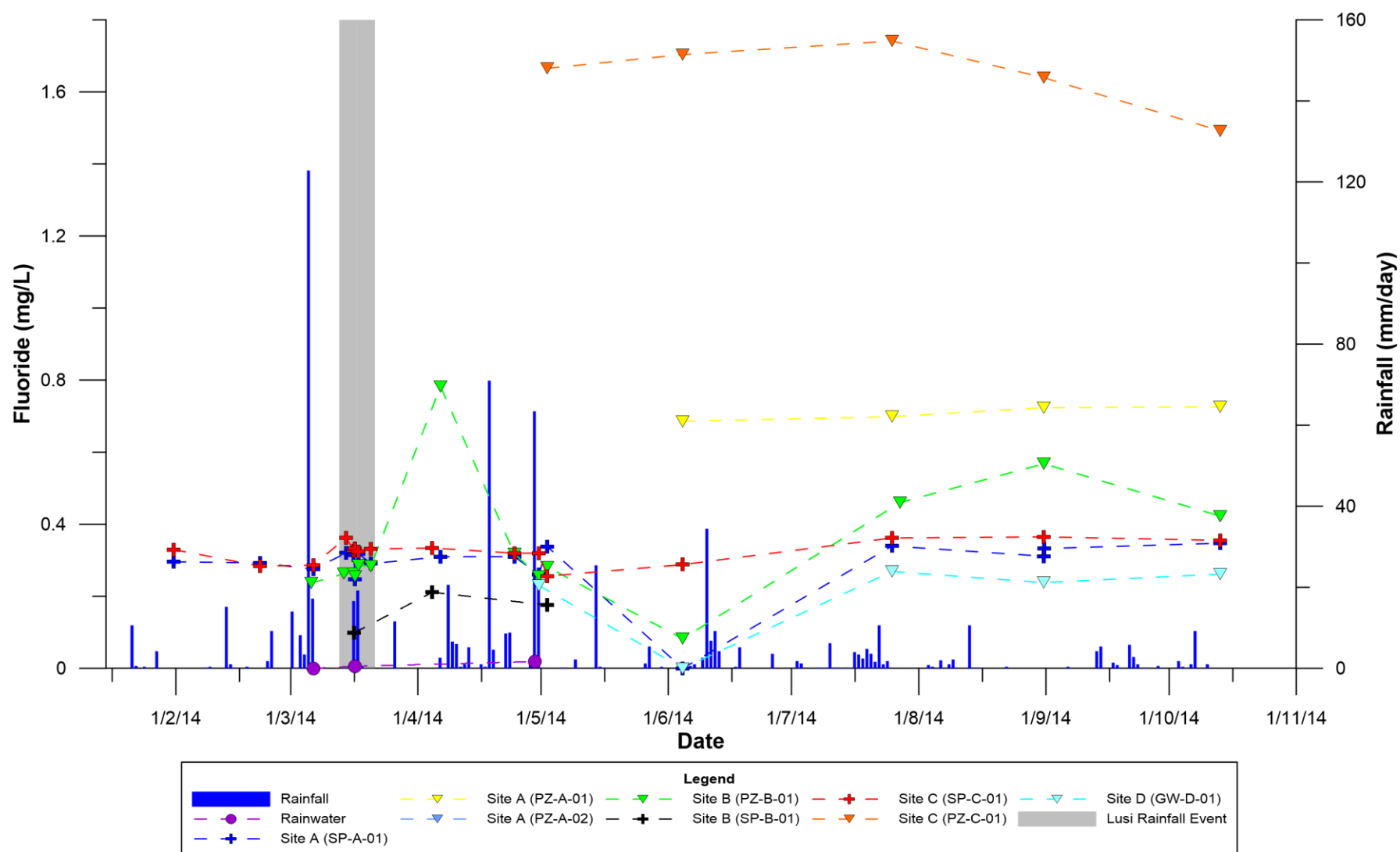


Figure 6.6: Fluoride anions (mg/L) for Hillsborough Valley water samples vs. rainfall

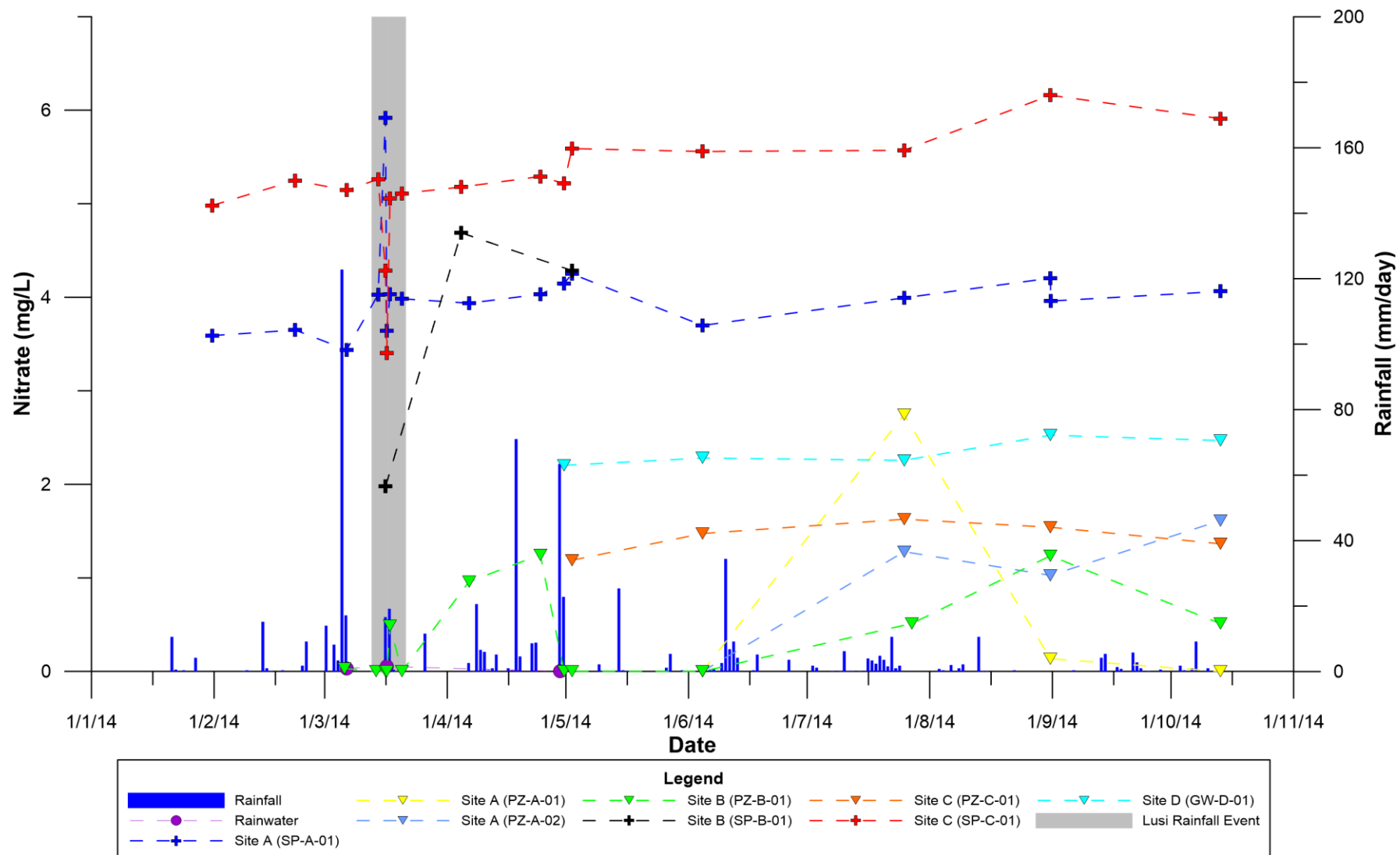


Figure 6.7: Nitrate anions (mg/L) for Hillsborough Valley water vs. rainfall.

## **Sulphate**

Sulphate concentrations range on average between a high of 46.3mg/L at the Site C spring and a low of 0.2 for the Site A piezometer PZ-A-01. High values (~50mg/L) occur in the spring waters throughout the Hillsborough area, yet the shallow ground waters sampled have considerably lower sulphate levels, and interestingly, the piezometers at Site A record sulphate concentrations as low as 0-2.6mg/L over the sample period, as opposed to the spring SP-A-01 which discharges three metres away (Figure 6.8). These values are comparable to rainwater sulphate concentrations, which range between 0.6 and 2.2mg/L. Interestingly, rainfall events dilute sulphate concentrations in both spring waters and ground waters. However, the spring waters appear to return to previous sulphate levels rapidly, in comparison with the groundwater in the sampled piezometers. This is particularly evident at Site B in PZ-B-01, where at the beginning of the test period which followed the early March 2014 1/100 year rainfall event, sulphate levels were at ~4mg/L, but by mid-March had risen to an average value for the testing period of 17.7mg/L. Values for each of the sampled waters for sulphate remained close to their respective average values for the duration of each sampling period. Sulphate values are higher in Banks Peninsula waters than Christchurch ground

## **Phosphate**

Phosphate concentrations are low in comparison to other anions (Figure 6.9) . Sampled phosphate concentrations range between concentrations as high as 3.5mg/L in rainwater from the Ex- Tropical Cyclone Lusi event and undetectably low levels during the same Lusi rainfall event in the Site B PZ-B-01. A similar dilution is observed in winter months. The phosphate concentrations in both ground waters and spring waters are highly variable between sampling periods. For example, both PZ-B-01 and the spring SP-B-01) at Site B at the beginning of June 2014 had Phosphate concentrations of 1.2mg/L and 1.4mg/L respectively, but by the end of July 2014 had dropped to very low concentrations which were unable to be accurately recorded (below the detectable limit of ~0.3mg/L).



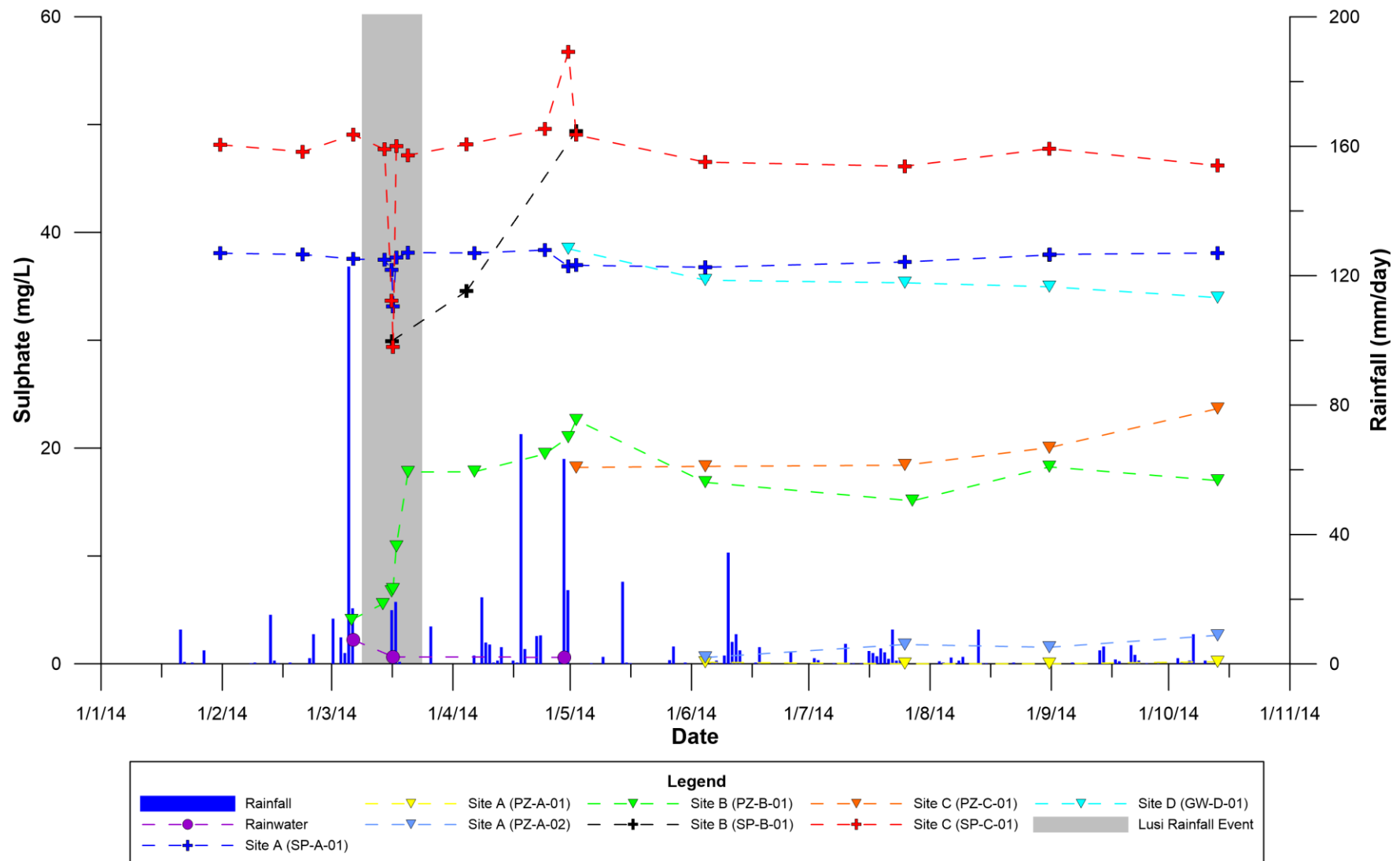


Figure 6.8: Sulphate anions (mg/L) for Hillsborough Valley water samples vs. rainfall

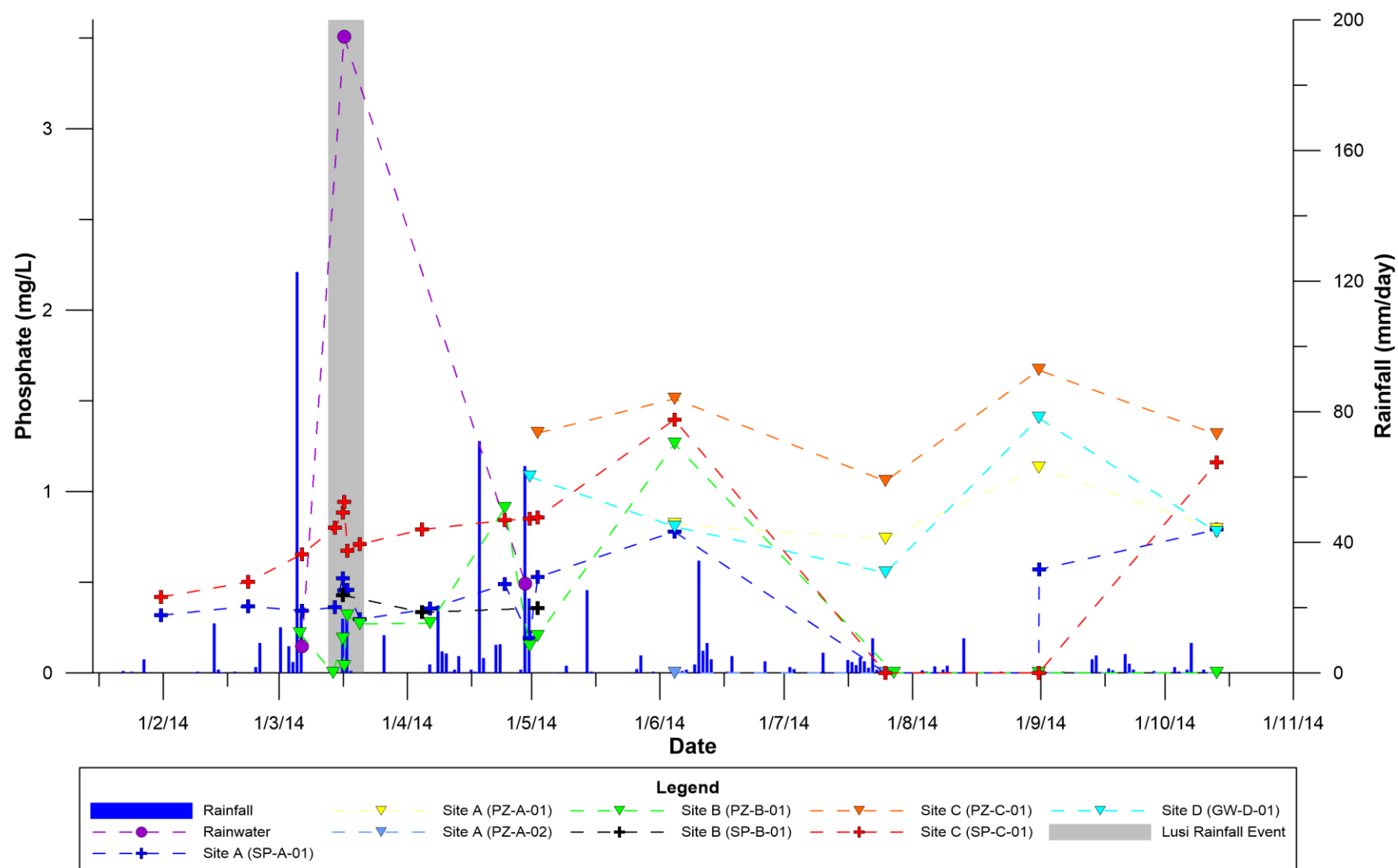


Figure 6.9: Phosphate anions (mg/L) for Hillsborough Valley water vs. rainfall

## Bicarbonate

Concentrations of bicarbonate ( $\text{HCO}_3$ ) is highly variable in the Hillsborough Valley spring waters, with a 279 percent variation in values between sites. The highest concentrations are observed at site E with 184mg/L in the spring water, whereas the lowest concentrations are seen in the Site A spring, with 48.6mg/L recorded (**Error! Reference source not found.**). Bicarbonate is seen in higher ratios in CAAS groundwater's than in Banks Peninsula waters.

## Chloride

Chloride mean concentrations range between a low of 23.6mg/l at Site C Piezometer to a high 251.4mg/L for piezometer PZ-A-01, as shown in **Error! Reference source not found.**. Therefore, chloride forms the most abundant anion in the Hillsborough Valley water samples. Although there is a range in chloride values collected in the area, levels remain relatively constant over the sampling period, with spring water values decreasing during rainfall events and groundwater chloride concentrations increasing following rainfall events (Figure 6.10). Rainwater collected in the area had much lower concentrations of chloride, ranging from 0.2-15.9mg/l. Although the piezometers at study site A are close in proximity to one and other, chloride values vary significantly between them, with PZ-A-01 averaging 251 mg/L while PZ-A-02 only averaged 134 mg/L over the same sampling period. The high levels of sodium and chloride in the spring and ground waters suggests that there is dissolved NaCl in the groundwater throughout the Hillsborough Valley. High Chloride values may be indicating seawater interactions, however Chloride salts are known to be in Banks Peninsula Birdlings Flat Loess (Griffiths 1973). Chloride is also observed in Banks Peninsula spring water, possibly an effect of deep circulating water and the insolubility of Chloride allowing enrichment in deep circulating waters (Feth 1981).

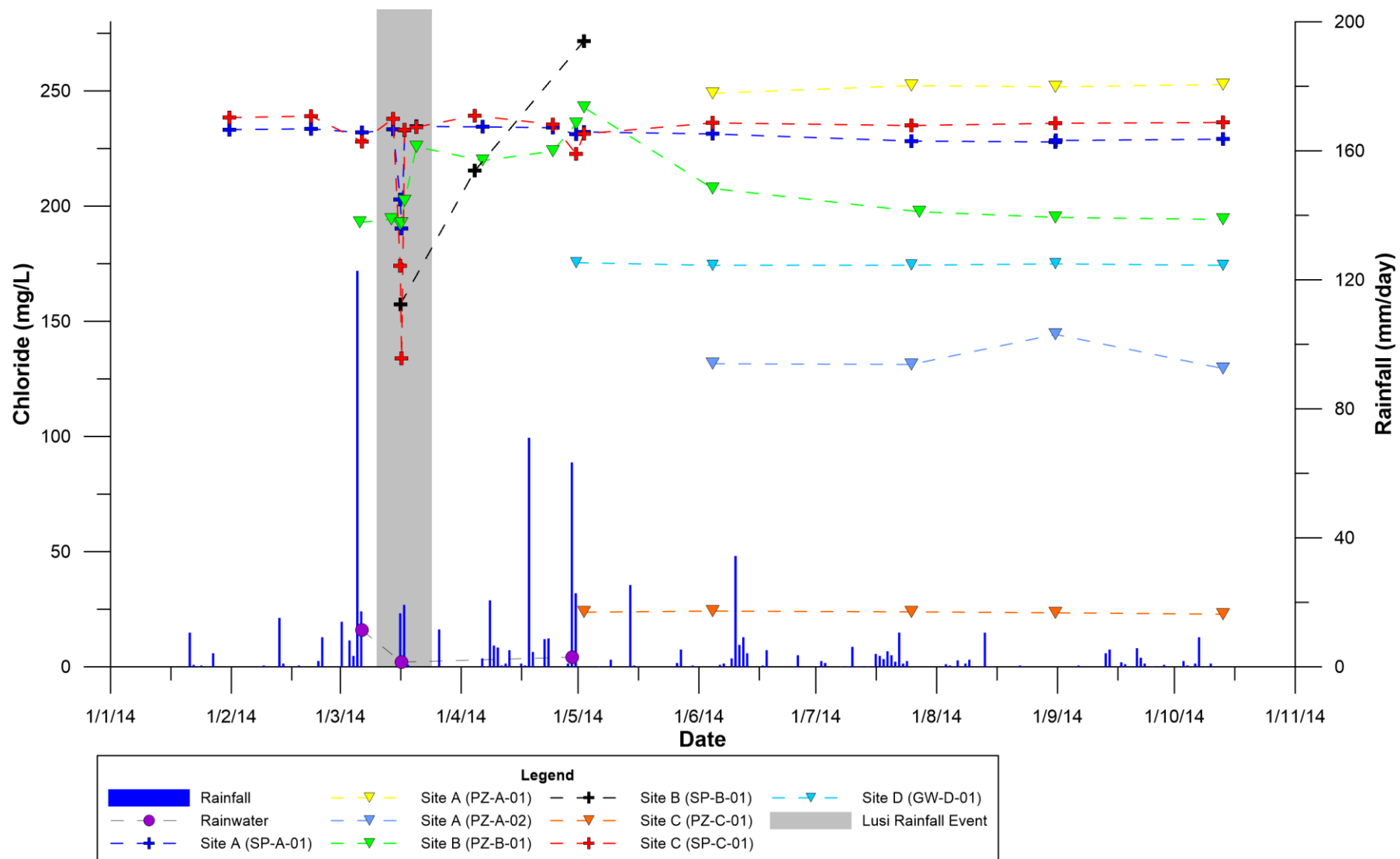
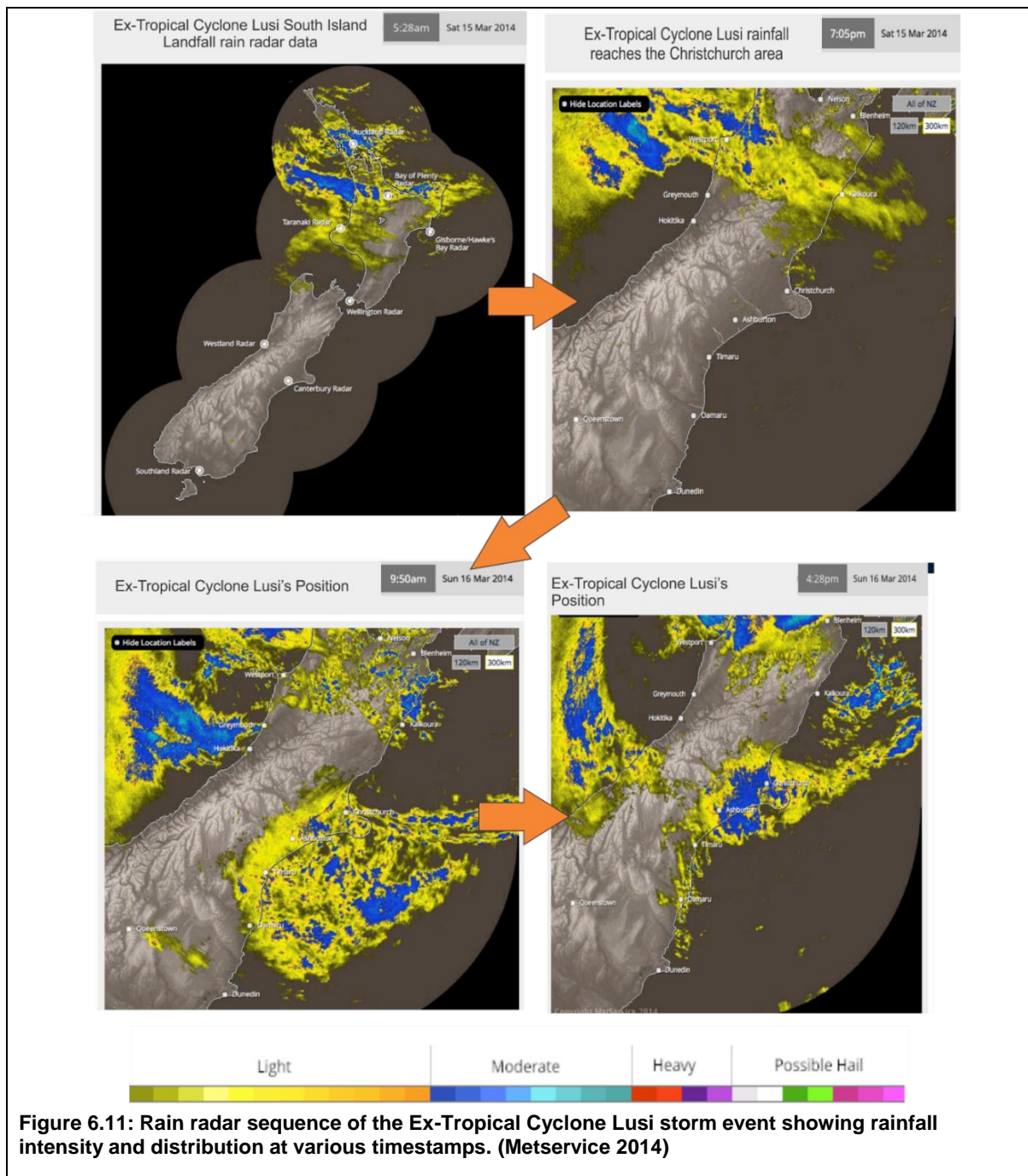


Figure 6.10: Chloride anions (mg/L) for Hillsborough Valley water vs. rainfall

## 6.8 Ex-Tropical Cyclone Lusi

Tropical Cyclone Lusi was the second severe tropical cyclone of the 2013-2014 season and affected the Pacific Islands of Fiji and Vanuatu and less severely, New Zealand. The storm was forecast to hit New Zealand on the 14<sup>th</sup> March 2014 (Metservice 2014). Lusi rainfall began falling at ~12:00am.



### **6.8.1 Significance**

Due to the Lusi storm being well forecast, the period prior to, during and following the event was chosen to observe the short-term response of spring discharge and groundwater level. Due to isotopic fractionation, the waters were expected to be depleted in the heavier  $\delta^{18}\text{O}$  stable isotope. The precipitation was in fact more enriched in  $\delta^{18}\text{O}$  and  $\delta^2\text{H}$  than expected, which subsequently still derives a distinct rainfall isotope signature which can be used to observe the groundwater-surface water interaction and recharge characteristics over time. The rainfall amounted to a total of 35mm for the Christchurch area (Metservice 2014)

### **6.8.2 High frequency sampling**

Samples of springs across sites A, B and C as well as groundwater from Piezometer PZ-B-01 were collected during the Lusi Storm event. Samples were collected at 12:00pm on the 14/03/2014, at 9:00am and 4:30pm on the 16/03/14 and at 12.00pm on the 17/03/2014 (Table 6.4).

### **6.8.3 Spring and Groundwater response**

The results show a variation due to rainfall infiltration. The springs spiked quickly and decreased rapidly, whereas groundwater increased more slowly and did not recede for the duration of the measurement. Rainfall has much lower (less negative)  $\delta^{18}\text{O}$  and chloride concentrations as when compared to the groundwater and springwater in the valley (Figure 6.12; 6.13)



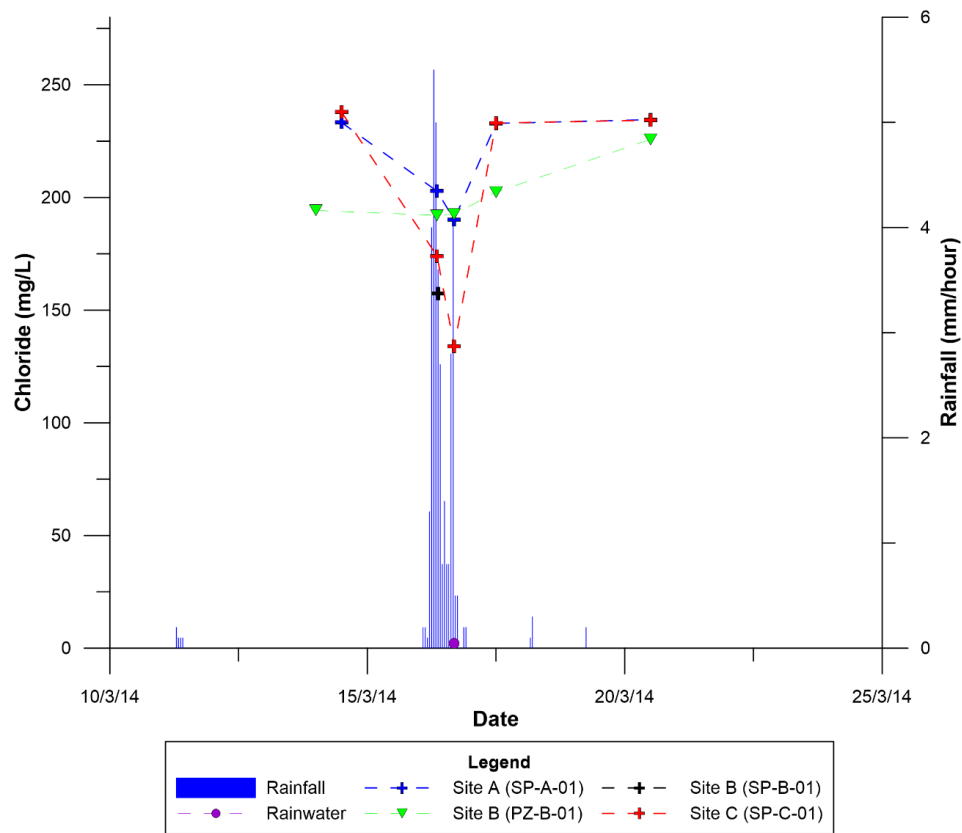
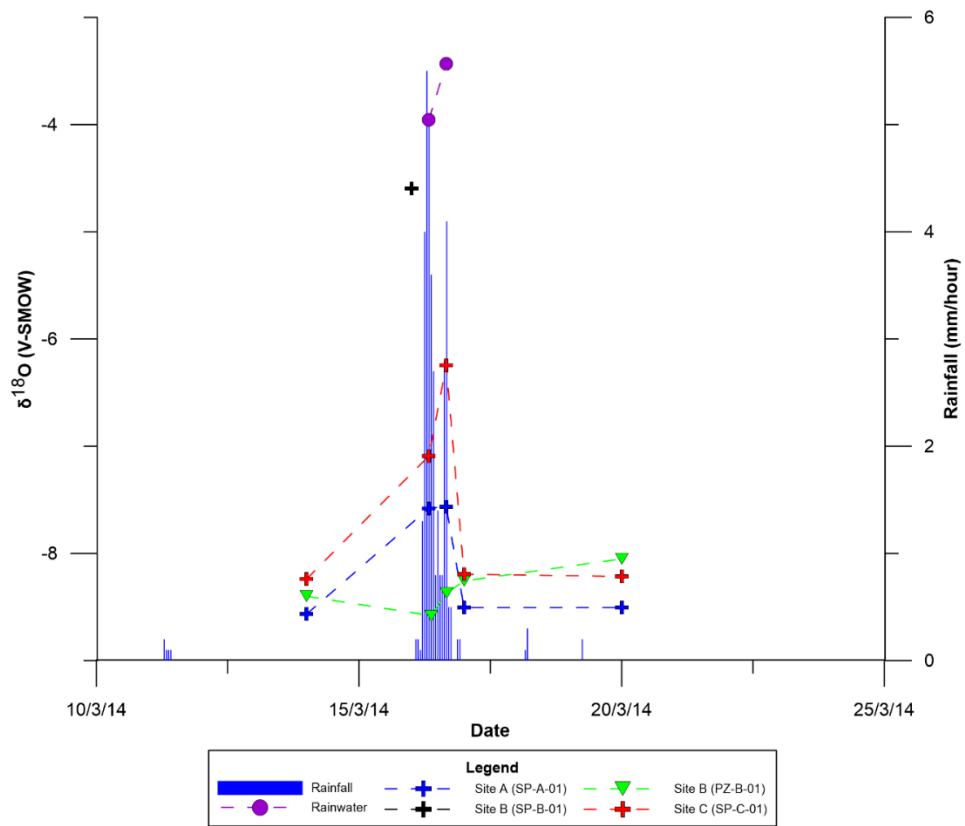


Table 6.6: Summary chart of ex-tropical cyclone Lusi storm event. Red Cells indicate a decrease in values and green cells increases of specific data. White cells are indicative of no measureable change.

	14/03/2014 12:00			16/03/2014 9:00			16/03/2014 16:00			17/03/2014 12:00			20/03/2014 12:00		
Water Level (M/bgs)/ Spring Discharge (L/min)	-0.27	6.00		-0.22	13.80		-0.30	14.40		-0.11	8.60		-0.35	7.80	
Temperature / Air Temp. (°C)	17.3/20	18.5/20	14.9/20	17.2/16	16.9/16	16.5/16	16.5/17	17.8/17	16.6/17	15.7/26	17.4/26	15.7/26	16.6/18	17.6/18	15.8/18
pH	6.71	7.24	7.35	6.24	7.47	6.06	6.33	6.37	6.16	6.42	6.43	6.42	6.44	6.46	6.44
$\delta^{18}\text{O}$ (V- SMOW)	-8.40	-8.57	-8.24	-8.58	-7.58	-7.09	-8.37	-7.56	-6.24	-8.26	-8.51	-8.19	-8.05	-8.51	-8.21
$\delta^2\text{H}$ (V- SMOW)	-57.42	-58.67	-56.36	-55.79	-50.28	-47.06	-57.05	-50.26	-41.60	-56.65	-58.42	-55.65	-55.39	-58.67	-56.11
FI (mg/L)	0.26	0.32	0.36	0.26	0.31	0.33	0.26	0.25	0.33	0.29	0.32	0.32	0.28	0.29	0.33
Cl (mg/L)	194.21	233.23	237.86	192.03	202.77	174.01	192.57	190.17	133.95	202.31	232.83	233.04	225.76	234.54	234.26
Br (mg/L)	0.58	0.59	0.65	0.54	0.47	0.57	0.57	0.02	0.47	0.61	0.58	0.63	0.65	0.61	0.63
$\text{NO}_3$ (mg/L)	0.00	4.02	5.26	0.00	5.92	4.29	0.00	3.64	3.40	0.49	4.03	5.05	0.00	3.98	5.11
$\text{SO}_4$ (mg/L)	5.55	37.46	47.70	6.69	36.52	33.67	6.93	33.13	29.39	10.89	37.65	47.99	17.77	38.13	47.15
$\text{PO}_4$ (mg/L)	0.00	0.36	0.80	0.19	0.52	0.88	0.04	0.46	0.94	0.32	0.46	0.67	0.27	0.30	0.71
	PZ-B-01	SP-A-01	SP-C-01	PZ-B-01	SP-A-01	SP-C-01	PZ-B-01	SP-A-01	SP-C-01	PZ-B-01	SP-A-01	SP-C-01	PZ-B-01	SP-A-01	SP-C-01

## 6.9 Hydrochemical comparison with Canterbury natural water

Water samples collected by Aqualinc Research Ltd and Griffin. (in prep) allow for the geochemical classification of the Hillsborough Valley water based on the ratios of major ions in the water. The piper plot of the chemical constituents of the Hillsborough Valley spring water and other spring and groundwater data from Christchurch and Banks Peninsula are displayed in Figure 6.14. Spring water from Site A and Site B plot closely to the Palatine well, which is sourcing water from the riccarton gravel aquifer and may be mixing with the adjacent Port Hills bedrock sourced water. This water plots closely to the milliequivalent composition of a freshwater-seawater mixture (Appelo & Postma 1993). The water sample from Site E plots with a similar composition as other bedrock sourced springs within Banks Peninsula. The Christchurch Artesian Aquifer System, Heathcote Valley, Alluvial Banks Peninsula groundwater and the Lyttelton Railway tunnel each possess distinctly different geochemical signatures.

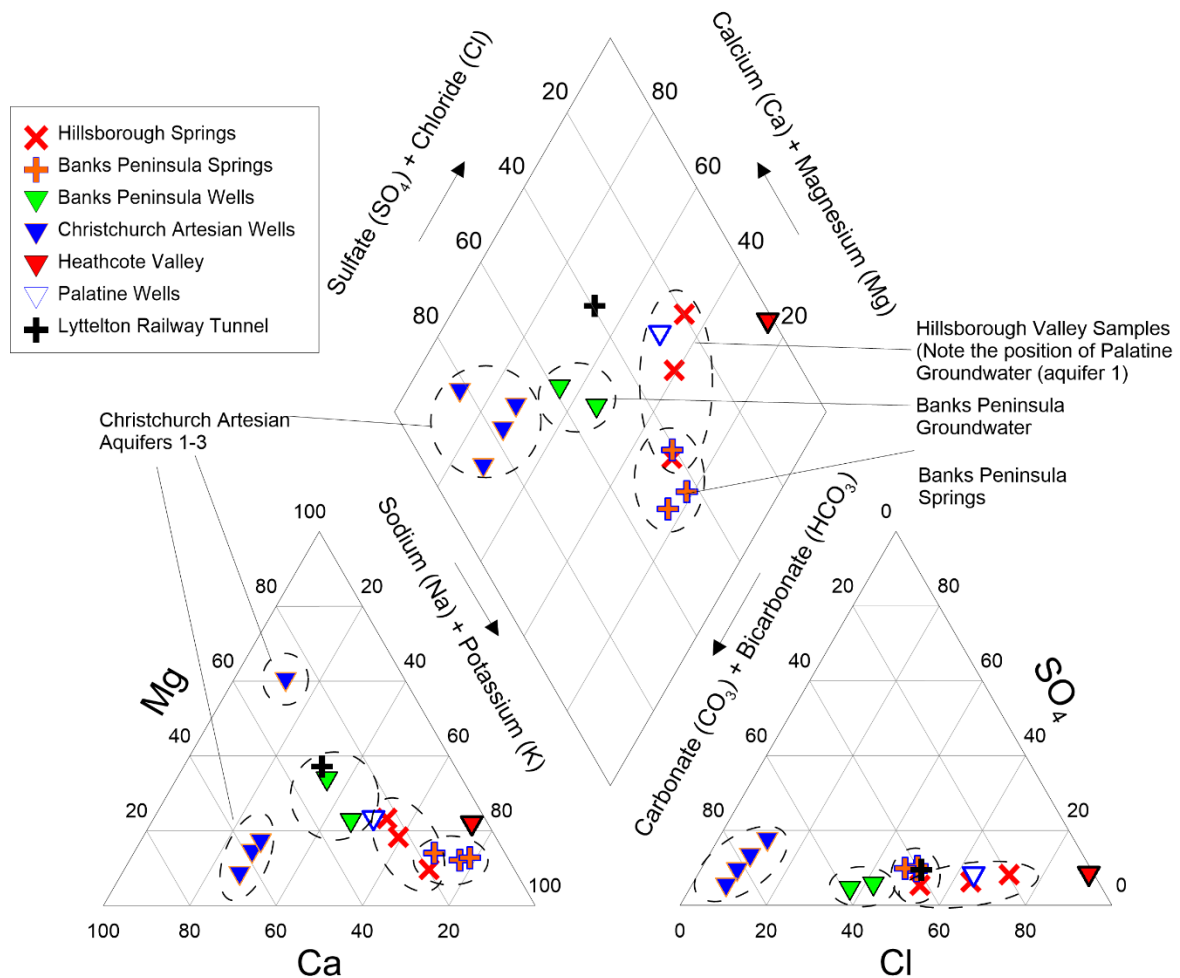


Figure 6.14: Piper plot of various spring and groundwater water samples from the greater Christchurch area

Geospatial variations in the water sample are apparent when displayed as geographically oriented stiff plots (Figure 6.15), where patterns are observed in the various water samples.

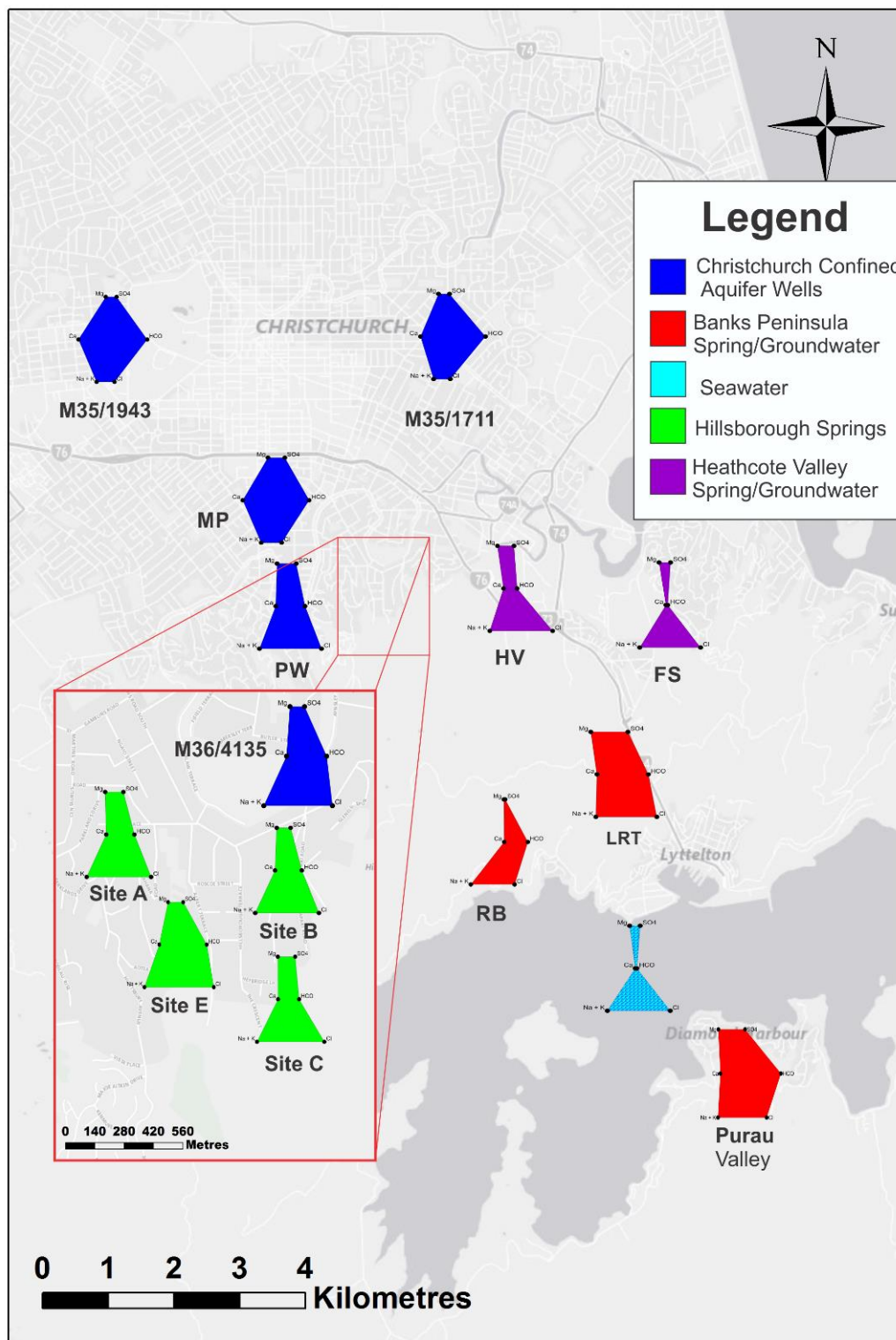


Figure 6.15: Stiff plots for selected Christchurch spring and well waters. Spring water samples from the Hillsborough Valley study sites are shown in the inset. PW=Palatine Place and MP= Colombo Street “Main Pumps” Community water Supply well waters, HV= Heathcote Valley Well, FS= Ferrymead Spring, LRT= Lyttelton Railway Tunnel Spring, RB= Rapaki Bay Spring.

Spring water from sites A, B and C show a similar geochemical consistency, with slightly higher Na+K and Cl milliequivalent percentages observed in the Site C spring (SP-C-01). The less mineralised spring water from Site E shows higher amounts of Ca and HCO<sub>3</sub> when contrasted to the other Hillsborough Valley springs. The thermal and mineralised water of the  $\geq 55.2$ m well M36/4135 (Brown & Weeber 1994) and the Palatine Terrace Community supply well appear geochemically similar to the Banks Peninsula bedrock sourced groundwater of the Purau Valley (Parker 1989). The CAAS derived waters from wells distributed though Christchurch show a distinctly similar chemistry, with higher ratios of calcium and bicarbonate as opposed to the other major ions. The effects of seawater intrusion are evident in the Heathcote Valley spring and borehole, with more NaCl rich water measured in the Ferrymead thermal spring closer to the coastline and Avon-Heathcote Estuary. The spring at Rapaki Bay resembles the chemical characteristics of a deep-circulated sodium-bicarbonate thermal spring (Brown & Weeber 1994; White 2010)

## Chapter 7. Summary and Conclusions

### 7.1 *Thesis Objectives and Methodology*

The primary aims for this thesis project were to determine the locations, morphology, source and cause of the 2010-2011 Canterbury earthquake sequence related springs in footslope positions of the Port Hills of Christchurch, New Zealand. The objectives for this thesis are outlined in the section below,

The Hillsborough Valley in St. Martins, Christchurch was selected as the study area for this project, as it displayed a noteworthy combination of earthquake related ground deformation and spring formation, as highlighted by previous studies. Specific objectives were:

- To Produce relevant maps and site plans documenting the geospatial features of the study area, infrastructure, areas of particular spring activity and ground deformation, and the locations of springs that were studied.
- Measure and record geophysical and chemical data for the springs over a 10-12 month period to better understand both short-term and seasonal fluxes in spring discharge and chemistry.
- Produce hydrogeological models of the valley based on geotechnical and hydrochemical investigations which detail the spring morphologies, water source and flow mechanism(s) within the Hillsborough Valley.
- Display the results of the investigations in clear and understandable outputs that are of use to third parties and are scientifically accurate and consistent.

To achieve these objectives, three key methodologies were followed. These were Site Investigations and Mapping, Physical groundwater level and spring discharge measurements and Geochemical and Stable Isotope analysis of the spring water, ground water and rain water.

Site investigations logged the location of extensional and compressional ground deformation in the Hillsborough Valley and documented the location of  $\geq 40$  spring features in the study area. The majority of these springs formed in areas of either mass-movement related ground compression or earthquake related ground fissures formed as a result of mass-movement induced ground extension.



Spring discharge was measured by a combination of short-term, high frequency automatically gauged weir measurements or by long-term single-sample manual spring discharge measurements. Similarly, groundwater was measured by either automatic level troll barometers or by manually measuring the water samples from the piezometer using a dip meter.

Samples of groundwater, spring water and rainwater were also collected during the sampling period and analysed for their relative isotopic composition and ionic concentrations. Testing was carried out at the University of Canterbury.

## ***7.2 Physical Hydrogeology***

Piezometric investigations show that the Hillsborough Valley water table is shallow (<1m b/gl) throughout the valley floor and has a slight upward gradient through the valley ridge slopes. This shallow groundwater table was a pre-existing hydrogeological feature of the valley, as shown in historic borehole data.

Investigation of the spring location, discharge quantity and orifice morphology allowed them to be classified into Artesian and Gravitational type springs. Both spring types appear to be fed through artesian-like vents, where groundwater is able to emerge at the land surface due to the earthquake related compressional fractures or extensional fissures. The springs may also be secondary in nature, where the colluvial deposits of the Hillsborough Valley may be overlying the original subsurface discharge location of the spring water.

The presence of peat deposits associated with swampy land that existed in the valley prior to infilling correlates with the location of springs in the Valley Floor. This may be due to the peat distributing subsurface water flow from the centre of the valley to the outer margins.

### **7.2.1 Spring discharge**

Spring discharge is variable between the two monitored springs (SP-A-01 and SP-B-01), with both springs also showing high levels of variable discharge rate over the study period.

Monthly discharge measurements were made for the Site A spring over an 8 month sampling period, with additional sampling carried out over 8-12 hours of the ex-tropical cyclone Lusi event, collected over a four day period. These discharge measurements showed a high degree

of variability between 4.2 and 14.4L/min (a 243% variation). A season trend appears to be visible, with lowest discharge levels observed during the drier spring months, as opposed to the unseasonably wet March-May 2014 where spring flows were on average higher.

Secondary discharge variation is observed during rainfall, where spring discharges levels spike during rainfall events and then recede to lower discharge levels in the days following the rainfall. This was observed during the high frequency monitoring of Site A spring during the Ex-Tropical cyclone Lusi Event. Similar spike and rapid recession trends were observed for the Site B spring during rainfall events. This implies groundwater infiltration is increasing spring flow, or that rainfall events increase the groundwater potentiometric surface on the underlying aquifer system which feed the springs, thus increasing pore pressure and subsequently spring discharge.

### **7.2.2 Piezometric levels**

Groundwater levels show similar seasonal and rainfall response trends as the spring discharge fluctuations, with rapid spikes in groundwater level following rainfall events being observed. However, groundwater level recession occurs over weeks and not days as it does for spring discharge. This implies that rainfall infiltration and the potentiometric surface in the valley may both be influencing the shallow water table.

## **7.3 Chemical Hydrogeology**

Ionic composition of the Hillsborough Valley water show that the spring water in the Hillsborough Valley is mineralised when compared to Christchurch Artesian Aquifer water. With slight variations observed geospatially throughout the valley.

Fluctuations in the chemical composition of the sampled waters varies with rainfall input, which coincides with increases in groundwater level and associated. Spring chemistry values are more constant when compared to those of the shallow ground water. This implies that the source for the spring water is deeper than the shallow (~3m) groundwater.

The residential nature of the valley may be altering the samples, with subsurface wastewater and storm water drains occurring throughout the valley

Stiff and Piper plots of the Hillsborough Valley spring waters seem to show that springs which occur at the entrance of the valley most-related to Banks Peninsula bedrock derived groundwater, with possibly some seawater interactions as is observed occurring in the Heathcote Valley to the east.

#### ***7.4 Isotope Hydrogeology***

The stable oxygen and hydrogen isotopic composition of the spring and groundwater's in the Hillsborough is most similar to Banks Peninsula bedrock derived spring and groundwater.

Isotopic compositions remain relatively consistent over the 10 month sampling period. Some fluctuations in isotopic composition especially during rainfall where increased groundwater level and spring discharge occurs. As was observed with the ionic data, spring water fluctuations in stable isotope composition show a rapid spike in values during major rainfall events, but quickly return to their pre-rainfall values in the 24 hours following rainfall

#### ***7.5 Principal Conclusions***

Principle conclusions for this thesis study are as follows:

- Groundwater springs emerged in the Hillsborough Valley as a results of ground deformation and increased pore pressures. This is inferred to be due to increased bedrock permeability, which resulted from earthquake shaking. These spring water discharge rates became exaggerated with subsequent earthquakes, in particular the 22<sup>nd</sup> February 2011 event.
- The spring water is most closely related to Banks Peninsula bedrock derived groundwater, with variability observed towards the valley entrance with the implication of mixing with Christchurch Artesian Aquifer System waters derived as underflow from the Waimakariri River.

- The spring waters are clearly not related to direct rainfall infiltration, as evidenced by isotopic data, anion chemistry and slightly elevated temperatures.
- The isotopic composition values remained relatively constant through the study period, indicating that the springs are sourced deeply and are not directly related to the shallow groundwater.

## **7.6 *Future Research***

- Future research requires deeper bores within the central part of the valley to identify a source aquifer, and carefully constrained screen intervals.
- The influence of peats in the Hillsborough Valley also requires further investigation as a source of spring waters.
- Higher frequency or continuous sampling during rainfall events is a requirement to better understand the relation between deeper bedrock waters and rainfall events.

## References

- AAM, 2011. Christchurch City Council Christchurch lidar survey. May 2011. , 18797(May), pp.1–9.
- Almond, P.C. et al., 2007. An OSL, radiocarbon and tephra isochron-based chronology for Birdlings Flat loess at Ahuriri Quarry, Banks Peninsula, Canterbury, New Zealand. *Quaternary Geochronology*, 2(1-4), pp.4–8.
- Appelo, C.A.J. & Postma, D., 1993. Geochemistry, groundwater and pollution .
- Bannister, S. & Gledhill, K., 2012. Evolution of the 2010–2012 Canterbury earthquake sequence. *New Zealand Journal of Geology and Geophysics*, 55(3), pp.295–304.
- Beavan, J. et al., 2012. Fault slip models of the 2010–2011 Canterbury, New Zealand, earthquakes from geodetic data and observations of postseismic ground deformation. *New Zealand Journal of Geology and Geophysics*, 55(3), pp.207–221.
- Bell, D.H. & Trangmar, B.B., 1987. Regolith Materials and Erosion Processes on the Port Hills, Christchurch, New Zealand. In *5th International Conference and Field Workshop on Landslides. Christchurch*. pp. 93–105.
- Brassington, R., 2007. *Field hydrogeology*, Hoboken, NJ; Chichester, England: John Wiley.
- Brown, L.J. et al., 1995. Geology of Christchurch, New Zealand. *Environmental & Engineering Geoscience U6*, 1(4), pp.427–488.
- Brown, L.J. & Weeber, J.H., 1992. *Geology of the Christchurch Urban Area.*, Institute of Geological & Nuclear Sciences.
- Brown, L.J. & Weeber, J.H., 1994. Hydrogeological implications of geology at the boundary of Banks Peninsula volcanic rock aquifers and Canterbury Plains fluvial gravel aquifers. *New Zealand Journal of Geology and Geophysics*, 37(2), pp.181–193.
- Brown, L.J., Weeber, J.H. & Reay, M.B., 1992. *Geology of the Christchurch Urban Area*,
- Browne, G.H. et al., 2012. The geological setting of the Darfield and Christchurch earthquakes. *New Zealand Journal of Geology and Geophysics*, 55(3), pp.193–197.
- Bryan, K., 1919. Classification of Springs. *The Journal of Geology*, 27(7), pp.522–561.
- CERA, 2015. Project Orbit (Canterbury Geotechnical Database).
- Christchurch City Council, 2015. Chemsitry of Christchurch Groundwater. Available at: <http://www.ccc.govt.nz/homeliving/watersupply/ourwater/chemicalanalysis.aspx>.
- Christchurch City Council, 2010. *Waterways, wetlands and drainage guide: Ko te anga whakaora mō ngā arawai rēpō*, Christchurch, N.Z: Christchurch City Council.
- Coates, G., 2002. *The Rise and Fall of the Southern Alps*, Christchurch: Canterbury University

Press.

- Cox, S. et al., 2012. 7.1 Darfield (Canterbury) earthquake, 4 September 2010, New Zealand. *New Zealand Journal of Geology and Geophysics*, 55(3), pp.231–247.
- Cubrinovski, M. et al., 2011. Geotechnical aspects of the 22 February 2011 Christchurch earthquake. *Bulletin of the New Zealand Society for Earthquake Engineering*, 44(4), pp.205–226.
- DeMets, C., Gordon, R.G. & Argus, D.F., 2010. Geologically current plate motions. *Geophysical Journal International*, 181(1), pp.1–80.
- Elliott, J.R. et al., 2012. Slip in the 2010-2011 Canterbury earthquakes, New Zealand. *Journal of Geophysical Research: Solid Earth*, 117(B3), p.n/a–n/a.
- Environment Canterbury, 2015. Canterbury Maps.
- Fetter, C.W., 2001. Applied Hydrogeology. *Applied Hydrogeology*, p.615.
- Forsyth, P.J., Barrell, D.J.A. & Jongens, R., 2008. *The Geology of the Christchurch Area*, Lower Hutt, New Zealand: Institute of Geological & Nuclear Sciences 1:250 000 geological map 16. 1 sheet.
- Gat, J., 2010. Isotope hydrology: a study of the water cycle . , 6;6.; .
- Geotechnical Extreme Events Reconnaissance (GEER), 2011. Geotechnical reconnaissance of the 2011 Christchurch, New Zealand earthquake. Available at: [http://www.geerassociation.org/GEER\\_PostEQReports/Christchurch\\_2011/Cover\\_Christchurch\\_2011.html](http://www.geerassociation.org/GEER_PostEQReports/Christchurch_2011/Cover_Christchurch_2011.html) [Accessed April 24, 2015].
- Gledhill, K. et al., 2011. The darfield (Canterbury, New Zealand) Mw 7.1 earthquake of september 2010: A preliminary seismological report . *Seismological Research Letters* , 82 (3 ), pp.378–386.
- GNS Science, 2010. GNS Science. Available at: <http://www.gns.cri.nz/> [Accessed February 16, 2015].
- GNS Science, 2015. GNS Science Christchurch Fault Map. Available at: <http://www.gns.cri.nz/Home/Our-Science/Natural-Hazards/Recent-Events/Canterbury-quake/Recent-aftershock-map> [Accessed April 4, 2015].
- Google Earth, 2015. No Title.
- Griffin, S., *Geochemical tracing of the source of dissolved inorganic carbon and chloride in Banks Peninsula warm springs, New Zealand*. University of Canterbury.
- Griffiths, E., 1973. Loess of Banks Peninsula. *New Zealand Journal of Geology and Geophysics*, 16(3), pp.657–675.
- Gulley, A.K. et al., 2013. Groundwater responses to the recent Canterbury earthquakes: A

- comparison. *Journal of Hydrology*, 504, pp.171–181.
- Hampton, S.J., 2010. *Growth, structure and evolution of the Lyttelton Volcanic Complex, Banks Peninsula, New Zealand: a thesis submitted in fulfilment of the requirements for the degree of Doctor of Philosophy in Geology at the University of Canterbury*.
- Heath, R.C., 1983. Basic Ground-Water Hydrology. *US Geological Survey Water Supply Paper*.
- Hiscock, K.M., 2005. *Hydrogeology: principles and practice*, Malden, MA: Blackwell Pub.
- Hornblow, S. et al., 2014. Paleoseismology of the 2010 Mw 7.1 Darfield (Canterbury) earthquake source, Greendale Fault, New Zealand. *Tectonophysics*, 637, pp.178–190.
- Hunt, T.M. & Bibby, H.M., 1992. Geothermal Hydrology. In M. P. Mosely, ed. *Waters of New Zealand*. New Zealand Hydrological Society.
- In-Situ Inc., 2015. Operators Manual: Level TROLL® 300, 500, 700, 700H Instruments. Available at: <https://in-situ.com/wp-content/uploads/2015/03/Level-TROLL-300-Manual.pdf> [Accessed March 5, 2015].
- Jayet, D.F., 1986. *An examination of observed climatic trends/changes over Banks Peninsula and the surrounding plains area, and their synoptic climatology*. University of Canterbury. Department of Geography.
- Kaiser, a et al., 2012. 6.2 Christchurch earthquake of February 2011: preliminary report. *New Zealand Journal of Geology and Geophysics*, 55(1), pp.67–90.
- Kalbus, E., Reinstorf, F. & Schirmer, M., 2006. Measuring methods for groundwater, surface water and their interactions: a review. *Hydrology and Earth System Sciences Discussions*, 3(4), pp.1809–1850.
- Kresic, N., 2010. *Types and classifications of springs* 1st ed., Elsevier Inc.
- Kresic, N. & Bonacci, O., 2010. Spring discharge hydrograph. *Groundwater Hydrology of Springs*, pp.129–163.
- Li, Y.G. et al., 2014. Fault damage zones of the M7.1 Darfield and M6.3 Christchurch earthquakes characterized by fault-zone trapped waves. *Tectonophysics*, 618, pp.79–101.
- Lowry, C.S., Fratta, D. & Anderson, M.P., 2009. Ground penetrating radar and spring formation in a groundwater dominated peat wetland. *Journal of Hydrology*, 373(1), pp.68–79.
- Manga, M. & Wang, C.Y., 2007. Earthquake Hydrology. *Treatise on Geophysics*, 4, pp.293–320.
- Macdonald, G.A., 1953. Pahoehoe, aa, and block lava . *American Journal of Science* , 251 (3 ), pp.169–191.
- Macdonald, G.A., Abbott, A.T. & Peterson, F.L., 1983. Volcanoes in the sea: the geology of



- Hawaii . , 2nd .
- McGann, R.P., 1983. *The Climate of Christchurch*, Wellington, N.Z.
- Meinzer, O.E., 1923. *The occurrence of ground water in the United States, with a discussion of principles* - ed.,
- Metservice, 2015. [www.metservice.com](http://www.metservice.com).
- Moore, P.D., 1989. The ecology of peat-forming processes: a review . *International Journal of Coal Geology* , 12 (1 ), pp.89–103.
- Namjou, P., 1988. *Hydrogeological and geophysical investigation of the groundwater system in the Kaituna Valley, Banks Peninsula*. University of Canterbury. Geology U6 - ctx\_ver=Z39.88-2004&ctx\_enc=info%3Aofi%2Fenc%3AUTF-8&rft\_id=info:sid/summon.serialssolutions.com&rft\_val\_fmt=info:ofi/fmt:kev:mtx:dissertation&rft.genre=dissertation&rft.title=Hydrogeological+and+geophysical+investi.
- NIWA, 2015. Niwa CliFlo Database. Available at: [cliflo.niwa.co.nz](http://cliflo.niwa.co.nz).
- Ogilvie, G., 2009. *The Port Hills of Christchurch*, Christchurch, N.Z: Phillips & King.
- Parker, S.K., 1989. *The hydrogeology of the Diamond Harbour region, Banks Peninsula: a thesis submitted in partial fulfilment of the requirements for the degree of Master of Science in Engineering Geology, University of Canterbury*,
- Piccaro, 2010. ChemCorrect™- Solving the Problem of Chemical Contaminants in H2O Stable Isotope Research. Available at: [http://www.picarro.com/assets/docs/Picarro\\_-\\_ChemCorrect\\_White\\_Paper.pdf](http://www.picarro.com/assets/docs/Picarro_-_ChemCorrect_White_Paper.pdf) [Accessed March 21, 2015].
- Quigley, M. et al., 2012. Surface rupture during the 2010 M-w 7.1 Darfield (Canterbury) earthquake: Implications for fault rupture dynamics and seismic-hazard analysis . *GEOLOGY* , 40 (1 ), pp.55–58.
- Ring, U. & Hampton, S., 2012. Faulting in Banks Peninsula: tectonic setting and structural controls for late Miocene intraplate volcanism, New Zealand. *Journal of the Geological Society*, 169(6), pp.773–785.
- Rojstaczer, S. & Carolina, N., 1992. Permeability changes associated with large earthquakes: An example from Loma Prieta, California. *Geology*, 20, pp.211–214.
- Rutter, H., 2011. Earthquake Related Springs. *qualinc Report No. C11069. Prepared for the New Zealand Earthquake and War Damage Commission (EQC). Christchurch, New Zealand*, (February).
- Ryan, A.P., 1987. *The climate and weather of Canterbury, including Aorangi*, Wellington, N.Z: New Zealand Meteorological Service.
- Sanders, R.A., 1986. *Hydrogeological studies of springs in Akaroa County, Banks Peninsula*.
- Sewell, R.J., 1985. *The volcanic geology and geochemistry of central Banks Peninsula and*

*relationships to Lyttelton and Akaroa volcanoes : a thesis submitted in partial fulfillment of the requirements for the degree of Doctor of Philosophy in Geology in the University of Can.*

- Sodemann, H. & Stohl, A., 2009. Asymmetries in the moisture origin of Antarctic precipitation. *Geophysical Research Letters*, 36(22).
- Stephen-Brownie, C., 2012. *Earthquake - Induced Ground Fissuring in Foot - Slope Positions of the Port Hills , Christchurch.*
- Stewart, M.K., 2012. A 40-year record of carbon-14 and tritium in the Christchurch groundwater system, New Zealand: Dating of young samples with carbon-14. *Journal of Hydrology*, 430-431, pp.50–68.
- Sturman, A., 2008. Weather and Climate. In M. Winterbourn et al., eds. *The Natural History of Canterbury*. Christchurch: Canterbury University Press, pp. 119–142.
- Sundaram, B. et al., 2010. *Groundwater Sampling and Analysis-A Field Guide*,
- Todd, D.K. & Mays, L.W., 2005. *Groundwater hydrology*, Hoboken, NJ: Wiley.
- Trček, B. & Zojer, H., 2010. Recharge of springs. In *Groundwater Hydrology of Springs*. pp. 87–127.
- Tutbury, R.W.O., 2015. An isotopic and anionic study of the hydrologic connectivity between the Waimakariri River and the Avon River, Christchurch, New Zealand .
- U. S. Department of the Interior Bureau of water., 2001. Water measurement manual. , p.317.
- White, W.B., 2010. Groundwater Hydrology of Springs. In *Groundwater Hydrology of Springs*. Elsevier, pp. 231–268.
- Wilson, J., 2005. *Contextual historical overview for Christchurch City*, Christchurch, N.Z.: Christchurch City Council.